



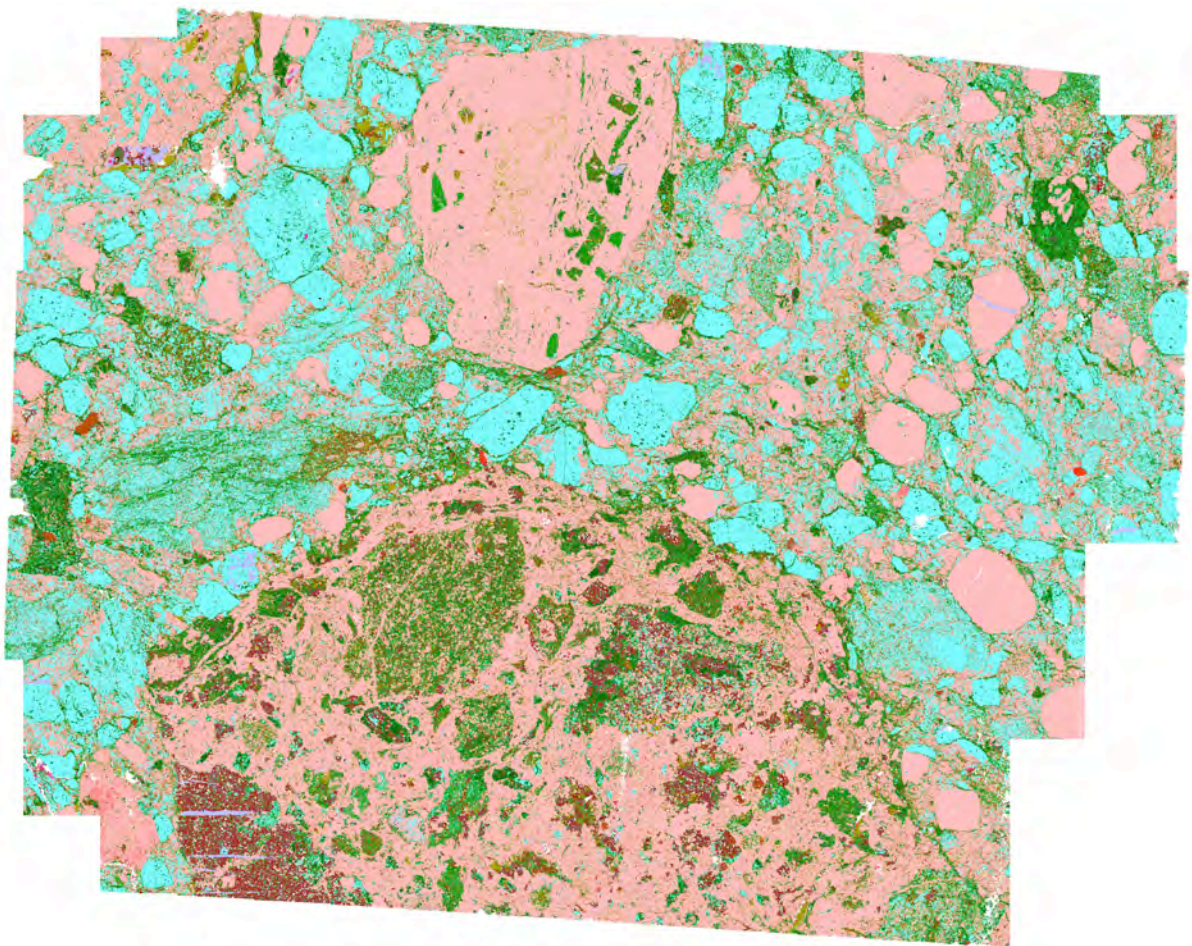
Stockholm
University

Bachelor Thesis

Degree Project in
Geology 15 hp

DeLong archipelago rock analysis: QEMSCAN compared to traditional methods

Andreas Sjöqvist



Stockholm 2015

Department of Geological Sciences
Stockholm University
SE-106 91 Stockholm

Table of contents

Abstract	4
Introduction	5
Background	5
<i>The DeLong archipelago</i>	<i>5</i>
<i>Location and history.....</i>	<i>5</i>
<i>Tectonic setting and geology.....</i>	<i>5</i>
<i>Volcaniclastic terminology.....</i>	<i>7</i>
<i>Pyroclasts and volcaniclastics.....</i>	<i>7</i>
<i>Accidental clasts and lithic fragments.....</i>	<i>7</i>
<i>Volcanic glass</i>	<i>7</i>
<i>Hyaloclastites</i>	<i>8</i>
<i>Volcaniclastic deposits and formation</i>	<i>8</i>
<i>QEMSCAN.....</i>	<i>10</i>
<i>Sample analysis.....</i>	<i>10</i>
<i>Software and data processing.....</i>	<i>10</i>
Data analysis	11
<i>Thin sections</i>	<i>11</i>
<i>XRF data.....</i>	<i>11</i>
<i>Point counting and grain angularity</i>	<i>12</i>
<i>QEMSCAN</i>	<i>13</i>
Results	14
<i>Traditional methods</i>	<i>14</i>
<i>Thin sections</i>	<i>14</i>
<i>XRF data.....</i>	<i>14</i>

<i>Grain angularity</i>	14
<i>Point counting data</i>	15
QEMSCAN data	17
<i>Element concentrations</i>	17
<i>Mineral percentages</i>	18
<i>Mineral maps</i>	19
Discussion	20
<i>Comparison</i>	20
<i>Element concentrations vs. XRF</i>	20
<i>Mineral maps vs. thin sections</i>	22
<i>Mineral abundances vs. point counting</i>	23
<i>Grain angularity</i>	24
<i>Results and future potential</i>	24
<i>Tectonic environment</i>	25
Conclusions	27
Acknowledgements	27
References	28

Appendices

Appendix A – Thin section descriptions, mineral identification confidence, QEMSCAN oxide conversion factors, metadata for the XRF.

Appendix B – Mineral abundance data, primary list.

Appendix C – QEMSCAN mineral maps.

Appendix D – QEMSCAN grain sphericity data.

Abstract

The DeLong archipelago is located off the northern coast of Siberia and is still largely unexplored. In 2013 a joint Russian-Swedish expedition investigated the geology of the archipelago, including the island Jeanette. Volcanic rocks occur across the archipelago and volcanoclastic sediments (mixed volcanic and non-volcanic sediment) were found. The goal of this study is to analyse the samples to determine a formational environment, but also to compare the analytical methods used with a relatively new instrument called a QEMSCAN (Quantitative Estimation of Mineralogy using Scanning Electron Microscopy). The QEMSCAN data proves superior for identifying the mineralogy of the samples since they were too fine-grained and too heavily altered for regular petrography. While the QEMSCANs analysis of element concentrations is not as accurate as that of an XRF, it is superior in terms of mineral abundances compared to point counting. The samples from Jeanette Island are identified as mostly volcanoclastic samples and a few volcanic samples, probably from an island arc setting and of andesitic mineralogy.

Introduction

The purpose of this study is a twofold one: i) to classify and, if possible, identify the tectonic origin of a number of rock samples from the island Jeanette located in the DeLong archipelago north of the Siberian coast, and ii) to compare the data acquired with equivalent data generated by a new instrument called QEMSCAN (Quantitative Estimation of Mineralogy using Scanning Electron Microscopy) to assess its capabilities. Data is acquired through traditional methods such as petrographic microscope observations on thin sections, XRF analysis, point counting and measuring grain angularity. The results of this study include a “traditional” analysis and an analysis performed by the QEMSCAN, and a comparison between the two. The data is used to classify the samples determine their formational environment.

Background

The DeLong archipelago

The DeLong archipelago includes five small islands located at 77°N 152°E in the East Siberian Sea. The islands are Bennett, Zhokov, Vilkitsky, Henrietta and Jeanette. Due to their remoteness, Bennett, Henrietta and Jeanette Islands were not discovered until 1881, and Zhokov and Vilkitsky Islands were discovered as late as 1914. Until recently the DeLong islands were little studied, and they are still an “unknown” on the geological map.

Location and history

Due to the remoteness of the DeLong archipelago, it was not discovered until 1881 by the Jeanette expedition. The expedition was led by US Navy Lieutenant Commander George W. DeLong, a veteran Arctic explorer, with a crew of 33 including 3 civilians. Their goal was to reach the North Pole. They were also to search for the famous Swedish polar explorer Adolf Erik Nordenskjöld whose expedition was long overdue. The ship Jeanette was purchased and provided for the expedition by James Gordon Bennett Jr.; an Arctic enthusiast, and they set off in June 1879. Just a few months later, Jeanette was trapped in sea ice and for almost two years drifted closer and closer to the North Pole before finally being crushed in 1881. During this time however, Henrietta, Jeanette and Bennett Islands had been discovered and the latter claimed for the US.

The crew of Jeanette was forced to abandon her and split up in three groups in an attempt to find their way back to civilisation. Only one of the groups survived, along with two of the crew from the second group who were sent ahead to find help. DeLong himself died from starvation in November 1881 (NHHHC, 2015-06-03).

Tectonic setting and geology

The geology of the five islands of the De Long archipelago is quite varied, and not all of the islands are related to each other from a geological perspective. The islands Zhokov and Vilkitsky are much younger than Henrietta, Jeanette and Bennett Islands (Pease and Tegner, 2014) as they were formed during the Neogene-Quaternary periods (Kos’ko and Korago, 2009). They are volcanic in origin (Pease and Tegner, 2014). Mantle and crustal xenoliths

are also present, as is spinel lherzolite, suggesting that the parent magma came from a depth of at least 60 km (Kos'ko and Korago, 2009). The mantle xenoliths suggest a depleted mantle origin (Kos'ko and Korago, 2009). Intraplate volcanism on continental lithosphere has been suggested as the formational environment of Zhokov and Vilkitsky Islands, according to Kos'ko and Korago (2009).

Amongst the three remaining islands, Henrietta, Jeanette and Bennett, the former two share many geological traits while the latter differs. Bennett Island is the largest of the five islands. Broadly speaking, Bennett Island is comprised of two units: a siliciclastic unit of Cambrian-Ordovician origin and a Cretaceous volcanic unit (Kos'ko and Korago, 2009). The first unit is dominated by mudstones and siltstones while the second unit is comprised of basalt, tuffaceous mudstones and sandstones (Kos'ko and Korago, 2009). The units are only weakly deformed and not metamorphosed (Pease, 2011).

Henrietta and Jeanette Islands are quite similar to each other in geological terms, but there are naturally a few differences. Jeanette Island is the smaller of the two: only around 3 km² compared to Henrietta Island that is 10 km². In contrast to Bennett Island, Jeanette Island is the least studied island of the De Long archipelago islands. M. M. Ermolaev was the last geologist to visit Jeanette Island back in 1933, and the only geological observations available until recently are from Ermolaev.

The coasts of Jeanette Island are steep cliffs ranging between 100 m and 350 m in height and a permanent ice cap is present on the island (Sobolev et. al., 2014). Ermolaev, who was the last person to study the island back in 1933, found coarse to medium grained sediments and conglomerates (Sobolev et. al., 2014). The conglomerate was made up of sedimentary, metamorphic and igneous, both mafic and felsic, clasts. The geology of Jeanette Island may be correlated to Henrietta Island (Pease and Tegner, 2014; Sobolev et. al., 2014). Pease and Tegner (2014) reported that sandstones, shales, dikes and volcanogenic rocks were found during the Russian-Swedish New Siberian Islands Expedition.

Finally, Henrietta Island is the northernmost island in the archipelago. Like the coasts of Jeanette Island, the coasts are made up of steep cliffs. Four geological units have been identified: quartz sandstone, volcanic mudstone, sandstone spliced with tuff, basalt and siltstone, and basalt (Kos'ko and Korago, 2009; Pease and Tegner, 2014). The volcanic unit is 160 m thick and comprised of flow basalts and andesite-basalts with intermittent tuff layers. Dolerite dikes are present in the middle two units, while diorite porphyritic dikes are present in all units but the quartz sandstone. Basaltic flows are present as well (Pease and Tegner, 2014). The clastics, volcanoclastics and calc-alkaline basalts that can be found on Henrietta Island suggest that it has an island arc origin that was intruded by sills and dikes at a later stage (Pease, 2011).

The islands in the De Long archipelago are of different age and origin. Zhokov and Vilkitsky Islands are suspected of being intraplate volcanic in origin (Kos'ko and Korago, 2009), while Bennett Islands is interpreted as remnants of an eroded lava plateau (Kos'ko and Korago, 2009). An island arc setting during the Caledonian orogeny is not ruled out however, and might fit very well with Henrietta and Jeanette Islands (Pease, 2011).

Observations of the rocks of Jeanette Island show that pyroclasts, volcanic glass and non-volcanic particles are present, and this study focuses on these components.

Volcaniclastic terminology

Pyroclasts and volcaniclastics

“Mixed sediments of both volcanic and non-volcanic origin” is a good way to describe volcaniclastic sediments (Fisher, 1961) or volcaniclastics as they will be referred as for the rest of this study. They differ from regular sediments in that they are mainly composed of pyroclasts instead of igneous or sedimentary rocks. A pyroclast is basically a particle of any size that is ejected from a volcanic vent (Fisher, 1961). They are mostly composed of volcanic glass and crystals and are usually angular to subrounded. Volcaniclastics are composed of a mixture of pyroclasts and grains of other origin. Since pyroclasts must be particles ejected from a volcanic vent, particles cannot be called pyroclasts if they i) are not formed in the volcanic vent, ii) are formed from flowing lava, iii) are formed from weathering, or iv) are not ejected from the vent, even if they were formed in it (Fisher, 1961). Tephra is another term for pyroclast, as proposed by Thorarinsson in 1944.

As tephra is deposited and lithified pyroclastic rock is formed. The difference between a volcaniclastic and pyroclastic rock, or deposit, is that while a pyroclastic rock must be composed of only pyroclasts, a volcaniclastic rock can be composed of a much broader array of clasts that are of volcanic origin but not necessarily of pyroclastic origin (Fisher, 1961).

Accidental clasts and lithic fragments

Volcaniclastic deposits might contain particles and fragments that are not pyroclast. These particles can be either volcanic or non-volcanic in origin. New volcanic particles that are ejected from the latest eruption are called juvenile clasts, while clasts from a previous eruption are called cognate (Fisher and Schmincke, 1984). There are also accidental clasts, which are clasts from the volcanic basement or host rock that have broken off during the eruption. These are usually not volcanic in origin (Fisher and Schmincke, 1984). Sometimes the name lithic clasts is used as an umbrella term for all clasts that did not form during the latest eruption, regardless of whether they are volcanic or non-volcanic in origin (Fisher and Schmincke, 1984; McPhie et. al., 1993). Alloclast is also a term for clasts of either volcanic or non-volcanic origin that are redeposited by a later eruption.

Volcanic glass

Volcanic glass is often referred to as obsidian, but this term has a genetic component to it since obsidian, *sensu stricto*, has high silica content (Ericson, 1975). There are numerous other types of volcanic glass with their own names, including tachylite which is basaltic (Fisher and Schmincke, 1984), so in order to minimize confusion the term “volcanic glass” will be used broadly for any type of glass with volcanic origin, regardless of how it is formed and its chemistry.

Glass is a major component of volcaniclastics due to the often rapid expulsion of hot magma into the comparatively cold air, which results in quenching of the magma and the formation of glass (Fisher and Schmincke, 1984). This sets volcaniclastics apart from other sedimentary deposits, making them relatively easy to identify. However, glass is inherently unstable, especially in water, and it weathers and decays very quickly (Fisher and

Schmincke, 1984), making volcanoclastic challenging to study. Even diagenesis itself affects volcanic glass: it breaks down in a process called devitrification and a matrix of clays, zeolites and palagonite is formed in its stead (Fisher and Schmincke, 1984; McPhie et. al., 1993). However, the clay can be used as an indicator of volcanoclastic or volcanic origin, and also hint at the original mineralogy of the pyroclast.

Different minerals weather into different clays, as do glass. Smectites are a common weathering product of glasses, so the presence of smectite might suggest that the sediments are volcanic in origin (Fisher and Schmincke, 1984). Montmorillonite is more common in basaltic glasses, as is chlorite, and kaolinite in more feldspathic ones. Furthermore, if euhedral phenocrysts of quartz, feldspar, biotite, pyroxene, olivine and/or amphibole are found in clay matrixes it is also a good sign that the origin was volcanic (Fisher and Schmincke, 1984). This is not an infallible method however, as other minerals might decay into the same clays. Kaolinite for instance is the end product in many weathered soils, as is smectite. Many mafic minerals are weathered into chlorite, thus making chlorite a rather poor indicator of basaltic glass, but an excellent indicator of a basaltic origin.

Hyaloclastites

Since glass is so unstable it readily alters, especially when in contact with water. Such hydrated glass is called hyaloclastite and not obsidian or tachylite. Regular basaltic glass, called sideromelane, is one such glass that readily hydrates and alters (Bonatti, 1965). Under the petrographic microscope sideromelane is clear and transparent but isotropic under crossed polars, and it is usually lacking vesicles. Over time, sideromelane alters to palagonite: a brown semi-transparent glass (McPhie et. al., 1993). Palagonite is often formed around vesicles as well. Interaction between mafic lava and water often forms palagonite directly (Bonatti, 1965) but since sideromelane also alters into palagonite it cannot be used as an exclusive indicator for either of the two processes. According to Bonatti (1965) however, at normal temperatures sideromelane alters rather slowly into palagonite, even in water.

Volcanoclastic deposits and formation

Volcanoclastic deposits might contain clasts of varying origin, not just pyroclastic origin. Until the middle of the last century there was no proper classification for different types of volcanic clasts, and the word pyroclast was sometimes erroneously used to describe volcanic clasts that did not match the above requirements. Thus, in 1961, Fisher proposed a new classification of volcanogenic clasts. Since then there have been several additions and new propositions to the classification.

Pyroclastic deposits are composed of only aerially ejected tephra (pyroclasts). Autoclastic deposits are formed by the mechanical fragmentation of solidified lava due to flow during effusive eruptions. Hyaloclastite deposits, or hydroclastic deposits as proposed by Walker and Blake (1966), are formed from effusive eruptions in a subaqueous environment. Finally, epiclastic deposits are deposits of reworked volcanoclastics through weathering. The original deposit could have been pyroclastic, autoclastic and/or hydroclastic.

In his classification in 1961, Fisher also proposed that the term volcanoclastic deposit be used for any deposit that contains volcanoclastic particles, regardless of the formational

process of the particles, the agent of transportation and the amount of non-volcanic particles present in the deposit.

There are also subaqueous volcanoclastic deposits. Note that “subaqueous” is used over “submarine” as this does not rule out volcanoclastic eruptions in freshwater environments. There are two ways of forming subaqueous volcanoclastic deposits: 1; a volcanic eruption takes place under water, forming deposits of particles on the sea floor, and 2; particles from a subaerial volcanic eruption is deposited into a marine, lacustrine, or otherwise aqueous environment and is subsequently deposited on the sea floor (Fisher, 1984). Just as when hot magma is ejected from a subaerial volcanic vent and is quenched when it comes into contact with the cold air, magma is quenched when it comes into contact with the cold water (Rittmann, 1962 in Fisher, 1984). This is called thermal spalling, and it forms volcanic glass.

If volatiles are present in the lava, explosions can occur, especially in silicic magmas. Due to the high viscosity of these magmas, volatiles in the magma are not as readily released and remain in the magma. As the magma is then cooled, the volatiles are still rather hot due to the close proximity to the magma, which results in the expansion of the volatiles. This expansion might violently shatter the solidified magma in an explosion, increasing the amount of magma that contacts the water further (Fisher, 1984). These types of eruptions are thus called explosive eruptions, while eruptions that do not involve explosions are called effusive (Fisher, 1984).

Explosive eruptions cannot occur at any depth however. Below a certain depth the hydrostatic pressure is greater than the internal gas pressure of the magma, preventing the formation of gas bubbles. At these depths, explosive eruptions cannot occur since no gas bubbles can form. The critical depth at which the hydrostatic pressure exceeds the internal gas pressure of the magma is called the PCL: the pressure compensation level. Since water pressure is relatively constant at specific depths around the globe, the main factor that affects PCL is the chemical composition of the magma (Fisher, 1984). The PCL for silicic magmas lies around 1000 meters below sea level or even deeper, while the PCL for mafic magmas lies around 500 meters below sea level (Fisher, 1984).

The chemical composition of the magma affects how the magma interacts with the water and the type of particle produced. While mafic magmas are the most common type since divergent plate boundaries in the oceans produce a lot of magma, andesitic and even rhyolitic magmas are erupted into the oceans as well. At ocean-ocean convergence zones andesitic magma is common, and at ocean-continent convergence zones andesitic to rhyolitic magmas are erupted. While these eruptions are often voluminous they cannot match the massive amounts of magma erupted at ocean spreading zones, which skews the proportions of the different erupted magma types. Intraplate volcanism is responsible for only a small amount of magma eruption compared to convergent and especially divergent plate boundaries. Most *volcanoclastic* deposits, i.e. mixed volcanic and non-volcanic sediments, are found near ocean islands and island arcs though (Fisher, 1984) since pyroclasts at these locations are mixed with eroded terrestrial sediment. The abundance and size of *pyroclastic* deposits, i.e. deposits of only volcanic sediments, on the other hand are more directly linked to the volume of erupted lava, and in this case divergent margins dominate.

QEMSCAN

Quantitative Estimation of Mineralogy using Scanning electron microscopy, QEMSCAN, is a relatively new instrument mainly used by the mining industry to quickly and reliably acquire element and mineral data in samples of varying type. It can analyse samples of any shape and form as long as it is dry, as any volatiles would vaporize and interfere with the probe. Samples with a flat surface are preferred, as a sample with too much topography would block the electron beam used to probe the sample. Thin sections and resin pucks are examples of good samples.

QEMSCAN is at its core a scanning electron microscope, or SEM. It uses a narrow beam of electrons to excite the electrons in the target atoms shells so that they emit x-rays. The x-rays can then be read by an EDS detector: an Energy Dispersive Spectrometer. The EDS contains a quartz crystal that is hit by the incoming x-ray, which causes a piezoelectric strain in the crystal. This strain is proportional to the amount of energy in the x-ray, which in turn is linked to the element that emitted the x-ray. This particular QEMSCAN uses a Burker EDS. Depending on the atom that ejected the x-ray pulse, the electron will have multiple “pathways” when returning to an inner shell. This means that each atom has a unique signature, a so called spectrum, and these spectra can be identified and compared to a library to determine the atom that produced each x-ray pulse.

The QEMSCAN also measures the relative proportions of the various element spectra, and then compares these against a library to determine what is currently being analysed. Thus, the mineralogy of the matter being analysed can be acquired.

Sample analysis

The QEMSCAN analyses samples in two more ways. One of them is called BSE, or Back Scatter Electron. The BSE is a low-count analysis that generates an image of the sample and density data. Electrons are more easily reflected off larger atoms, and the larger the atom the heavier it is, thus correlating the number of reflected electrons to the density of the atom.

The third type of data is called SE, or Secondary Electron. As the electron beam is moved over a sample, some of the atoms in the sample are ionized by the electron beam. In order to restore their neutral charge, the atoms eject electrons, which can then be collected by an SE detector. While this particular QEMSCAN is not equipped with an SE detector, it is a great tool that can render high-resolution images of the type regular SEMs produce.

Software and data processing

The QEMSCAN only generates raw data; the identification of elements and minerals is performed at a later stage by a software program called iDiscover. The mineral library that the raw data is compared against is called a SIP, or Species Identification Protocol. The SIP can be adjusted to accommodate new minerals or alternative appearances of minerals.

Since the SIP is very extensive, mineralogical results are usually condensed into a secondary mineral list that is easier to work with. Post processing is also possible in the software, which can be used to clean up the data or to process the data in various ways. One such tool

in the post processing that is very useful is the so called “gangue buster”. The gangue buster is a processor that can “bust out” certain minerals and remove the rest, only showing the remaining minerals. This is useful to determine the physical distribution of a mineral in a sample, which in turn can be used to for instance determine if a mineral often is associated with certain grains or in other patterns. Another tool is the particulator, which can separate grains to analyse them separately. The software can also generate element oxide concentration data similar to the data an XRF generates.

Data analysis

Thin sections

The thin sections were studied under the petrographic microscope, and descriptions of them were made.

A template based on basic sedimentary and igneous classification factors and important textures observed in the thin sections was used when making the descriptions. Refer to table 1 for the template, and to appendix A for the full descriptions.

Table 1: The template used for the descriptions of the thin sections.

Parameter	Definition
Mineralogy	E.g. quartz, feldspar and calcite
Crystal size	Estimation of size; small, medium, large
Crystal shape	Anhedral to euhedral, rounded to angular
Crystal surface textures	Boundary textures and dissolution textures
Crystal orientation	E.g. crystals aligned with flow direction
Matrix composition	E.g. chlorite, smectite and muscovite
Crystal/matrix abundance	Estimation of the abundances. E.g. 10/70/20 (percent)
Vesicles/pore spaces	Size and shape (if present)
Compositional variations	Spatial variations in the matrix or mineralogy
Textural relationships	Associations of certain minerals or textures, e.g. chlorite associated with fragment-rich areas
Structures	E.g. fractures, veins, larger fragments
Bedding	Bedding and/or layering
Sorting	Very good to very poor

The thin sections were observed in detail and the template was filled in as accurately as possible. However, due to the extensive alteration and extremely fine grain size of some of the samples, the matrix composition parameter could not be determined using the thin sections only. Instead the element maps from the QEMSCAN were used to complement the thin sections. For the comparison between the thin section observations and the QEMSCAN data, this parameter was left out.

XRF data

The samples were crushed and ground to a powder, mixed with flux and fused at 1100°C into glass beads to be used for XRF analysis. The XRF data was produced at Stockholm University with a ZSX Primus II Sequential X-Ray Fluorescence Spectrometer from Rigaku Industrial Corporation of Osaka, Japan. Since the data was generated prior to and independently of this study, XRF data is available only for samples DL13-03, DL13-08a, DL13-09, DL13-11 and DL13-12. The comparison between QEMSCAN element data and the

XRF data is therefore limited to these samples. The results from the XRF can be found in table 3 in the results section.

Point counting and grain angularity

Point counting was done on the thin sections using a Leica DMLSP petrographic microscope and the software Pelcon Point Counter as a way of determining the relative proportions of the minerals that make up each sample. Roughly 500 points were counted on each sample. The results are presented in tables 5 and 6 in the results section.

Grain angularity is a way of measuring the maturity of a sedimentary sample. More mature sediments often have grains that are more rounded since they are abraded by the transport. There are other ways of estimating maturity of sediment. For instance, feldspar tend to weather away and break apart during transport while quartz remains intact and is thus concentrated as other minerals are removed or broken down. A sample with euhedral feldspar is regarded as more juvenile than a sample with mostly quartz and only a few rounded feldspars is considerably more mature. Grain angularity measurements can thus be combined with point counting data to estimate the maturity of the sediment.

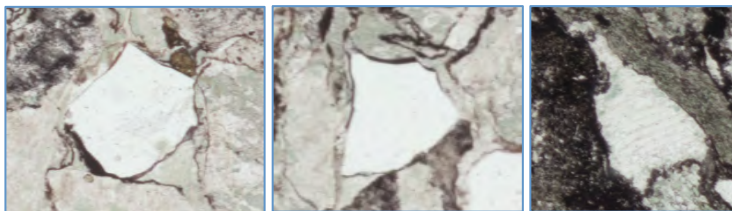


Image 1a: Examples of angular grains.



Image 1b: Examples of subangular to subrounded grains.

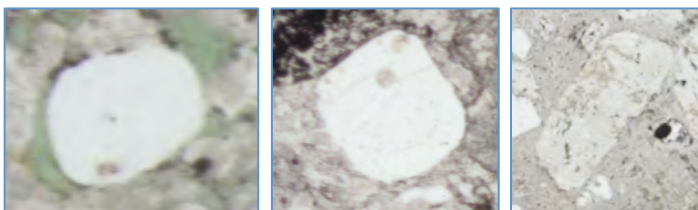


Image 1c: Examples of rounded grains.

Grain angularity was measured semi-quantitatively through observation and estimation. The variation in grain angularity throughout the samples was condensed into a spectrum with three entries: angular, subrounded to subangular and rounded. Microphotographs were then made of the thin sections and grains were manually compared against the example grains and counted. See image 1 for examples of category.

The key trait that determines the grain angularity is the presence of sharp or blunt corners. If the grain has a single sharp corner it is considered to be angular. If a grain has no corners, as with the first grain in image 1c, it is

considered to be rounded. If the grain has perfectly smooth edges, it is also considered to be rounded. Finally, anything in between, i.e. with corners that are neither sharp nor smooth, are considered to be subangular or subrounded. Since these measurements are broad generalisations of the grain angularity and not a meticulous, highly accurate analysis, no distinction was made between subangular and subrounded. This method leaves some room for interpretation, but is relatively accurate and fast, and provides information on the general angularity of each sample.

QEMSCAN

Rock chips left from the making of the thin sections were mounted into epoxy, polished and put into the QEMSCAN and analysed at a 2.5 by 2.5 micron resolution. This raw data was then processed in iDiscover to acquire element concentrations in the form of oxide weight percent and mineral abundances. Also, using the same software, mineral maps of each chip were made. The element oxide concentrations can be found in the results section in table 7, the mineral abundances can be found in table 9 and 10, and the mineral maps can be found in appendix C.

In order to acquire this data some processing was required. Samples were cleaned up, the SIP was updated once to a new and improved SIP, and the primary mineral list was condensed into a secondary list that was easier to work with. After the analysis, the erroneous identification of some minerals was detected. Garnet was the most notable one; it was actually epidote, but due to its wide range of compositions it was erroneously identified. Misclassifications such as these are fortunately easy to correct to within an acceptable level of error by simply assuming that all garnet found was actually epidote. Thin section observations can strengthen the validity of this assumption further. There are however other minerals that the QEMSCAN cannot classify with acceptable accuracy and that are not as easy to correct for during the post processing stage. The secondary list with information about the QEMSCAN's accuracy in classifying each mineral can be found in appendix A, but a shorter list with only the most abundant and/or important minerals found in the samples can be found in table 2.

Table 2. Mineral identification confidence for the QEMSCAN.

Mineral	Identification confidence
Muscovite	Good; may include minor misidentifications with other K-Al silicates (e.g. illite, K-feldspar)
Hematite/ Magnetite/ Ilmenite	Very difficult to differentiate magnetite and hematite; ilmenite is easily identified
Calcite	Good, includes aragonite
Garnet group	Wide range of compositions in garnet group. Some garnet compositions are very close to other silicates, which may cause misclassifications/misidentifications. E.g. grossular garnet is very similar to epidote
Epidote group	Moderate. Epidote composition very similar to grossular garnet. Zoisite and allanite compositions should be good
K-Feldspar group	Good; may include minor misidentifications with other K-Al silicates (predominantly illite, minor muscovite)
Albite	Good; although the composition of albite is close to jadeite which means that jadeite and albite might be misclassified as each other
Plagioclase group	Good
Chlorite group	Good to moderate
Kaolinite/Dickite (S)	Impure kaolinite definitions may capture other phases, such as tourmaline; kaolinite concentrations might be too high
Montmorillonite/ Smectite group	Wide range of compositions; some pixels might be misclassified
Fe Oxides	Very difficult to differentiate between magnetite and hematite under non-optimal conditions; magnetite/hematite should be differentiated well against goethite and siderite. Siderite and goethite can be difficult to determine from each other as well
Quartz	Good
Illite	Moderate. May include minor misidentifications with other K-Al silicates (especially K-feldspar); can contain impurities, which may cause misidentification/overlap with other silicates

Results

Traditional methods

Thin sections

The results from the thin section observations using a petrographic microscope can be found in appendix C.

XRF data

Table 3. XRF data for some of the samples.

	SiO ₂ wt%	Al ₂ O ₃ wt%	CaO wt%	MgO wt%	MnO wt%	P ₂ O ₅ wt%	Fe ₂ O ₃ wt%	Na ₂ O wt%	K ₂ O wt%	TiO wt%	Totals
DL13-03	55.76	14.34	5.66	4.44	0.46	0.25	14.6	0.67	1.79	2.08	100,00
DL13-8a	58.53	16.46	4.18	3.24	0.20	0.59	9.03	4.84	1.08	1.86	100,00
DL13-09	67.19	17.69	2.16	1.60	0.11	0.05	3.46	5.88	1.63	0.23	100,00
DL13-11	51.53	14.18	9.16	6.46	0.25	0.19	14.0	2.17	0.21	1.86	100,00
DL13-12	57.91	19.63	4.15	2.77	0.22	0.05	7.77	4.56	2.43	0.52	100,00

Grain angularity

Table 4. Grain angularity data presented as number of grains in each category. In some samples one of the categories was very dominant. This is highlighted as numbers such as 100+. Samples with grain size too fine to accurately determine the angularity are labelled N/A. Sample DL13-11 contained a very large amount of vesicles and volcanic glass shards, making it difficult to identify grains for the angularity analysis.

Sample	Angular	Subangular to subrounded	Rounded	General roundness
DL13-01	62	100+	1	Subangular to subrounded
DL13-02	N/A	N/A	N/A	N/A
DL13-03	45	29	1	Angular
DL13-04	N/A	N/A	N/A	N/A
DL13-05	N/A	N/A	N/A	N/A
DL13-06	39	46	4	Subangular to subrounded
DL13-07	67	31	5	Angular
DL13-08a	N/A	N/A	N/A	N/A
DL13-08b	68	49	0	Angular
DL13-09	41	85	5	Subangular to subrounded
DL13-10	N/A	N/A	N/A	N/A
DL13-11	---	---	---	---
DL13-12	43	200+	5	Subangular to subrounded
DL13-13	32	120+	2	Subangular to subrounded

Point counting data

Table 5: Point counting data from the samples.

* "Matrix" is everything that is too altered or tiny to identify.

** In one sample the sericitation was so extensive that it was near impossible to identify the feldspar beneath it, and in this sample only fresh feldspar crystals were counted as feldspar

*** In one sample there were abundant vesicles, some of which were glassy and not filled with a mineral. These were counted as "vesicles".

	Quartz	Feldspar	Chlorite	Calcite	Matrix*	Epidote	Muscovite	Opaques	Sericite**	Vesicle***	Total points counted	Lines counted
DL13-01	25	301	0	24	82	7	3	17	0	0	459	20
DL13-02	4	241	101	72	13	0	0	9	0	0	440	18
DL13-03	11	232	2	57	228	0	3	12	0	0	545	20
DL13-04	0	457	39	49	32	107	2	3	0	0	689	20
DL13-05	3	216	5	5	217	3	0	53	0	0	502	21
DL13-06	38	448	2	0	15	29	0	29	0	0	561	20
DL13-07	5	419	9	3	39	5	0	33	0	0	513	18
DL13-08a	0	387	84	13	0	2	1	18	0	0	505	21
DL13-08b	20	496	47	55	0	0	0	26	0	0	664	22
DL13-09	50	284	12	26	67	0	0	6	0	0	445	21
DL13-10	7	23	4	17	35	0	0	9	383	0	478	17
DL13-11	0	164	0	44	183	64	2	23	0	59	539	19
DL13-12	7	431	71	53	24	1	3	36	0	0	626	20
DL13-13	4	442	10	17	10	0	3	51	0	0	537	22

Notes regarding the point counting data:

In sample DL13-03, the matrix probably contains a lot of glass, which means that some of the points classified as opaques might be glass and some of the matrix might be opaques.

In sample DL13-05, a significant part of the matrix is probably fine-grained feldspar but the extensive alteration makes it hard to accurately identify minerals.

In sample DL13-09, clusters of sericite where there is no feldspar visible beneath it is also counted as matrix here.

In general, some feldspar might actually be quartz but since it's too fine grained and altered it makes identification difficult. Most of the quartz is rather fresh though, so alteration (even though it is not sericitation) is usually a sign that it is feldspar. Plagioclase was not distinguished from feldspar at all due to heavy alteration and small size, which made identification difficult.

Table 6. Point counting data presented as mineral percentages out of 100% instead of absolute values.

Mineral abundance (%)	DL13-01	DL13-02	DL13-03	DL13-04	DL13-05	DL13-06	DL13-07	DL13-08a	DL13-08b	DL13-09	DL13-10	DL13-11	DL13-12	DL13-13
Quartz	5	1	2	0	1	7	1	0	3	11	1	0	1	1
Feldspar	66	55	43	66	43	80	82	77	77	64	5	30	69	82
Chlorite	0	23	0	6	1	0	2	17	7	3	1	0	11	2
Calcite	5	16	10	7	1	0	1	3	9	6	4	8	8	3
Matrix	18	3	42	5	43	3	8	0	0	15	7	34	4	2
Epidote	2	0	0	16	1	5	1	0	0	0	0	12	0	0
Muscovite	1	0	1	0	0	0	0	0	0	0	0	0	0	1
Opaques	4	2	2	0	11	5	6	4	4	1	2	4	6	9
Sericite	0	0	0	0	0	0	0	0	0	0	80	0	0	0
Vesicle	0	0	0	0	0	0	0	0	0	0	0	11	0	0
Total	100	100	100	100	100	100	100	100	100	100	100	100	100	100

QEMSCAN data

Element concentrations

Table 7: Element oxide percent for the major elements. Based on the area percent of the elements in the sample.

Element oxide	DL13-01	DL13-02	DL13-03	DL13-04	DL13-05	DL13-06	DL13-07	DL13-08a	DL13-08b	DL13-09	DL13-10	DL13-11	DL13-12	DL13-13
Al ₂ O ₃	15.29	12.40	10.49	15.35	16.66	14.01	13.21	14.87	16.41	16.16	14.24	11.83	16.16	16.74
CO ₂	3.15	5.14	3.80	1.38	0.43	0.18	0.28	0.54	1.42	1.42	1.54	3.57	3.18	0.56
CaO	4.68	7.43	5.43	4.04	1.49	1.54	1.32	3.04	2.71	2.48	2.42	7.39	4.87	1.39
Cl	0.01	0.02	0.03	0.01	0.01	0.00	0.01	0.07	0.01	0.00	0.00	0.01	0.01	0.00
Cr ₂ O ₃	0.00	0.00	0.00	0.04	0.00	0.00	0.00	0.00	0.00	0.00	0.00	0.00	0.00	0.00
F	0.10	0.07	0.23	0.01	0.12	0.09	0.15	0.08	0.02	0.09	0.11	0.02	0.13	0.19
Fe ₂ O ₃	4.11	13.24	10.32	11.17	9.73	2.98	11.83	9.47	6.04	2.58	2.91	12.30	8.05	6.99
H ₂ O	3.58	4.98	7.01	11.78	12.29	4.66	4.60	3.72	1.85	1.80	5.34	4.88	4.09	3.26
K ₂ O	1.74	0.78	2.08	0.06	0.81	2.19	3.19	0.73	0.15	1.71	2.50	0.22	1.90	2.77
MgO	1.36	3.40	2.90	3.86	3.22	1.16	3.94	2.41	1.32	1.10	0.76	3.91	2.00	1.50
Mn ₂ O ₂	0.00	0.00	0.00	0.01	0.01	0.00	0.00	0.00	0.00	0.00	0.00	0.00	0.00	0.00
Na ₂ O	3.83	2.27	0.38	1.75	3.08	2.73	2.34	4.82	7.46	5.84	2.08	2.08	4.41	4.81
P ₂ O ₅	0.13	0.34	0.48	0.14	0.20	0.09	0.23	1.19	0.10	0.06	0.07	0.26	0.12	0.04
SO ₃	0.00	0.03	0.00	0.07	0.00	0.05	0.01	0.00	0.00	0.00	0.00	0.01	0.00	0.00
SiO ₂	61.94	48.48	56.20	50.10	52.66	69.96	57.01	57.93	62.21	66.63	67.22	53.97	54.40	61.40
TiO ₂	0.16	1.96	1.15	0.90	0.07	0.14	2.09	1.50	0.65	0.18	0.55	0.08	1.03	0.61
Sum	100.08	100.54	100.51	100.65	100.77	99.79	100.22	100.37	100.36	100.05	99.73	100.54	100.34	100.27

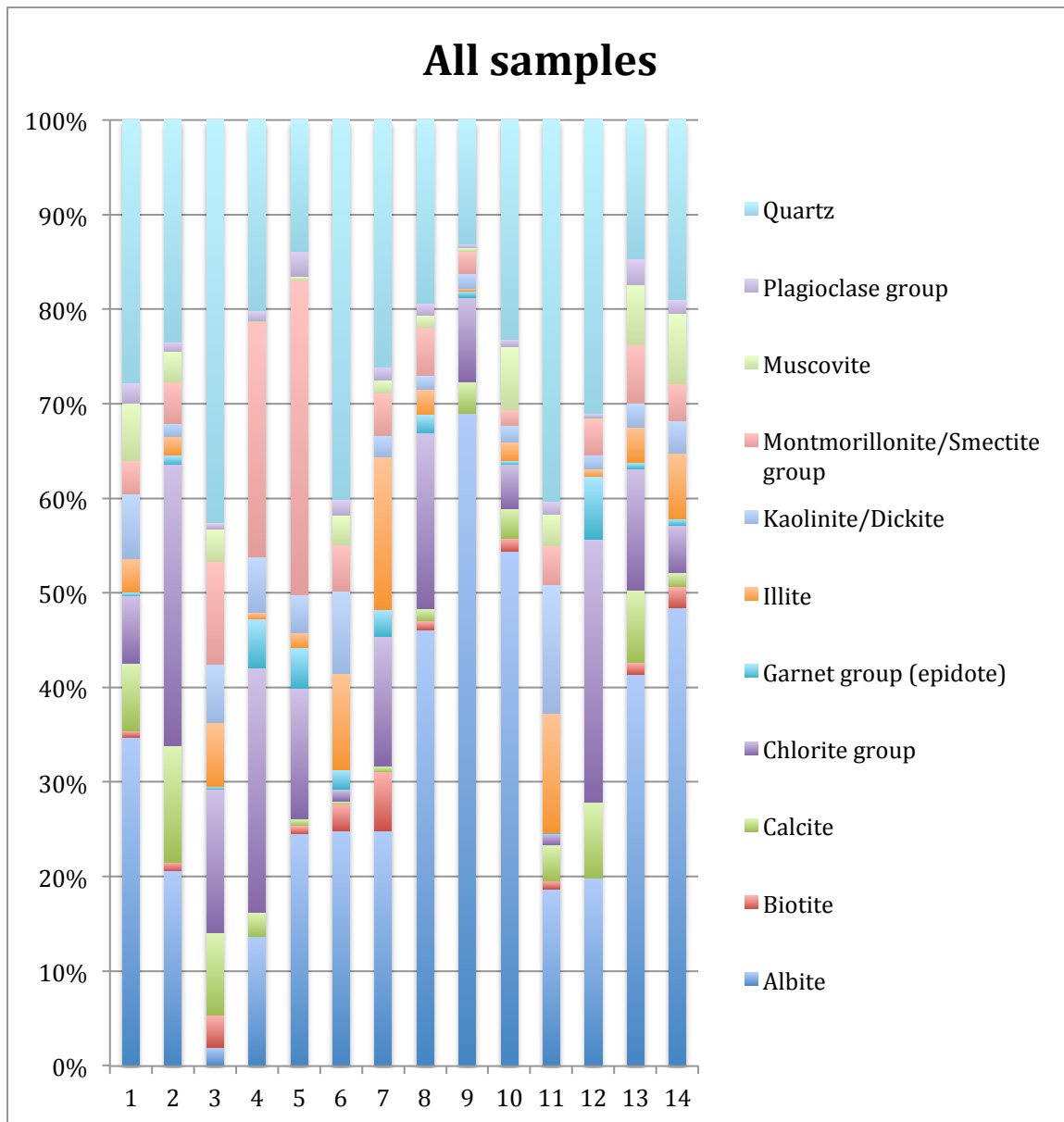
Table 8. QEMSCAN element concentrations for the elements analysed by the XRF, renormalized to 100.

	SiO2 wt%	Al2O3 wt%	CaO wt%	MgO wt%	MnO wt%	P2O5 wt%	Fe2O3 wt%	Na2O wt%	K2O wt%	TiO2 wt%	Totals
DL13-03	62.84	11.73	6.07	3.24	0.00	0.54	11.54	0.43	2.32	1.29	100.00
DL13-08a	60.37	15.50	3.17	2.51	0.00	1.24	9.87	5.02	0.76	1.56	100.00
DL13-09	68.88	16.71	2.56	1.13	0.00	0.06	2.67	6.03	1.76	0.19	100.00
DL13-11	58.63	12.85	8.03	4.24	0.00	0.28	13.36	2.26	0.24	0.09	100.00
DL13-12	58.54	17.39	5.24	2.16	0.00	0.13	8.66	4.74	2.04	1.11	100.00

Mineral percentages

Table 9. Mineral percentage by area. The most abundant minerals are included in the table, with the total sum they amount to. For a full list of all the minerals found in each sample, refer to appendix B.

Mineral area %	DL13-01	DL13-02	DL13-03	DL13-04	DL13-05	DL13-06	DL13-07	DL13-08a	DL13-08b	DL13-09	DL13-10	DL13-11	DL13-12	DL13-13
Albite	33	20	2	13	23	23	21	43	67	52	17	18	38	43
Biotite	1	1	3	0	1	3	5	1	0	1	1	0	1	2
Calcite	7	12	8	2	1	0	1	1	3	3	3	7	7	1
Chlorite group	7	29	14	24	13	1	12	17	9	4	1	26	12	5
Garnet group	0	1	0	5	4	2	2	2	1	0	0	6	1	1
Illite	3	2	6	1	1	9	14	2	0	2	11	1	3	6
Kaolinite/Dickite	6	1	6	5	4	8	2	1	2	2	12	1	2	3
Montmorillonite (Smectite)	3	4	10	23	31	5	4	5	2	2	4	4	6	4
Muscovite	6	3	3	0	0	3	1	1	0	6	3	0	6	7
Other silicates	4	1	5	0	3	4	8	2	1	3	6	1	5	6
Plagioclase group	2	1	1	1	3	2	1	1	0	1	1	0	3	1
Quartz	26	23	39	19	13	37	22	18	13	22	37	29	14	17
Total	98	97	96	93	98	97	93	95	98	99	97	94	97	96



Graph 1: Stacked tabular graph of the most abundant minerals by volume found in the samples.

Mineral maps

Mineral maps of the samples can be found in appendix C.

Discussion

Comparison

Element concentrations vs. XRF

Both XRF and QEMSCAN gather element data in the same way: by exciting electrons in the atoms of the sample so that x-rays are emitted from the atoms. While the XRF uses x-rays to excite the atoms, the QEMSCAN uses an electron beam, but the results should be the same. Therefore, since the QEMSCAN also has other functions, such as SEM imaging, it would be a very useful and versatile tool if it could generate data of the same accuracy and precision as the XRF. Results for the XRF analysis can be found in table 3 and the results from the QEMSCAN element concentration analysis can be found in table 7, both in the results section.

XRF is a tried and trusted method that has a documented high accuracy and very high precision. The QEMSCAN has not been as rigorously tested yet. A comparison between the QEMSCAN and XRF data can be found in table 10. Since the XRF used at Stockholm University only measures 10 elements: Al, Ca, Fe, K, Mg, Mn, Na, P, Si and Ti, and the QEMSCAN measures many more elements, the QEMSCAN data was renormalized to match the XRF data. The results after the renormalization can be found in table 8. The two data sets were then compared and presented as ratios in (see table 10).

As clearly shown by the comparison, the QEMSCAN data is not as accurate as the XRF data with errors of more than 25% being very common and errors within the 5-25% range being typical. A few measurements are within a 5% error margin, which still is quite high compared to the Mean Relative Deviation of the XRF at Stockholm University for a number of USGS standards. While a 5% error would be unacceptable in most cases, if all the QEMSCAN data were within the 5% error range it would be considerably more acceptable than what it currently is. In addition, XRF analysis was performed on other, larger, pieces of rock, so there is a chance that the chemistry varies between the two samples. If this is the case then a 5% error margin may be acceptable.

Of the 10 elements, the QEMSCAN measurements for P_2O_5 and MgO are the least accurate. The P_2O_5 concentrations are mostly within the lower range of major element concentrations, approaching minor element concentrations, but the MgO concentrations are well within major element abundances, and thus should be measured with much greater accuracy. Also, according to the QEMSCAN, no MnO was present in the samples, hence the extremely high ratios in the comparison. Low concentrations of Mn, lower than around 2%, might not be detected by the QEMSCAN.

It should be noted that since these numbers are not absolute values but percentages, the lack of MnO in the sample means that the relative concentrations of the other elements to the XRF concentrations are increased. To find out the significance of this, MgO was given concentrations based on those reported by the XRF, and the QEMSCAN concentrations were then renormalized with the new MnO concentrations. The results were compared to the old results as a ratio in table 11.

Table 10. Comparison of element concentrations measured by QEMSCAN and XRF.

Values of <1 means that the QEMSCAN reported higher concentrations of the element than the XRF
 Values of >1 means that the QEMSCAN reported lower concentrations of the element than the XRF
 Values of 1 means that the QEMSCAN reported the same concentration as the XRF
 Red fields have a 25% or greater error, yellow fields have a 5-25% error and green fields have an error of 5% or less.

Comparison										
Samples	SiO2 wt%	Al2O3 wt%	CaO wt%	MgO wt%	MnO wt%	P2O5 wt%	Fe2O3 wt%	Na2O wt%	K2O wt%	TiO2 wt%
DL13-03	0.89	1.22	0.93	1.37	147.50	0.47	1.26	1.56	0.77	1.62
DL13-08a	0.97	1.06	1.32	1.29	547.33	0.47	0.91	0.96	1.43	1.19
DL13-09	0.98	1.06	0.84	1.41	33.50	0.79	1.30	0.97	0.93	1.23
DL13-11	0.88	1.10	1.14	1.52	81.69	0.66	1.05	0.96	0.87	20.82
DL13-12	0.99	1.13	0.79	1.28	219.48	0.37	0.90	0.96	1.19	0.47

Table 11. Comparison between original QEMSCAN element concentrations and QEMSCAN element concentrations with values from the XRF added to MnO. Presented as a ratio of modified values/original values.

Comparison											
Samples	SiO2 wt%	Al2O3 wt%	CaO wt%	MgO wt%	MnO wt%	P2O5 wt%	Fe2O3 wt%	Na2O wt%	K2O wt%	TiO2 wt%	Totals
DL13-03	0.99	0.99	0.99	0.99	164.08	0.99	0.99	0.99	0.99	0.99	1.00
DL13-08a	1.00	1.00	1.00	1.00	569.19	1.00	1.00	1.00	1.00	1.00	1.00
DL13-09	1.00	1.00	1.00	1.00	34.60	1.00	1.00	1.00	1.00	1.00	1.00
DL13-11	1.00	1.00	1.00	1.00	88.51	1.00	1.00	1.00	1.00	1.00	1.00
DL13-12	1.00	1.00	1.00	1.00	235.62	1.00	1.00	1.00	1.00	1.00	1.00

Clearly, the rather drastic change in MnO concentrations had little to no effect on the concentrations of the other elements, which means that even with more accurate Mn measurements the QEMSCAN data would still suffer from unacceptably low accuracy.

SiO₂ and Na₂O are the elements with the highest accuracy. Since Si is such a common and abundant element in rocks, it is no surprise that it is one of the elements that are measured with the most accuracy. The surprise is Na. It is the lightest of the 10 elements and is difficult to measure with the XRF, in part because it can be volatile. This trait and/or its low weight may or may not be a partial explanation, but it is unlikely since Mg is only slightly heavier and yet has the lowest accuracy of all the measured elements. Furthermore, Al, Si and P all have the same number of electron shells as Na and Mg, and while Si is measured with acceptable accuracy, Al and P are not. The problem with non-accurate measurements seems to originate not in the chemical nature of the elements but somewhere else.

The likely reason for the differences in concentrations reported by QEMSCAN and XRF is the process that the QEMSCAN uses to quantify elements. The QEMSCAN does not measure

the absolute quantity of elements in each pixel; instead it compares the relative concentrations of them. These relative concentrations are then compared against the SIP for mineral identification, and the mineral with the closest relative concentration is assigned to that pixel. The QEMSCAN then quantifies the absolute concentrations of the elements in that pixel based on the standard chemical composition of the mineral that the pixel was assigned as. While certain minerals have several entries in the SIP for different chemical compositions, this method is still a rather inaccurate way of quantifying element abundances, and needs to be improved in order for QEMSCAN to truly compete with for instance XRF. Metadata on QEMSCAN accuracy and precision was requested but could not be obtained from the manufacturer in time. This is very unfortunate as without any measurements of accuracy or precision all the QEMSCAN data used in this study cannot be completely trusted, and this study should thus not be taken as a completely fair assessment of the QEMSCAN's capabilities.

Mineral maps vs. thin sections

Since QEMSCAN can identify minerals at a 2.5 micron resolution it is an extremely powerful tool when it comes to identifying very fine grained minerals, alteration products and substances that are hard to identify through the petrographic microscope. For heavily altered samples such as the ones in this study, the QEMSCAN is truly superior. However, as with the case of the garnet-epidote misidentification, the instrument is not infallible and manual quality control on the minerals identified is recommended when possible.

- Albite
- Annite-Phlogopite
- Apatite
- Background
- Barite
- Biotite
- Calcic amphiboles
- Calcite
- Chlorite group
- Chloritoid
- Clinopyroxenes
- Dolomite-Ankerite group
- Epidote group
- Fe Oxides
- Fe-Mg-Mn amphiboles
- Garnet group
- Glaucophane
- Gypsum/Anhydrite
- Halides
- Hematite/Magnetite/Ilmenite
- Illite
- Kaolinite/Dickite (S)
- K-Feldspar group
- Low Confidence
- Montmorillonite/Smectite group
- Muscovite
- Olivine
- Orthopyroxenes
- Other
- Other carbonates
- Other oxides
- Other phosphates
- Other sheet silicates
- Other silicates
- Other sulphates/sulphides
- Plagioclase group
- Pores
- Pyrite
- Quartz
- Rutile/Anatase/Brookite
- Siderite
- Sillimanite/Kyanite/Andalusite
- Sodic amphiboles
- Spinel group
- Staurilite
- Titanite
- Tourmaline group
- Unclassified
- Zircon

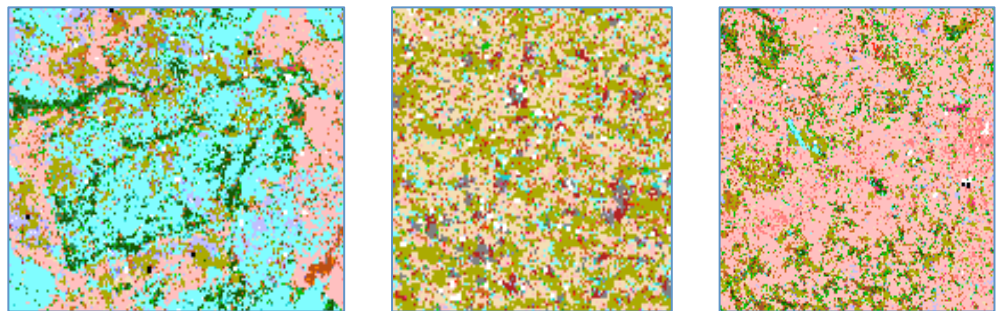


Image 2. From left to right: alteration textures in a plagioclase grain, a fine-grained matrix, isotropic silicic glass.

The mineral maps offer a quick overview of the sample and the geographical locations of the minerals. Grains are visible on the maps, as are alteration textures (see image 2, left picture) and boundary textures that include a change of mineralogy. The mineralogy of fine-grained matrixes is easily identified (see image 2, centre picture) and changes in chemistry in single grains can be identified as well.

A welcome but not surprising “side effect” of the mineral identification becomes apparent when volcanic glass is analysed. The rough chemistry of the glass can be seen on the mineral maps since the QEMSCAN identified the glass as quartz, as in sample DL13-03 (see image 2, right picture). While it might not be a perfect match the fact that it is close to quartz offers some insight into the approximate chemistry of the glass.

Figure 1. QEMSCAN mineral map legend.

Regular thin section observations have advantages too. For instance, a mineral might be in disequilibrium but not altered to another mineral. Such changes are hard if not impossible for the QEMSCAN to detect; since the change in chemistry will be small it will probably fall within the parameters of the original mineral, and not show on the mineral maps. Such processes that affect the optical properties of the mineral but not its chemistry, at least not in a significant way, is one of the advantages of thin section observations over QEMSCAN analysis.

Mineral abundances vs. point counting

Since the QEMSCAN measures the chemistry of each pixel and converts it into mineralogy, it can produce mineral abundance data in addition to element concentrations. The most traditional method of acquiring this data is through point counting, which is time-consuming and susceptible to misinterpretations by the operator. Also, with its 2.5 micron resolution, the QEMSCAN can analyse a sample with far greater resolution. This in turn reduces the risk involved in point counting of unintentionally introducing bias in the results through accidentally counting more of a certain mineral than what is proportionally correct. The QEMSCAN counts every pixel in the entire sample, which eliminates this risk completely. Graph 1 shows the relative concentrations of the most abundant minerals in the samples.

As long as the QEMSCAN can identify minerals accurately it is vastly superior to point counting. Compare the data from tables 6 and 9. The QEMSCAN identifies a larger number of minerals, most of which are too low in concentration or too small in size to be identified in thin section, and also bases this data on a much larger number of counts.

Table 12 is a comparison between the data acquired from the point counting and from the QEMSCAN. Since only a few minerals were identified in thin section during the point counting, the QEMSCAN data was renormalized to just those minerals. The two were then compared as a ratio.

*Table 12. Comparison of the point counting data and the QEMSCAN data for each mineral and sample in the form of ratios. The entries were assigned to groups for easier recognition. The groups are:
 A means that the mineral was found during point counting but not by the QEMSCAN.
 B means that the mineral was found by the QEMSCAN but not during point counting.
 Values of >1.15 (blue fields) means that 15% more of the mineral was found during point counting than by the QEMSCAN.
 Values of <0.85 (orange fields) means that 15% less of the mineral was found during point counting than by the QEMSCAN.
 Values of 0.85-1.15 (green fields) means that the same amount of mineral, plus or minus 15%, was found during both point counting and by the QEMSCAN.*

Mineral %	DL13 -01	DL13 -02	DL13 -03	DL13 -04	DL13 -05	DL13 -06	DL13 -07	DL13 -08a	DL13 -08b	DL13 -09	DL13 -10	DL13 -11	DL13 -12	DL13 -13
Quartz	0.19	B	0.03	0.11	B	0.03	0.32	0.06	B	0.14	0.30	0.03	B	0.06
Feldspar	3.14	B	3.93	1.65	2.64	1.95	1.82	1.22	1.45	4.28	3.56	0.12	0.68	A
Chlorite	B	B	1.64	B	0.46	1.00	B	0.12	1.89	1.75	3.00	0.04	B	2.20
Calcite	0.71	B	2.00	5.00	7.00	A	B	1	1.00	3.00	2.00	0.57	1.14	8.00
Epidote	A	B	A	B	4.00	0.50	2.50	0.50	B	A	A	B	12.00	B
Muscovite	0.17	B	B	A	A	B	B	B	A	B	B	A	B	B

As the comparison shows, the point counting data is quite far off from the QEMSCAN data. The quantity of each group found in table 12 is presented in table 13. In many cases there is

Table 13. Sums of the different entry types found in table 12.

Type	Quantity
A	10
B	26
>1.15	24
<0.85	11
0.85-1.15	11

a difference of several hundred percent between the QEMSCAN and the point counting data. Some of the more extreme differences though, for instance epidote in sample DL13-12, can be attributed to human error during the point counting; epidote might be mistaken for muscovite based on birefringence, and in the case of sample DL13-12 the QEMSCAN reported that muscovite was present but not a lot of epidote (after the data was corrected for the garnet misidentification), while the point counting data suggests the opposite.

Grain angularity

Measuring grain angularity with the QEMSCAN is not easily done. Grain sphericity can be measured rather easily by gangue busting each mineral one at a time and then measuring the shortest axis and the longest axis. By comparing these, grain sphericity can be derived. This method is not without errors though. Since each mineral is gangue busted one at a time, grains that have composite mineralogy or grains with several interlocking minerals will not be analysed as whole grains. Instead, each component mineral will be analysed as a grain on its own, which may be more irregular and angular than the actual grain. Also, grains that are touching each other as well as matrixes that contain the mineral will be counted as grains as well, and these are often highly irregular and angular. Both of these side effects introduce bias towards angular grains. The QEMSCAN grain sphericity data can be found in appendix D. The manual grain angularity measurements can be found in table 4.

This is grain sphericity data however, which is often related to angularity but cannot be used as a proxy or substitute for it. No angularity measurements could be generated during the QEMSCAN session, mostly due to lack of knowledge of the instruments capabilities. There might be ways to acquire grain angularity measurements from the QEMSCAN, but it was not found during this session. As grain angularity measurements were not generated, a comparison could not be done. However, a manual measurement of grain angularity using the mineral maps could possibly be done. Since grains are visible on the mineral maps, and since grains of a single mineral can be gangue busted, manual measurements can be made to roughly equal standards as the microphotograph method used in this study. A completely automated method would be preferable though.

Results and future potential

The QEMSCAN is overall a very useful tool that can generate many types of data, all useful for classifying rocks. It's greatest weakness is that the accuracy of the element concentration data is not equivalent to other methods currently in use, for instance XRF. When it comes to mineral identification there is still room for improvement, mainly mineral identification accuracy, but the QEMSCAN is already a very powerful tool that is especially useful for identifying minerals that are either too altered or too tiny to accurately identify under the petrographic microscope.

If the element concentration analysis could be refined and determined to acceptable standards and the SIP updated to be even more accurate for existing and new minerals, the QEMSCAN will truly be of great aid to the geoscience community. Fast and reliable data generation, extremely simple sample preparation in comparison to other instruments and the fact that a plethora of data including high-resolution SEM imaging can be acquired from a single instrument makes it extremely useful.

Accurate element identification and an improved SIP should make it possible to detect cryptic layering in crystals on a scale that is too fine for manual instruments and methods to detect. For this study, the samples were analysed at a 2.5 micron resolution, but they could have been analysed at a 1 micron resolution. Future versions of the QEMSCAN might have even higher resolution, and one of the greatest advantages of the QEMSCAN is its ability to generate accurate data with very high resolution, and to generate it very quickly.

It might even be possible that future versions of the QEMSCAN can be fitted with other types of EDS's and BSE detectors, and maybe other instruments as well. For instance, since the analysis chamber is put under vacuum, an ICP-MS could possibly be fitted to the QEMSCAN to allow for additional element concentration data.

Tectonic environment

The samples in this study are mostly volcanoclastic in origin and contain both volcanic glass and lithic clasts, which by definition makes them volcanoclastic. Whether they are reworked and transported or a primary deposit, as well as how and where they were formed, still needs to be determined.

The volcanoclastic samples share a number of traits: they contain volcanic glass, either sideromelane or palagonite, they contain chlorite, they contain quartz and feldspar, they are not vesiculated (with one exception), grain size usually varies, they are often heavily altered with most feldspar altering into sericite, and they contain calcite. Most grains are either subrounded/subangular or angular, though the spectra that the angularity classification was based on would generally be classified as subrounded-subangular. This suggests that the samples are relatively proximal.

The palagonite found in the samples is of an aqueous origin or have at least been deposited in an aqueous environment long enough for palagonite to form. The combination of chlorite and the lack of vesicles offer good insight into the type of aqueous formational environment. Vesicles are more easily formed in silicic, high-viscosity lava compared to mafic, low-viscosity lava, and most mafic minerals are quickly altered to chlorite. This suggests that the lava was mafic in origin, or possibly andesitic. The high concentrations of quartz and feldspar suggest otherwise, unless they are lithic clasts and not pyroclasts. The shape and size of the feldspars supports the theory that they are lithic clasts; while most feldspar was either rounded or subrounded-subangular, they were still relatively large and intact. Since chlorite was found in the sample, there is a good chance that mafic minerals such as pyroxene and possibly biotite was present in the sample, but that all of it is now altered into chlorite. It is known that feldspar is very quickly altered and weathered, so finding large amounts of feldspar in rather good shape while all the mafic minerals have weathered away seems contradictory. Also, palagonite is more common than sideromelane. While sideromelane alters into palagonite, it does so rather slowly unless at elevated

temperatures. Interaction between mafic lava and water can form palagonite directly, which might explain the higher amounts of palagonite. This supports the other observations that the lava was basaltic, or possibly andesitic.

The only observation speaking against this is sample DL13-03, which contains a glassy matrix that according to the QEMSCAN resembles quartz chemically. While the glass is not made up of pure silica SiO_2 , it has to contain a lot of silica for the QEMSCAN to identify it as quartz. This suggests that the lava that formed the glass was silica-rich, which in turn means that vesicles would likely be present, unless the lava was erupted below the PCL.

Tectonic environments where mafic or andesitic lava is erupted include spreading zones for mafic lava and island arcs for both mafic and andesitic lava. A spreading zone would most likely be located beneath the PCL, which the lack of vesicles in the samples supports. However, an island arc would also most likely be located beneath the PCL, at least initially.

The concentration of SiO_2 in the samples is rather high: around 55-60% in general. If all silica was provided by the lava and none from lithic clasts then a basaltic or even andesitic lava would be out of the question. However, since there are a lot of lithic clasts present the actual Si content for the lava is likely much lower than 55-60%. How much lower, and if it is basaltic or andesitic, is impossible to say without additional data.

Out of the 14 samples, DL13-01, 06, 07, 08b, 11 and 12 are volcanoclastic. Samples 03, 09 and 13 are not as definitive but are likely also volcanoclastic. Sample 10 might be a volcanoclastic but it exhibits a layering that is not seen in the other samples. Out of these samples, only DL13-03 has a silicic glass; the rest have matrixes made up of chlorite and other clays, such as montmorillonite, illite and muscovite/sericite. Taking crystal fractionation into account, sample DL13-03 could have been formed at an earlier or later stage during the formation of Jeanette Island, which could explain the different chemistry. Since spreading zones only erupt mafic lava and andesitic lava is indicative of island arcs, and assuming that sample DL13-03 is of the same origin as the rest of the samples on Jeanette Island, a spreading zone setting can be ruled out in favour of an island arc setting.

The remaining samples (DL13-02, 04, 05 and 08a) are not volcanoclastic but volcanic in origin. Samples DL13-02, 04 and 08a exhibit abundant feldspar laths, sometimes even microlaths, which are oriented in a general direction for sample 04 and in some regard sample 08a. All three samples have a clayey matrix consisting of chlorite, and in the case of sample 04: a lot of montmorillonite. Sample DL13-05 also contains a lot of montmorillonite. Montmorillonite is, like chlorite, a common alteration product in basaltic lava. These samples are thus likely to be basalts.

One section of sample DL13-04 is different from the rest of the sample. This section resembles samples DL13-06 and 07 most closely, both in thin section and the mineral map, and is clearly not part of the rest of sample 04. The boundary between its two parts is rich in chlorite and what appears to be quartz, although it's probably a silicic glass and not quartz crystals. Calcite is also present, and the margin is interlaced with calcite veinlets. Overall, the boundary appears to be a chill margin, such as those related to an intruding dike or sill, which further strengthens the suggestion that these samples are basaltic lava.

Conclusions

QEMSCAN is a new and interesting instrument that shows great potential as a tool for geoscientists in the future. It can generate multiple forms of data, including element concentrations, mineral maps, mineral abundances and SEM images. While it cannot fully compete with XRF yet, the mineral maps and mineral abundances are invaluable for work on fine-grained and altered samples. Since it is a relatively new instrument, it will certainly evolve and improve over time, and it could very well become the new standard instrument at every university.

During this study it proved very useful for identifying the mineralogy of the samples from Jeanette Island in the DeLong archipelago, and either complemented or completely replaced the data acquired through more traditional means. The samples were volcanoclastic, subaqueous, likely andesitic and likely formed under the pressure compensation level, which is around 500 meter below sea level for basaltic lavas. Island arcs are typically andesitic. The presence of non-volcanic particles also suggests an island arc setting since island arcs supply eroded terrestrial material.

Acknowledgements

I would like to thank Dr Jenny Omma, Dr Martin Rittner and Aukje Benedictus from Rocktype Ltd, who helped me with all things related to the QEMSCAN, and Victoria Pease, my supervisor from Stockholm University, who helped me on this thesis from start to finish.

References

- Bonatti, E., 1965: Palagonite, hyaloclastites and alteration of volcanic glass in the ocean. *Bulletin Volcanologique* 28, 257-269.
- Ericson, J. E., Makishima, A., Mackenzie, J. D. and Berger, R., 1975: Chemical and physical properties of obsidian: a naturally occurring glass. *Journal of Non-Crystalline Solids* 17, 129-142.
- Fisher, R. V. and Schmincke, H.-U., 1984: *Pyroclastic Rocks*. Springer Berlin Heidelberg New York Tokyo, pp 472.
- Fisher, R. V., 1961: Proposed Classification of Volcaniclastic Sediments and Rocks. *Geological Society of America Bulletin* 72, 1409-1414.
- Fisher, R. V., 1984: Submarine Volcaniclastic Rocks. Geological Society, London. *Special Publications* 16, 5-27.
- Kos'ko, M. and Korago, E., 2009: Review of geology of the New Siberian Islands between the Laptev and the East Siberian Seas, North East Russia. *Stephan Mueller Special Publication Series* 4, 45-69.
- McPhie, J., Doyle, M. and Allen, R., 1993: *Volcanic textures: A guide to the interpretation of textures in volcanic rocks*. Centre for Ore Deposit and Exploration Studies, University of Tasmania, pp 198.
- NHHC (Naval History and Heritage Command), 2015-06-03: A Lengthy Deployment: The Jeanette Expedition in Arctic Waters. (<http://www.history.navy.mil/research/library/online-reading-room/title-list-alphabetically/l/uss-jeannette-expedition.html>)
- Pease, V. and Tegner, C., 2014: The DeLong islands and Arctic tectonic reconstruction. *Geophysical research abstracts* 16: EGU2014-3345.
- Pease, V., 2011: Eurasian orogens and Arctic tectonics: an overview. In Spencer, A. M., Embry, A. F., Gautier, D. L., Stoupakova, A. V. and Sorensen, K. (eds.): *Arctic Petroleum Geology*. Geological Society, London. *Memoirs* 35, 311-324.
- Silvestri, S. C., 1963: Proposal for a genetic classification of hyaloclastites. *Bulletin Volcanologique* 25, 315-321.
- Sobolev, N. N., Metelkin, D. V., Vernikovskiy, V. A., Matyshkin, N. Yu., Prokop, A. V., Ershova, V. B., Shmanyak, A. V. and Petrov, E. O., 2014: The First Data on the Geology of Jeanette Island (De Long Archipelago, New Siberian Islands). *Doklady Earth Sciences*, 459, part 2, pp. 1504-1509.
- Thorarinsson, S., 1944: Tefrakronologiska Studier På Island. *Geografiska Annaler* 26, 1-217.
- Walker, G. P. L. and Blake, D. H., 1966: The formation of a palagonite breccia mass beneath a valley glacier in Iceland. *Quarterly Journal of the Geological Society* 122, 45-58.

Appendix A

Table of contents

“Traditional” methods **2**

Thin section descriptions 2

QEMSCAN data **7**

Mineral identification confidence 7

QEMSCAN oxide conversion factors 9

Metadata for XRF **13**

“Traditional” methods

Thin section descriptions

Tables DL13-01 to DL13-13. Thin section descriptions of the samples.

DL13-01	
Parameter	Definition
Mineralogy	Quartz, plagioclase, epidote in small amounts, muscovite in small amounts, opaques, palagonite
Crystal size:	Varying but mostly large
Crystal shape:	Varying shape, roundness and sphericity
Crystal surface textures:	Sericitation, possibly alteration into calcite
Crystal orientation:	No preferred
Matrix composition:	No matrix
Crystal/matrix abundance:	100/0
Vesicles/pore spaces:	None
Compositional variations:	Variation due to the sedimentary nature of the sample, but nothing else
Textural relationships:	None
Structures:	None
Bedding:	None
Sorting:	Rather poor

DL13-02	
Parameter	Definition
Mineralogy	Abundant plagioclase, quartz, chlorite, calcite, epidote, muscovite
Crystal size:	Small to medium
Crystal shape:	Felspar grains are subhedral (retain the tabular shape but with rounded corners), other grains are mostly anhedral
Crystal surface textures:	Dissolution and alteration of grains, chloritisation present, calcite alteration present
Crystal orientation:	No preferred
Matrix composition:	Mainly chlorite but some illite and muscovite is present as well
Crystal/matrix abundance:	75/25
Vesicles/pore spaces:	None
Compositional variations:	None
Textural relationships:	None
Structures:	None
Bedding:	None
Sorting:	Rather good
Other notes	A large portion of the matrix might actually be heavily altered feldspar and quartz (altered to chlorite), and this makes it difficult to accurately determine the abundance of matrix and crystals

DL13-03	
Parameter	Definition
Mineralogy	Calcite, possibly feldspar, abundant opaques, veinlets of chlorite
Crystal size:	Varying but an abundance of large crystals
Crystal shape:	Mostly anhedral but some are subhedral
Crystal surface textures:	Sericitation, minor chloritisation, extreme alteration of most crystals into clays and weathering products
Crystal orientation:	Crystals are somewhat oriented
Matrix composition:	Most of the matrix is comprised of opaques, which appears to be quartz or, more likely, silicic glass
Crystal/matrix abundance:	40/60
Vesicles/pore spaces:	None
Compositional variations:	Alteration seems to be random and does not seem to follow any specific paths or structures
Textural relationships:	Chlorite seems to be associated with calcite, but it is also present as veinlets shooting through the sample
Structures:	None
Bedding:	None
Sorting:	Rather poor

DL13-04	
Parameter	Definition
Mineralogy	Epidote, feldspar (probably plagioclase), calcite
Crystal size:	Small
Crystal shape:	Anhedral and rounded
Crystal surface textures:	Dissolution of boundaries
Crystal orientation:	Feldspar laths have a preferred orientation when present. Other grains seems to be similarly aligned as well.
Matrix composition:	Mainly chlorite and montmorillonite (smectite)
Crystal/matrix abundance:	10/90
Vesicles/pore spaces:	None
Compositional variations:	None
Textural relationships:	Chlorite is often present in large amounts on clasts due to alteration
Structures:	Chill margin present; rock on the other side of the chill margin has different mineralogy to the sample. The chill margin itself has calcite veinlets shooting through it at a normal angle to the margin boundary and also the crystal orientation direction. Chlorite is abundant in the chill margin.
Bedding:	Possibly some bedding
Sorting:	Good

DL13-05	
Parameter	Definition
Mineralogy	Feldspar (probably plagioclase) in laths, quartz, minor amounts of epidote, opaques
Crystal size:	Small
Crystal shape:	Anhedral
Crystal surface textures:	Dissolution of crystal boundaries, sericitation, possibly calcite alteration
Crystal orientation:	No preferred
Matrix composition:	Clays; mostly montmorillonite (smectite) but also some chlorite and minor amounts of kaolinite
Crystal/matrix abundance:	10/90
Vesicles/pore spaces:	None
Compositional variations:	Matrix dominated by montmorillonite but spatial variations do occur
Textural relationships:	None
Structures:	None
Bedding:	Possibly bedding in the form of alternating darker and lighter bands
Sorting:	Good

DL13-06	
Parameter	Definition
Mineralogy	Quartz, plagioclase, muscovite, epidote, calcite, opaques
Crystal size:	Varying but a lot of large crystals
Crystal shape:	Mostly anhedral but some are subhedral
Crystal surface textures:	Some chloritisation, extensive sericitation
Crystal orientation:	No preferred
Matrix composition:	Sericite, chlorite, illite and kaolinite
Crystal/matrix abundance:	50/50
Vesicles/pore spaces:	None
Compositional variations:	Variations between the large fragments
Textural relationships:	
Structures:	The sample is comprised of 2-5 large fragments of varying mineralogy
Bedding:	None
Sorting:	Very poor

DL13-07	
Parameter	Definition
Mineralogy	Quartz, plagioclase, epidote, chlorite
Crystal size:	Varying but mostly medium
Crystal shape:	Varying from anhedral to almost euhedral
Crystal surface textures:	Extensive sericitation of entire sample
Crystal orientation:	No preferred
Matrix composition:	Sericite and illite
Crystal/matrix abundance:	40/60
Vesicles/pore spaces:	None
Compositional variations:	The fragments have different mineralogy, shape, size, etc., suggesting different origins
Textural relationships:	None
Structures:	The sample is made up of 3-5 fragments
Bedding:	None
Sorting:	Poor sorting within the fragments

DL13-08a	
Parameter	Definition
Mineralogy	Feldspar, plagioclase, calcite, quartz, possibly some muscovite, abundant small opaques
Crystal size:	Feldspar present as small laths, quartz present as small rounded grains and calcite present as small to medium sized grains of varying shape. A few larger plagioclase laths are present as well
Crystal shape:	Feldspars are subhedral to euhedral, other grains anhedral to subhedral
Crystal surface textures:	Extensive chloritisation throughout the sample, possibly some minor sericitation as well
Crystal orientation:	Feldspar laths have a preferred orientation, other crystals share this orientation
Matrix composition:	Mostly chlorite with minor amounts of muscovite, illite and montmorillonite (smectite)
Crystal/matrix abundance:	85/15
Vesicles/pore spaces:	None
Compositional variations:	None
Textural relationships:	None
Structures:	None
Bedding:	None
Sorting:	Good

DL13-08b	
Parameter	Definition
Mineralogy	Plagioclase, calcite, quartz
Crystal size:	Varying
Crystal shape:	Varying but mostly anhedral to subhedral
Crystal surface textures:	Some sericitation and chloritisation present but not very extensive, also some dissolution of grain edges
Crystal orientation:	None
Matrix composition:	Mostly chlorite with minor amounts of muscovite
Crystal/matrix abundance:	90/10
Vesicles/pore spaces:	None
Compositional variations:	None
Textural relationships:	None
Structures:	None
Bedding:	None
Sorting:	Very poor

DL13-09	
Parameter	Definition
Mineralogy	Plagioclase, quartz, calcite, possibly epidote, muscovite
Crystal size:	Varying but abundant large grains
Crystal shape:	Mostly anhedral
Crystal surface textures:	Extensive sericitation
Crystal orientation:	No preferred
Matrix composition:	Mainly muscovite and chlorite
Crystal/matrix abundance:	95/5
Vesicles/pore spaces:	None
Compositional variations:	None
Textural relationships:	None
Structures:	None
Bedding:	None
Sorting:	Moderate

DL13-10	
Parameter	Definition
Mineralogy	Calcite, quartz, feldspar, abundant small opaques
Crystal size:	Very small
Crystal shape:	Plagioclase laths often more tabular, quartz and calcite more spherical
Crystal surface textures:	Sericitation of entire sample, dissolution and some alteration of grains, chloritisation of a calcite vein
Crystal orientation:	None
Matrix composition:	Illite and muscovite in moderate amounts, quartz seems to make up most of the matrix (as silica glass or silica gel)
Crystal/matrix abundance:	5/95
Vesicles/pore spaces:	None
Compositional variations:	Possibly some variation in mineralogy between layers (see bedding)
Textural relationships:	Chlorite possibly associated with calcite
Structures:	Calcite vein crossing through entire sample at an angle to the bedding
Bedding:	Alternating bands of finer and coarser material throughout sample
Sorting:	Good to very good (within each band)

DL13-11	
Parameter	Definition
Mineralogy	Calcite, quartz, plagioclase, epidote, palagonite
Crystal size:	Varying
Crystal shape:	Mostly rounded, rather low sphericity
Crystal surface textures:	Extensive alteration of entire sample into calcite, epidote, chlorite and possibly sericite
Crystal orientation:	None
Matrix composition:	Mainly chlorite with some muscovite and minor amounts of illite as well as palagonite
Crystal/matrix abundance:	80/20
Vesicles/pore spaces:	Yes. Vesicles filled with (presumably precipitated or secondary) calcite, quartz or plagioclase present in the sample. The vesicles are of varying size and some are undeformed while others are elongated/heavily deformed. The elongation direction varies. Some vesicles are more fresh than others/less alteration. The calcite filled ones are the least altered. Some of the vesicles filled with plagioclase are altered and contain some calcite, suggesting that plagioclase is altered into calcite.
Compositional variations:	Spatial variations in vesicle abundance
Textural relationships:	Palagonite surrounds vesicles, chlorite associated with the palagonite
Structures:	None ???
Bedding:	None
Sorting:	Very poor

DL13-12	
Parameter	Definition
Mineralogy	Quartz, feldspar, calcite, opaques of varying shape and size
Crystal size:	Medium
Crystal shape:	Rounded and anhedral and often with high sphericity
Crystal surface textures:	Sericitation over entire sample, some chloritisation
Crystal orientation:	No preferred
Matrix composition:	Mainly chlorite but some muscovite as well
Crystal/matrix abundance:	95/5
Vesicles/pore spaces:	None
Compositional variations:	None
Textural relationships:	None
Structures:	None
Bedding:	Possibly some bedding
Sorting:	Good

DL13-13	
Parameter	Definition
Mineralogy	Quartz, plagioclase, calcite, epidote, abundant opaques of varying shape and size
Crystal size:	Varying but mostly large and medium size
Crystal shape:	Mostly anhedral
Crystal surface textures:	Extensive sericitation and minor chloritisation
Crystal orientation:	No preferred
Matrix composition:	Mainly muscovite but also chlorite and minor amounts of illite
Crystal/matrix abundance:	90/10
Vesicles/pore spaces:	None
Compositional variations:	None
Textural relationships:	None
Structures:	None???
Bedding:	Bedding???
Sorting:	Poor

QEMSCAN data

Mineral identification confidence

Table I. Mineral identification confidence for the QEMSCAN.

Mineral Volume (%)	Identification confidence
Biotite	Good
Muscovite	Good; may include minor misidentifications with other K-Al silicates (e.g. illite, K-feldspar)
Annite-Phlogopite	Good, is essentially biotite
Rutile/Anatase/Brookite	Good, although polymorphs are not differentiated
Hematite/Magnetite/Ilmenite	Very difficult to differentiate magnetite and hematite; ilmenite is easily identified
Calcite	Good, includes aragonite
Dolomite-Ankerite group	Good
Pyrite	Good
Apatite	Good
Zircon	Good
Titanite	Good
Tourmaline group	Poor, is often classed as Mg rich kaolinite. We're working on this.
Garnet group	Wide range of compositions in garnet group. Some garnet compositions are very close to other silicates, which may cause misclassifications/misidentifications. E.g. grossular garnet is very similar to epidote
Staurolite	Good
Sillimanite/Kyanite/Andalusite	Good
Epidote group	Moderate. Epidote composition very similar to grossular garnet. Zoisite and allanite compositions should be good
K-Feldspar group	Good; may include minor misidentifications with other K-Al silicates (predominantly illite, minor muscovite)
Albite	Good; although composition close to jadeite and jadeite may be misidentified as albite
Plagioclase group	Good
Chlorite group	Good-moderate
Chloritoid	Untested
Olivine	Good
Orthopyroxenes	Good-moderate; may be minor misidentification of olivine cracks as OPX; may be misidentified as talc
Clinopyroxenes	Moderate. Range of compositions; may be similar in composition to Ca-amphiboles and some misidentification expected
Calcic amphiboles	Moderate. Wide range of compositions; may be similar in composition to CPX and some misidentification expected
Sodic amphiboles	Poor, is often characterised as lots of different silicate phases
Fe-Mg-Mn amphiboles	Poor, is often characterised as lots of different silicate phases
Kaolinite/Dickite (S)	Impure kaolinite definitions may capture other phases, such as tourmaline
Glauconite	Untested
Montmorillonite/Smectite group	Wide range of compositions; difficult
Barite	Good
Halides	Good
Fe Oxides	Very difficult to differentiate magnetite and hematite under non-optimal conditions; mag/hem vs goethite and siderite should be differentiated well. Siderite vs goethite can be difficult as well
Quartz	Good
Illite	Moderate. may include minor misidentifications with other K-Al silicates (especially K-feldspar); can contain impurities, which may cause misidentification/overlap with other silicates
Gypsum/Anhydrite	Good. Impossible to differentiate gypsum from anhydrite

Siderite	Can be difficult to differentiate from goethite (and mag/hem to lesser extent)
Spinel group	Should be good, but wide range of possible compositions, so need to be added to the SIP to cover range (most common?)
Other sulphates/sulphides	Combination of high-confidence phases of very low concentrations, boundary textures and poorly identified phases
Other phosphates	Combination of high-confidence phases of very low concentrations, boundary textures and poorly identified phases
Other oxides	Combination of high-confidence phases of very low concentrations, boundary textures and poorly identified phases
Other silicates	Combination of high-confidence phases of very low concentrations, boundary textures and poorly identified phases
Other carbonates	Combination of high-confidence phases of very low concentrations, boundary textures and poorly identified phases
Other sheet silicates	As classification is based on chemistry, poor-moderate confidence these are sheet silicates vs other silicates
Pores	Good; may include organic matter
Other	Combination of high-confidence phases of very low concentrations, boundary textures and poorly identified phases
Low Confidence	Poor confidence due to poor match of spectral engine with raw measurement spectrum. Can be investigated offline and potentially included in SIP
Unclassified	Unclassified measurement points - can become classified phases/textures through SIP development

QEMSCAN oxide conversion factors

Table II. Oxide conversion factors for the QEMSCAN. The QEMSCAN uses these conversion factors to determine the amount of element oxides in the sample based on the amount of each element in its non-oxide form.

Symbol	Atomic Weight	Oxide conversion	# Element	# Oxygen	Oxide Weight	Element weight	Calculated Oxide conversion	Match
H	1,0079	0,1119	2	1	18,0152	2,0158	0,1118944	SANT
He	4,0026	1						
Li	6,941	0,4645	2	1	29,8814	13,882	0,464569933	SANT
Be	9,0122	0,3603	1	1	25,0116	9,0122	0,360320811	SANT
B	10,811	0,3106	2	3	69,6202	21,622	0,310570783	SANT
C	12,0107	0,2729	1	2	44,0095	12,0107	0,27291153	SANT
N	14,0067	0,2594	2	5	108,0104	28,0134	0,259358358	SANT
O	15,9994	0						
F	18,9984	1						
Ne	20,1797	1						
Na	22,9898	0,7419	2	1	61,979	45,9796	0,741857726	SANT
Mg	24,305	0,6031	1	1	40,3044	24,305	0,603035897	SANT
Al	26,9815	0,5293	2	3	101,9612	53,963	0,529250342	SANT
Si	28,0855	0,4674	1	2	60,0843	28,0855	0,467434921	SANT
P	30,9738	0,4364	2	5	141,9446	61,9476	0,43642097	SANT
S	32,066	0,4005	1	3	80,0642	32,066	0,400503596	SANT
Cl	35,4527	1						
Ar	39,948	1						

Cr	51,9961	0,6842	2	3	151,9904	103,9922	0,684202423	SANT
Mn	54,938	0,7745	2	2	141,8748	109,876	0,774457479	SANT
Fe	55,845	0,6994	2	3	159,6882	111,69	0,699425505	SANT
Co	58,9332	0,7865	1	1	74,9326	58,9332	0,786482786	SANT
Ni	58,6934	0,7858	1	1	74,6928	58,6934	0,785797292	SANT
Cu	63,546	0,7989	1	1	79,5454	63,546	0,798864548	SANT
Zn	65,39	0,8034	1	1	81,3894	65,39	0,803421576	SANT
Ga	69,723	0,7439	2	3	187,4442	139,446	0,743933395	SANT
Ge	72,61	0,6941	1	2	104,6088	72,61	0,694109865	SANT
As	74,9216	0,7574	2	3	197,8414	149,8432	0,757390516	SANT
Se	78,96	0,6219	1	3	126,9582	78,96	0,621936984	SANT
Br	79,904	1						
Kr	83,8	1						
Rb	85,4678	0,914	2	1	186,935	170,9356	0,914411961	SANT
Sr	87,62	0,8456	1	1	103,6194	87,62	0,845594551	SANT
Y	88,9059	0,7874	2	3	225,81	177,8118	0,787439883	SANT
Zr	91,224	0,7403	1	2	123,2228	91,224	0,740317539	SANT
Nb	92,9064	0,699	2	5	265,8098	185,8128	0,699044204	SANT
Mo	95,94	0,6665	1	3	143,9382	95,94	0,666536055	SANT
Tc	-98	1						
Ru	101,07	1						
Rh	102,9055	1						
Pd	106,42	1						
Ag	107,8682	0,931	2	1	231,7358	215,7364	0,930958445	SANT
Cd	112,411	0,8754	1	1	128,4104	112,411	0,875404173	SANT
In	114,818	0,8271	2	3	277,6342	229,636	0,82711712	SANT
Sn	118,71	0,7877	1	2	150,7088	118,71	0,787677959	SANT
Sb	121,76	0,8353	2	3	291,5182	243,52	0,835350932	SANT
Te	127,6	0,7995	1	2	159,5988	127,6	0,799504758	SANT
I	126,9045	0,7604	2	5	333,806	253,809	0,760348825	SANT
Xe	131,29	1						
Cs	132,9055	0,9432	2	1	281,8104	265,811	0,943226368	SANT
Ba	137,327	0,8957	1	1	153,3264	137,327	0,895651369	SANT
La	138,9055	0,8527	2	3	325,8092	277,811	0,852680035	SANT

Ce	140,116	0,8538	2	3	328,2302	280,232	0,853766655	SANT
Pr	140,9076	0,8545	2	3	329,8134	281,8152	0,854468618	SANT
Nd	144,24	0,8574	2	3	336,4782	288,48	0,857351234	SANT
Pm	-145	0,8594						
Sm	150,36	0,8624	2	3	348,7182	300,72	0,862358202	SANT
Eu	151,964	0,8636	2	3	351,9262	303,928	0,863612882	SANT
Gd	157,25	0,8676	2	3	362,4982	314,5	0,867590515	SANT
Tb	158,9253	0,8688	2	3	365,8488	317,8506	0,868803178	SANT
Dy	162,5	0,8713	2	3	372,9982	325	0,871317878	SANT
Ho	164,9303	0,873	2	3	377,8588	329,8606	0,872973185	SANT
Er	167,26	0,8745	2	3	382,5182	334,52	0,87452048	SANT
Tm	168,9342	0,8756	2	3	385,8666	337,8684	0,875609343	SANT
Yb	173,04	0,8782	2	3	394,0782	346,08	0,878201332	SANT
Lu	174,967	0,8794	2	3	397,9322	349,934	0,87938096	SANT
Hf	178,49	0,848	1	2	210,4888	178,49	0,84797861	SANT
Ta	180,9479	0,819	2	5	441,8928	361,8958	0,818967406	SANT
W	183,84	0,8518	1	2	215,8388	183,84	0,851746767	SANT
Re	186,207	0,8534	1	2	218,2058	186,207	0,853354952	SANT
Os	190,23	1						
Ir	192,217	1						
Pt	195,078	1						
Au	196,9666	0,961	2	1	409,9326	393,9332	0,960970657	SANT
Hg	200,59	0,9261	1	1	216,5894	200,59	0,926130272	SANT
Tl	204,3833	0,8949	2	3	456,7648	408,7666	0,894917034	SANT
Pb	207,2	0,9283	1	1	223,1994	207,2	0,928317908	SANT
Bi	208,9804	0,897	2	3	465,959	417,9608	0,896990508	SANT
Po	-209	0,814						
At	-210	0,7895						
Rn	-222	1						
Fr	-223	0,9654						
Ra	226,025	0,9339	1	1	242,0244	226,025	0,933893442	SANT
Ac	227,028	0,9044	2	3	502,0542	454,056	0,904396378	SANT
Th	232,0381	0,8788	1	2	264,0369	232,0381	0,878809363	SANT
Pa	231,0359	0,9059	2	3	510,07	462,0718	0,905898798	SANT

U	238,0289	0,848	3	8	842,0819	714,0867	0,848001483	SANT
Np	237,048	0						
Pu	-244	0						
Am	-243	0						
Cm	-247	0						
Bk	-247	0						
Cf	-251	0						
Es	-252	0						
Fm	-257	6,5						
Md	-258	6,58						
No	-259	6,65						
Lr	-260	0						
Rf	0	0						
Ha	0	0						
Sg	0	0						
Ns	0	0						
Hs	0	0						
Mt	0	0						

Metadata for XRF

Table III. Stockholm University preferred values for International Standards utilised during calibration

standard name		AGV-1	MRG-1	AGV-2	BCR-2	GSP-2	RGM-1	SARM-1	SARM-3	SARM-6	GS-N	GA	AN-G	W-2	PCC-1	DTS-1	GS-2	SY-2	JB-1b	JB-2	JA-2	JG-2	JR-3	NBS 278	NBS 688
		USGS	USGS	USGS	USGS	USGS	USGS	SARM						USGS	USGS	USGS	USGS	CCRM P						NIST	NIST
SiO ₂	mass %	58.84		59.3	54.1	66.6	73.4	75.7	52.24	38.5					41.71	40.41		49.9	51.11	53.25	56.42	76.83	72.76	72.97	48.35
Al ₂ O ₃	mass %	17.15		16.91	13.5	14.9	13.7	12.08	13.64	0.22					0.675	0.19		20.69	14.38	14.64	15.41	12.47	11.9	14.15	17.35
CaO	mass %	4.94		5.2	7.12	2.1	1.15	0.78	3.22	0.29					0.52	0.17		8.05	9.6	9.82	6.29	0.7	0.093	0.983	12.17
MgO	mass %	1.53		1.79	3.59	0.96	0.28		0.28	43.2					43.43	49.59		0.54	8.14	4.62	7.6	0.037	0.05	0.23	8.46
MnO	mass %	0.1		0.1			0.036		0.77	0.22						0.12		0.108	0.147	0.218	0.108	0.016	0.083	0.052	0.167
P ₂ O ₅	mass %	0.5		0.48	0.35	0.29	0.07		0.06	0.01						0.002		0.131	0.256	0.101	0.146	0.002	0.017	0.036	0.133
Fe ₂ O ₃	mass %	6.77		6.69	13.8	4.9	1.86		9.96	16.79					8.25	8.68		6.21	9.02	14.25	6.21	0.97	4.72	2.04	10.34
Na ₂ O	mass %	4.26		4.19	3.16	2.78	4.07		8.37	0.03						0.01		7.1	2.63	2.04	3.11	3.54	4.69	4.84	2.16
K ₂ O	mass %	2.92		2.88	1.79	5.38	4.3	4.99	5.51	0.01						0.001		1.66	1.32	0.42	1.81	4.71	4.29	4.16	0.19
TiO ₂	mass %	1.05		1.05	2.26	0.66	0.27		0.48	0.02						0.005		0.287	1.26	1.19	0.66	0.044	0.21	0.245	1.168
Total		98.06	0	98.59	99.67	98.57	99.136	93.55	94.53	99.29	0	0	0	0	94.585	99.178	0	94.676	97.863	100.549	97.764	99.319	98.813	99.706	100.488
SiO ₂	mass %	60.01	39.72	60.15	54.17	67.57	74.04	76.47	55.34	38.84	66.85	70.75	46.68	52.48	44.02	40.74	69.76	52.71	52.23	52.96	57.71	77.36	73.63	73.19	48.12
Al ₂ O ₃	mass %	17.49	8.65	17.15	13.52	15.12	13.82	12.20	14.40	0.30	14.90	14.68	30.04	15.39	0.71	0.19	15.53	21.85	14.69	14.56	15.76	12.56	12.04	14.19	17.27
CaO	mass %	5.04	14.84	5.27	7.13	2.13	1.16	0.79	3.40	0.28	2.54	2.48	16.03	10.82	0.55	0.17	1.98	8.50	9.81	9.77	6.43	0.70	0.09	0.99	12.11

MgO	mass %	1.56	13.69	1.82	3.59	0.97	0.28	0.06	0.30	43.38	2.34	0.96	1.81	6.35	45.83	50.00	0.76	0.57	8.32	4.59	7.77	0.04	0.05	0.23	8.42
MnO	mass %	0.1	0.17	0.10	0.20	0.00	0.04	0.02	0.81	0.22	0.06	0.09	0.04	0.17	0.13	0.12	0.03	0.11	0.15	0.22	0.11	0.02	0.08	0.05	0.17
P2O5	mass %	0.51	0.06	0.49	0.35	0.29	0.07	0.01	0.06	0.01	0.28	0.12	0.01	0.13	0.00	0.00	0.14	0.14	0.26	0.10	0.15	0.00	0.02	0.04	0.13
Fe2O3	mass %	6.9	18.12	6.79	13.82	4.97	1.88	1.91	10.52	16.91	3.81	2.86	3.39	10.79	8.71	8.75	2.68	6.56	9.22	14.17	6.35	0.98	4.78	2.05	10.29
Na2O	mass %	4.34	0.75	4.25	3.16	2.82	4.11	3.41	8.84	0.04	3.83	3.59	1.64	2.19	0.03	0.01	4.12	7.50	2.69	2.03	3.18	3.56	4.75	4.85	2.15
K2O	mass %	2.98	0.17	2.92	1.79	5.46	4.34	5.04	5.82	0.01	4.70	4.08	0.13	0.62	0.01	0.00	4.52	1.75	1.35	0.42	1.85	4.74	4.34	4.17	0.19
TiO2	mass %	1.07	3.83	1.07	2.26	0.67	0.27	0.09	0.51	0.02	0.69	0.38	0.22	1.06	0.01	0.01	0.48	0.30	1.29	1.18	0.68	0.04	0.21	0.25	1.16
Ce	ppm	68	26	68	53	410	47	195	286	0	135	76	5	23	0	0	160	122		7	33	48	327	62	13
La	ppm	38	10	38	25	180	24	109	250	0	75	40	2	11	0	0	89	58		2	16	20	179	32	5
Th	ppm	6	1	6	6	105	15	51	66	1	41	17	0	2	0	0	25	1		0	5	2	112	12	0
Ni	ppm	16	193	19	18	17	4	2	11	2050	34	7	35	72	2380	2360	5	9	148	17	130	4		4	150
V	ppm	119	526	120	416	52	13	81	81	40	65	38	70	268	31	11	36	8	214	575	126	4	4	9	250
Ba	ppm	1200	61	1140	677	1340	810	120	450	10	1400	840	34	172	1	2	1880	340		222	321	81	66	1140	200
Cr	ppm	9	430	17	18	20	4	12	10	2900	55	12	50	93	2730	3990	9	12	439	28	436	6	4	6	332
Cu	ppm	58	134	53	21	43	12	12	13	10	20	16	19	105	10	7	11	7	56	225	30	0	3	6	96
Ga	ppm	20	17	20	23	22	15	27	54	0	22	16	18	18	1	1	23	35		17	17	19	37	13	18
Hf	ppm	5	4	5	5	14	6	12	190	0	6	4	0	2	0	0	8	11		1	3	5	40	8	2
Nb	ppm	15	20	15	13	27	9	53	960	0	21	12	1	8	1	2	12	13		2	9	15	510	18	6
Pb	ppm	37	10	13	11	42	24	40	43	7	53	30	2	8	10	12	30	10	7	5	19	32	33	16	3
Rb	ppm	67	9	69	47	245	150	325	190	0	185	175	1	21	0	0	170	55	39	7	73	301	453	128	2
Sr	ppm	660	266	658	340	240	110	10	4600	3	570	310	76	196	0	0	478	1191	439	178	248	18	10	64	169
Y	ppm	19	14	20	37	28	25	143	22	0	16	21	8	22	0	0	11	119		25	18	87	166	39	19
Zr	ppm	231	108	230	184	550	220	300	1100	20	235	150	11	92	10	0	309	517		51	116	98	1494	290	59

Table IV. Mean of Relative Deviation (RD%) from 25th June to 5th October 2008

	AGV 2	BCR 2	RGM 1		meanRD (Weighted)
SiO ₂	-0.08	-0.02	-0.40		-0.12
Al ₂ O ₃	-0.10	0.07	-0.02		-0.03
CaO	-0.62	-1.34	7.17		0.67
MgO	-0.44	0.42	4.82		0.82
MnO	0.23	2.24	-6.51		-0.49
P ₂ O ₅	5.13	-1.19	12.33		4.69
Fe ₂ O ₃	0.75	0.50	6.53		1.79
Na ₂ O	0.62	1.10	1.14		0.86
K ₂ O	0.35	-1.66	0.56		-0.19
TiO ₂	-0.56	0.21	0.06		-0.22
Ce	-3.05	-0.52	1.91		-1.37
La	-2.73	-9.64	7.08		-2.84
Th	8.68	-16.67	-7.33		-1.71
Ni	-3.12	-72.22	97.73		-3.66
V	1.23	-0.09	1.54		0.91
Ba	-0.40	-0.39	1.09		-0.11
Cr	6.10	83.33			27.21
Cu	-2.31	-32.74	3.33		-10.00
Ga	3.52	-15.76	18.00		0.74
Hf	4.26	14.80	-14.52		3.69
Nb	-11.60	1.19	-10.11		-7.63
Pb	4.56	-5.68	0.42		0.81
Rb	-0.82	-3.52	0.47		-1.35
Sr	1.23	-3.09	-6.45		-1.49
Y	-9.81	-19.59	5.60		-9.67
Zr	-3.75	0.48	-3.45		-2.48
n	27	15	10		52

Table V. Coefficients of Variation (CV%) from 25th June to 25th September 2008

	AGV 2	BCR 2	RGM 1	Argent,in Pease, 1997	Lee & McConchie, 1982
SiO ₂	0.07	0.09	0.06	0.07	0.13
Al ₂ O ₃	0.54	0.47	0.54	0.10	0.16
CaO	0.48	0.36	0.46	0.16	0.12
MgO	0.53	0.45	2.70	0.85	0.78
MnO	0.56	0.40	2.58	1.10	2.10
P ₂ O ₅	1.67	2.43	9.65	1.15	0.10
Fe ₂ O ₃	0.61	0.27	2.56	0.15	0.16
Na ₂ O	0.38	0.68	0.36	0.49	1.40
K ₂ O	0.41	0.58	0.30	0.14	0.14
TiO ₂	0.32	0.17	0.32	0.34	0.19
Ce	6.77	9.54	6.34		
La	5.88	11.51	12.04		
Th	10.37	12.03	4.08	4.80	
Ni	6.26	24.80	7.76	1.70	
V	2.01	0.84	9.97	2.40	4.30
Ba	0.41	0.68	0.87	0.60	0.50
Cr	4.21	8.82		3.40	
Cu	3.72	38.20	12.72	3.80	12.70
Ga	4.98	5.34	5.36	1.50	2.40
Hf	38.42	52.01	30.88		
Nb	4.95	7.72	8.33	4.10	
Pb	5.86	12.47	3.63	4.50	9.10
Rb	1.12	1.42	0.77	0.60	4.50
Sr	0.74	0.63	1.07	0.30	1.00
Y	11.96	13.54	1.96	4.50	13.00
Zr	1.67	4.15	3.22	0.30	2.20
n	27	15	10		

Table VI. Counts per second per unit of concentration for 2 standards.

	AGV 2 cps/weight% or cps/ppm	BCR 2 cps/weight% or cps/ppm	Lower limit of accurate detection Weight% (*) or ppm
Si-K α	14405	14349	0.032 *
Al-K α	15767	15424	0.078 *
Ca-K α	28331	29514	0.012 *
Mg-K α	3815	3791	0.075 *
Mn-K α	61543	59028	0.001 *
P-K α	34071	33508	0.031 *
Fe-K α	70470	68800	0.004 *
Na-K α	2536	2530	0.233 *
K-K α	124059	125228	0.021 *
Ti-K α	19070	19672	0.001 *
Ce-L β 1	0.64	0.61	10
La-L α	1.09	0.85	10
Th-L α	15.64	12.68	5
Ni-K α	29.64	22.53	15
V-K α	4.06	3.66	10
Ba-L α	0.54	0.60	15
Cr-K α	23.74	29.76	10
Cu-K α	15.12	19.70	10
Ga-K α	15.61	11.34	10
Hf-L α	4.21	1.35	5
Nb-K α	43.15	35.10	5
Pb-L β 1	20.28	13.93	5
Rb-K α	34.90	28.65	5
Sr-K α	39.32	31.52	5
Y-K α	94.10	51.25	10
Zr-K α	61.20	46.34	5

Appendix A

Table of contents

“Traditional” methods..... 2

Thin section descriptions 2

QEMSCAN data..... 7

Mineral identification confidence..... 7

QEMSCAN oxide conversion factors 9

Metadata for XRF 13

“Traditional” methods

Thin section descriptions

Tables DL13-01 to DL13-13. Thin section descriptions of the samples.

DL13-01	
Parameter	Definition
Mineralogy	Quartz, plagioclase, epidote in small amounts, muscovite in small amounts, opaques, palagonite
Crystal size:	Varying but mostly large
Crystal shape:	Varying shape, roundness and sphericity
Crystal surface textures:	Sericitation, possibly alteration into calcite
Crystal orientation:	No preferred
Matrix composition:	No matrix
Crystal/matrix abundance:	100/0
Vesicles/pore spaces:	None
Compositional variations:	Variation due to the sedimentary nature of the sample, but nothing else
Textural relationships:	None
Structures:	None
Bedding:	None
Sorting:	Rather poor

DL13-02	
Parameter	Definition
Mineralogy	Abundant plagioclase, quartz, chlorite, calcite, epidote, muscovite
Crystal size:	Small to medium
Crystal shape:	Feldspar grains are subhedral (retain the tabular shape but with rounded corners), other grains are mostly anhedral
Crystal surface textures:	Dissolution and alteration of grains, chloritisation present, calcite alteration present
Crystal orientation:	No preferred
Matrix composition:	Mainly chlorite but some illite and muscovite is present as well
Crystal/matrix abundance:	75/25
Vesicles/pore spaces:	None
Compositional variations:	None
Textural relationships:	None
Structures:	None
Bedding:	None
Sorting:	Rather good
Other notes	A large portion of the matrix might actually be heavily altered feldspar and quartz (altered to chlorite), and this makes it difficult to accurately determine the abundance of matrix and crystals

DL13-03	
Parameter	Definition
Mineralogy	Calcite, possibly feldspar, abundant opaques, veinlets of chlorite
Crystal size:	Varying but an abundance of large crystals
Crystal shape:	Mostly anhedral but some are subhedral
Crystal surface textures:	Sericitation, minor chloritisation, extreme alteration of most crystals into clays and weathering products
Crystal orientation:	Crystals are somewhat oriented
Matrix composition:	Most of the matrix is comprised of opaques, which appears to be quartz or, more likely, silicic glass
Crystal/matrix abundance:	40/60
Vesicles/pore spaces:	None
Compositional variations:	Alteration seems to be random and does not seem to follow any specific paths or structures
Textural relationships:	Chlorite seems to be associated with calcite, but it is also present as veinlets shooting through the sample
Structures:	None
Bedding:	None
Sorting:	Rather poor

DL13-04	
Parameter	Definition
Mineralogy	Epidote, feldspar (probably plagioclase), calcite
Crystal size:	Small
Crystal shape:	Anhedral and rounded
Crystal surface textures:	Dissolution of boundaries
Crystal orientation:	Feldspar laths have a preferred orientation when present. Other grains seems to be similarly aligned as well.
Matrix composition:	Mainly chlorite and montmorillonite (smectite)
Crystal/matrix abundance:	10/90
Vesicles/pore spaces:	None
Compositional variations:	None
Textural relationships:	Chlorite is often present in large amounts on clasts due to alteration
Structures:	Chill margin present; rock on the other side of the chill margin has different mineralogy to the sample. The chill margin itself has calcite veinlets shooting through it at a normal angle to the margin boundary and also the crystal orientation direction. Chlorite is abundant in the chill margin.
Bedding:	Possibly some bedding
Sorting:	Good

DL13-05	
Parameter	Definition
Mineralogy	Feldspar (probably plagioclase) in laths, quartz, minor amounts of epidote, opaques
Crystal size:	Small
Crystal shape:	Anhedral
Crystal surface textures:	Dissolution of crystal boundaries, sericitation, possibly calcite alteration
Crystal orientation:	No preferred
Matrix composition:	Clays; mostly montmorillonite (smectite) but also some chlorite and minor amounts of kaolinite
Crystal/matrix abundance:	10/90
Vesicles/pore spaces:	None
Compositional variations:	Matrix dominated by montmorillonite but spatial variations do occur
Textural relationships:	None
Structures:	None
Bedding:	Possibly bedding in the form of alternating darker and lighter bands
Sorting:	Good

DL13-06	
Parameter	Definition
Mineralogy	Quartz, plagioclase, muscovite, epidote, calcite, opaques
Crystal size:	Varying but a lot of large crystals
Crystal shape:	Mostly anhedral but some are subhedral
Crystal surface textures:	Some chloritisation, extensive sericitation
Crystal orientation:	No preferred
Matrix composition:	Sericite, chlorite, illite and kaolinite
Crystal/matrix abundance:	50/50
Vesicles/pore spaces:	None
Compositional variations:	Variations between the large fragments
Textural relationships:	
Structures:	The sample is comprised of 2-5 large fragments of varying mineralogy
Bedding:	None
Sorting:	Very poor

DL13-07	
Parameter	Definition
Mineralogy	Quartz, plagioclase, epidote, chlorite
Crystal size:	Varying but mostly medium
Crystal shape:	Varying from anhedral to almost euhedral
Crystal surface textures:	Extensive sericitation of entire sample
Crystal orientation:	No preferred
Matrix composition:	Sericite and illite
Crystal/matrix abundance:	40/60
Vesicles/pore spaces:	None
Compositional variations:	The fragments have different mineralogy, shape, size, etc., suggesting different origins
Textural relationships:	None
Structures:	The sample is made up of 3-5 fragments
Bedding:	None
Sorting:	Poor sorting within the fragments

DL13-08a	
Parameter	Definition
Mineralogy	Feldspar, plagioclase, calcite, quartz, possibly some muscovite, abundant small opaques
Crystal size:	Feldspar present as small laths, quartz present as small rounded grains and calcite present as small to medium sized grains of varying shape. A few larger plagioclase laths are present as well
Crystal shape:	Feldspars are subhedral to euhedral, other grains anhedral to subhedral
Crystal surface textures:	Extensive chloritisation throughout the sample, possibly some minor sericitation as well
Crystal orientation:	Feldspar laths have a preferred orientation, other crystals share this orientation
Matrix composition:	Mostly chlorite with minor amounts of muscovite, illite and montmorillonite (smectite)
Crystal/matrix abundance:	85/15
Vesicles/pore spaces:	None
Compositional variations:	None
Textural relationships:	None
Structures:	None
Bedding:	None
Sorting:	Good

DL13-08b	
Parameter	Definition
Mineralogy	Plagioclase, calcite, quartz
Crystal size:	Varying
Crystal shape:	Varying but mostly anhedral to subhedral
Crystal surface textures:	Some sericitation and chloritisation present but not very extensive, also some dissolution of grain edges
Crystal orientation:	None
Matrix composition:	Mostly chlorite with minor amounts of muscovite
Crystal/matrix abundance:	90/10
Vesicles/pore spaces:	None
Compositional variations:	None
Textural relationships:	None
Structures:	None
Bedding:	None
Sorting:	Very poor

DL13-09	
Parameter	Definition
Mineralogy	Plagioclase, quartz, calcite, possibly epidote, muscovite
Crystal size:	Varying but abundant large grains
Crystal shape:	Mostly anhedral
Crystal surface textures:	Extensive sericitation
Crystal orientation:	No preferred
Matrix composition:	Mainly muscovite and chlorite
Crystal/matrix abundance:	95/5
Vesicles/pore spaces:	None
Compositional variations:	None
Textural relationships:	None
Structures:	None
Bedding:	None
Sorting:	Moderate

DL13-10	
Parameter	Definition
Mineralogy	Calcite, quartz, feldspar, abundant small opaques
Crystal size:	Very small
Crystal shape:	Plagioclase laths often more tabular, quartz and calcite more spherical
Crystal surface textures:	Sericitation of entire sample, dissolution and some alteration of grains, chloritisation of a calcite vein
Crystal orientation:	None
Matrix composition:	Illite and muscovite in moderate amounts, quartz seems to make up most of the matrix (as silica glass or silica gel)
Crystal/matrix abundance:	5/95
Vesicles/pore spaces:	None
Compositional variations:	Possibly some variation in mineralogy between layers (see bedding)
Textural relationships:	Chlorite possibly associated with calcite
Structures:	Calcite vein crossing through entire sample at an angle to the bedding
Bedding:	Alternating bands of finer and coarser material throughout sample
Sorting:	Good to very good (within each band)

DL13-11	
Parameter	Definition
Mineralogy	Calcite, quartz, plagioclase, epidote, palagonite
Crystal size:	Varying
Crystal shape:	Mostly rounded, rather low sphericity
Crystal surface textures:	Extensive alteration of entire sample into calcite, epidote, chlorite and possibly sericite
Crystal orientation:	None
Matrix composition:	Mainly chlorite with some muscovite and minor amounts of illite as well as palagonite
Crystal/matrix abundance:	80/20
Vesicles/pore spaces:	Yes. Vesicles filled with (presumably precipitated or secondary) calcite, quartz or plagioclase present in the sample. The vesicles are of varying size and some are undeformed while others are elongated/heavily deformed. The elongation direction varies. Some vesicles are more fresh than others/less alteration. The calcite filled ones are the least altered. Some of the vesicles filled with plagioclase are altered and contain some calcite, suggesting that plagioclase is altered into calcite.
Compositional variations:	Spatial variations in vesicle abundance
Textural relationships:	Palagonite surrounds vesicles, chlorite associated with the palagonite
Structures:	None ???
Bedding:	None
Sorting:	Very poor

DL13-12	
Parameter	Definition
Mineralogy	Quartz, feldspar, calcite, opaques of varying shape and size
Crystal size:	Medium
Crystal shape:	Rounded and anhedral and often with high sphericity
Crystal surface textures:	Sericitation over entire sample, some chloritisation
Crystal orientation:	No preferred
Matrix composition:	Mainly chlorite but some muscovite as well
Crystal/matrix abundance:	95/5
Vesicles/pore spaces:	None
Compositional variations:	None
Textural relationships:	None
Structures:	None
Bedding:	Possibly some bedding
Sorting:	Good

DL13-13	
Parameter	Definition
Mineralogy	Quartz, plagioclase, calcite, epidote, abundant opaques of varying shape and size
Crystal size:	Varying but mostly large and medium size
Crystal shape:	Mostly anhedral
Crystal surface textures:	Extensive sericitation and minor chloritisation
Crystal orientation:	No preferred
Matrix composition:	Mainly muscovite but also chlorite and minor amounts of illite
Crystal/matrix abundance:	90/10
Vesicles/pore spaces:	None
Compositional variations:	None
Textural relationships:	None
Structures:	None???
Bedding:	Bedding???
Sorting:	Poor

QEMSCAN data

Mineral identification confidence

Table I. Mineral identification confidence for the QEMSCAN.

Mineral Volume (%)	Identification confidence
Biotite	Good
Muscovite	Good; may include minor misidentifications with other K-Al silicates (e.g. illite, K-feldspar)
Annite-Phlogopite	Good, is essentially biotite
Rutile/Anatase/Brookite	Good, although polymorphs are not differentiated
Hematite/Magnetite/Ilmenite	Very difficult to differentiate magnetite and hematite; ilmenite is easily identified
Calcite	Good, includes aragonite
Dolomite-Ankerite group	Good
Pyrite	Good
Apatite	Good
Zircon	Good
Titanite	Good
Tourmaline group	Poor, is often classed as Mg rich kaolinite. We're working on this.
Garnet group	Wide range of compositions in garnet group. Some garnet compositions are very close to other silicates, which may cause misclassifications/misidentifications. E.g. grossular garnet is very similar to epidote
Staurolite	Good
Sillimanite/Kyanite/Andalusite	Good
Epidote group	Moderate. Epidote composition very similar to grossular garnet. Zoisite and allanite compositions should be good
K-Feldspar group	Good; may include minor misidentifications with other K-Al silicates (predominantly illite, minor muscovite)
Albite	Good; although composition close to jadeite and jadeite may be misidentified as albite
Plagioclase group	Good
Chlorite group	Good-moderate
Chloritoid	Untested
Olivine	Good
Orthopyroxenes	Good-moderate; may be minor misidentification of olivine cracks as OPX; may be misidentified as talc
Clinopyroxenes	Moderate. Range of compositions; may be similar in composition to Ca-amphiboles and some misidentification expected
Calcic amphiboles	Moderate. Wide range of compositions; may be similar in composition to CPX and some misidentification expected
Sodic amphiboles	Poor, is often characterised as lots of different silicate phases
Fe-Mg-Mn amphiboles	Poor, is often characterised as lots of different silicate phases
Kaolinite/Dickite (S)	Impure kaolinite definitions may capture other phases, such as tourmaline
Glauconite	Untested
Montmorillonite/Smectite group	Wide range of compositions; difficult
Barite	Good
Halides	Good
Fe Oxides	Very difficult to differentiate magnetite and hematite under non-optimal conditions; mag/hem vs goethite and siderite should be differentiated well. Siderite vs goethite can be difficult as well
Quartz	Good
Illite	Moderate. may include minor misidentifications with other K-Al silicates (especially K-feldspar); can contain impurities, which may cause misidentification/overlap with other silicates
Gypsum/Anhydrite	Good. Impossible to differentiate gypsum from anhydrite

Siderite	Can be difficult to differentiate from goethite (and mag/hem to lesser extent)
Spinel group	Should be good, but wide range of possible compositions, so need to be added to the SIP to cover range (most common?)
Other sulphates/sulphides	Combination of high-confidence phases of very low concentrations, boundary textures and poorly identified phases
Other phosphates	Combination of high-confidence phases of very low concentrations, boundary textures and poorly identified phases
Other oxides	Combination of high-confidence phases of very low concentrations, boundary textures and poorly identified phases
Other silicates	Combination of high-confidence phases of very low concentrations, boundary textures and poorly identified phases
Other carbonates	Combination of high-confidence phases of very low concentrations, boundary textures and poorly identified phases
Other sheet silicates	As classification is based on chemistry, poor-moderate confidence these are sheet silicates vs other silicates
Pores	Good; may include organic matter
Other	Combination of high-confidence phases of very low concentrations, boundary textures and poorly identified phases
Low Confidence	Poor confidence due to poor match of spectral engine with raw measurement spectrum. Can be investigated offline and potentially included in SIP
Unclassified	Unclassified measurement points - can become classified phases/textures through SIP development

QEMSCAN oxide conversion factors

Table II. Oxide conversion factors for the QEMSCAN. The QEMSCAN uses these conversion factors to determine the amount of element oxides in the sample based on the amount of each element in its non-oxide form.

Symbol	Atomic Weight	Oxide conversion	# Element	# Oxygen	Oxide Weight	Element weight	Calculated Oxide conversion	Match
H	1,0079	0,1119	2	1	18,0152	2,0158	0,1118944	SANT
He	4,0026	1						
Li	6,941	0,4645	2	1	29,8814	13,882	0,464569933	SANT
Be	9,0122	0,3603	1	1	25,0116	9,0122	0,360320811	SANT
B	10,811	0,3106	2	3	69,6202	21,622	0,310570783	SANT
C	12,0107	0,2729	1	2	44,0095	12,0107	0,27291153	SANT
N	14,0067	0,2594	2	5	108,0104	28,0134	0,259358358	SANT
O	15,9994	0						
F	18,9984	1						
Ne	20,1797	1						
Na	22,9898	0,7419	2	1	61,979	45,9796	0,741857726	SANT
Mg	24,305	0,6031	1	1	40,3044	24,305	0,603035897	SANT
Al	26,9815	0,5293	2	3	101,9612	53,963	0,529250342	SANT
Si	28,0855	0,4674	1	2	60,0843	28,0855	0,467434921	SANT
P	30,9738	0,4364	2	5	141,9446	61,9476	0,43642097	SANT
S	32,066	0,4005	1	3	80,0642	32,066	0,400503596	SANT
Cl	35,4527	1						
Ar	39,948	1						
K	39,0983	0,8302	2	1	94,196	78,1966	0,830147777	SANT
Ca	40,078	0,7147	1	1	56,0774	40,078	0,714690767	SANT
Sc	44,9559	0,652	2	3	137,91	89,9118	0,651959974	SANT
Ti	47,867	0,5995	1	2	79,8658	47,867	0,599342898	SANT
V	50,9415	0,5602	2	5	181,88	101,883	0,560166044	SANT
Cr	51,9961	0,6842	2	3	151,9904	103,9922	0,684202423	SANT

Mn	54,938	0,7745	2	2	141,8748	109,876	0,774457479	SANT
Fe	55,845	0,6994	2	3	159,6882	111,69	0,699425505	SANT
Co	58,9332	0,7865	1	1	74,9326	58,9332	0,786482786	SANT
Ni	58,6934	0,7858	1	1	74,6928	58,6934	0,785797292	SANT
Cu	63,546	0,7989	1	1	79,5454	63,546	0,798864548	SANT
Zn	65,39	0,8034	1	1	81,3894	65,39	0,803421576	SANT
Ga	69,723	0,7439	2	3	187,4442	139,446	0,743933395	SANT
Ge	72,61	0,6941	1	2	104,6088	72,61	0,694109865	SANT
As	74,9216	0,7574	2	3	197,8414	149,8432	0,757390516	SANT
Se	78,96	0,6219	1	3	126,9582	78,96	0,621936984	SANT
Br	79,904	1						
Kr	83,8	1						
Rb	85,4678	0,914	2	1	186,935	170,9356	0,914411961	SANT
Sr	87,62	0,8456	1	1	103,6194	87,62	0,845594551	SANT
Y	88,9059	0,7874	2	3	225,81	177,8118	0,787439883	SANT
Zr	91,224	0,7403	1	2	123,2228	91,224	0,740317539	SANT
Nb	92,9064	0,699	2	5	265,8098	185,8128	0,699044204	SANT
Mo	95,94	0,6665	1	3	143,9382	95,94	0,666536055	SANT
Tc	-98	1						
Ru	101,07	1						
Rh	102,9055	1						
Pd	106,42	1						
Ag	107,8682	0,931	2	1	231,7358	215,7364	0,930958445	SANT
Cd	112,411	0,8754	1	1	128,4104	112,411	0,875404173	SANT
In	114,818	0,8271	2	3	277,6342	229,636	0,82711712	SANT
Sn	118,71	0,7877	1	2	150,7088	118,71	0,787677959	SANT
Sb	121,76	0,8353	2	3	291,5182	243,52	0,835350932	SANT
Te	127,6	0,7995	1	2	159,5988	127,6	0,799504758	SANT
I	126,9045	0,7604	2	5	333,806	253,809	0,760348825	SANT
Xe	131,29	1						
Cs	132,9055	0,9432	2	1	281,8104	265,811	0,943226368	SANT
Ba	137,327	0,8957	1	1	153,3264	137,327	0,895651369	SANT
La	138,9055	0,8527	2	3	325,8092	277,811	0,852680035	SANT
Ce	140,116	0,8538	2	3	328,2302	280,232	0,853766655	SANT

Pr	140,9076	0,8545	2	3	329,8134	281,8152	0,854468618	SANT
Nd	144,24	0,8574	2	3	336,4782	288,48	0,857351234	SANT
Pm	-145	0,8594						
Sm	150,36	0,8624	2	3	348,7182	300,72	0,862358202	SANT
Eu	151,964	0,8636	2	3	351,9262	303,928	0,863612882	SANT
Gd	157,25	0,8676	2	3	362,4982	314,5	0,867590515	SANT
Tb	158,9253	0,8688	2	3	365,8488	317,8506	0,868803178	SANT
Dy	162,5	0,8713	2	3	372,9982	325	0,871317878	SANT
Ho	164,9303	0,873	2	3	377,8588	329,8606	0,872973185	SANT
Er	167,26	0,8745	2	3	382,5182	334,52	0,87452048	SANT
Tm	168,9342	0,8756	2	3	385,8666	337,8684	0,875609343	SANT
Yb	173,04	0,8782	2	3	394,0782	346,08	0,878201332	SANT
Lu	174,967	0,8794	2	3	397,9322	349,934	0,87938096	SANT
Hf	178,49	0,848	1	2	210,4888	178,49	0,84797861	SANT
Ta	180,9479	0,819	2	5	441,8928	361,8958	0,818967406	SANT
W	183,84	0,8518	1	2	215,8388	183,84	0,851746767	SANT
Re	186,207	0,8534	1	2	218,2058	186,207	0,853354952	SANT
Os	190,23	1						
Ir	192,217	1						
Pt	195,078	1						
Au	196,9666	0,961	2	1	409,9326	393,9332	0,960970657	SANT
Hg	200,59	0,9261	1	1	216,5894	200,59	0,926130272	SANT
Tl	204,3833	0,8949	2	3	456,7648	408,7666	0,894917034	SANT
Pb	207,2	0,9283	1	1	223,1994	207,2	0,928317908	SANT
Bi	208,9804	0,897	2	3	465,959	417,9608	0,896990508	SANT
Po	-209	0,814						
At	-210	0,7895						
Rn	-222	1						
Fr	-223	0,9654						
Ra	226,025	0,9339	1	1	242,0244	226,025	0,933893442	SANT
Ac	227,028	0,9044	2	3	502,0542	454,056	0,904396378	SANT
Th	232,0381	0,8788	1	2	264,0369	232,0381	0,878809363	SANT
Pa	231,0359	0,9059	2	3	510,07	462,0718	0,905898798	SANT
U	238,0289	0,848	3	8	842,0819	714,0867	0,848001483	SANT

Np	237,048	0					
Pu	-244	0					
Am	-243	0					
Cm	-247	0					
Bk	-247	0					
Cf	-251	0					
Es	-252	0					
Fm	-257	6,5					
Md	-258	6,58					
No	-259	6,65					
Lr	-260	0					
Rf	0	0					
Ha	0	0					
Sg	0	0					
Ns	0	0					
Hs	0	0					
Mt	0	0					

Metadata for XRF

Table III. Stockholm University preferred values for International Standards utilised during calibration

standard name		AGV-1	MRG-1	AGV-2	BCR-2	GSP-2	RGM-1	SARM-1	SARM-3	SARM-6	GS-N	GA	AN-G	W-2	PCC-1	DTS-1	GS-2	SY-2	JB-1b	JB-2	JA-2	JG-2	JR-3	NBS 278	NBS 688
		USGS	USGS	USGS	USGS	USGS	USGS	SARM						USGS	USGS	USGS	USGS	CCRM P						NIST	NIST
SiO ₂	mass %	58.84		59.3	54.1	66.6	73.4	75.7	52.24	38.5					41.71	40.41		49.9	51.11	53.25	56.42	76.83	72.76	72.97	48.35
Al ₂ O ₃	mass %	17.15		16.91	13.5	14.9	13.7	12.08	13.64	0.22					0.675	0.19		20.69	14.38	14.64	15.41	12.47	11.9	14.15	17.35
CaO	mass %	4.94		5.2	7.12	2.1	1.15	0.78	3.22	0.29					0.52	0.17		8.05	9.6	9.82	6.29	0.7	0.093	0.983	12.17
MgO	mass %	1.53		1.79	3.59	0.96	0.28		0.28	43.2					43.43	49.59		0.54	8.14	4.62	7.6	0.037	0.05	0.23	8.46
MnO	mass %	0.1		0.1			0.036		0.77	0.22						0.12		0.108	0.147	0.218	0.108	0.016	0.083	0.052	0.167
P ₂ O ₅	mass %	0.5		0.48	0.35	0.29	0.07		0.06	0.01						0.002		0.131	0.256	0.101	0.146	0.002	0.017	0.036	0.133
Fe ₂ O ₃	mass %	6.77		6.69	13.8	4.9	1.86		9.96	16.79					8.25	8.68		6.21	9.02	14.25	6.21	0.97	4.72	2.04	10.34
Na ₂ O	mass %	4.26		4.19	3.16	2.78	4.07		8.37	0.03						0.01		7.1	2.63	2.04	3.11	3.54	4.69	4.84	2.16
K ₂ O	mass %	2.92		2.88	1.79	5.38	4.3	4.99	5.51	0.01						0.001		1.66	1.32	0.42	1.81	4.71	4.29	4.16	0.19
TiO ₂	mass %	1.05		1.05	2.26	0.66	0.27		0.48	0.02						0.005		0.287	1.26	1.19	0.66	0.044	0.21	0.245	1.168
Total		98.06	0	98.59	99.67	98.57	99.136	93.55	94.53	99.29	0	0	0	0	94.585	99.178	0	94.676	97.863	100.549	97.764	99.319	98.813	99.706	100.488
SiO ₂	mass %	60.01	39.72	60.15	54.17	67.57	74.04	76.47	55.34	38.84	66.85	70.75	46.68	52.48	44.02	40.74	69.76	52.71	52.23	52.96	57.71	77.36	73.63	73.19	48.12
Al ₂ O ₃	mass %	17.49	8.65	17.15	13.52	15.12	13.82	12.20	14.40	0.30	14.90	14.68	30.04	15.39	0.71	0.19	15.53	21.85	14.69	14.56	15.76	12.56	12.04	14.19	17.27
CaO	mass %	5.04	14.84	5.27	7.13	2.13	1.16	0.79	3.40	0.28	2.54	2.48	16.03	10.82	0.55	0.17	1.98	8.50	9.81	9.77	6.43	0.70	0.09	0.99	12.11

MgO	mass %	1.56	13.69	1.82	3.59	0.97	0.28	0.06	0.30	43.38	2.34	0.96	1.81	6.35	45.83	50.00	0.76	0.57	8.32	4.59	7.77	0.04	0.05	0.23	8.42
MnO	mass %	0.1	0.17	0.10	0.20	0.00	0.04	0.02	0.81	0.22	0.06	0.09	0.04	0.17	0.13	0.12	0.03	0.11	0.15	0.22	0.11	0.02	0.08	0.05	0.17
P2O5	mass %	0.51	0.06	0.49	0.35	0.29	0.07	0.01	0.06	0.01	0.28	0.12	0.01	0.13	0.00	0.00	0.14	0.14	0.26	0.10	0.15	0.00	0.02	0.04	0.13
Fe2O3	mass %	6.9	18.12	6.79	13.82	4.97	1.88	1.91	10.52	16.91	3.81	2.86	3.39	10.79	8.71	8.75	2.68	6.56	9.22	14.17	6.35	0.98	4.78	2.05	10.29
Na2O	mass %	4.34	0.75	4.25	3.16	2.82	4.11	3.41	8.84	0.04	3.83	3.59	1.64	2.19	0.03	0.01	4.12	7.50	2.69	2.03	3.18	3.56	4.75	4.85	2.15
K2O	mass %	2.98	0.17	2.92	1.79	5.46	4.34	5.04	5.82	0.01	4.70	4.08	0.13	0.62	0.01	0.00	4.52	1.75	1.35	0.42	1.85	4.74	4.34	4.17	0.19
TiO2	mass %	1.07	3.83	1.07	2.26	0.67	0.27	0.09	0.51	0.02	0.69	0.38	0.22	1.06	0.01	0.01	0.48	0.30	1.29	1.18	0.68	0.04	0.21	0.25	1.16
Ce	ppm	68	26	68	53	410	47	195	286	0	135	76	5	23	0	0	160	122		7	33	48	327	62	13
La	ppm	38	10	38	25	180	24	109	250	0	75	40	2	11	0	0	89	58		2	16	20	179	32	5
Th	ppm	6	1	6	6	105	15	51	66	1	41	17	0	2	0	0	25	1		0	5	2	112	12	0
Ni	ppm	16	193	19	18	17	4	2	11	2050	34	7	35	72	2380	2360	5	9	148	17	130	4		4	150
V	ppm	119	526	120	416	52	13	81	81	40	65	38	70	268	31	11	36	8	214	575	126	4	4	9	250
Ba	ppm	1200	61	1140	677	1340	810	120	450	10	1400	840	34	172	1	2	1880	340		222	321	81	66	1140	200
Cr	ppm	9	430	17	18	20	4	12	10	2900	55	12	50	93	2730	3990	9	12	439	28	436	6	4	6	332
Cu	ppm	58	134	53	21	43	12	12	13	10	20	16	19	105	10	7	11	7	56	225	30	0	3	6	96
Ga	ppm	20	17	20	23	22	15	27	54	0	22	16	18	18	1	1	23	35		17	17	19	37	13	18
Hf	ppm	5	4	5	5	14	6	12	190	0	6	4	0	2	0	0	8	11		1	3	5	40	8	2
Nb	ppm	15	20	15	13	27	9	53	960	0	21	12	1	8	1	2	12	13		2	9	15	510	18	6
Pb	ppm	37	10	13	11	42	24	40	43	7	53	30	2	8	10	12	30	10	7	5	19	32	33	16	3
Rb	ppm	67	9	69	47	245	150	325	190	0	185	175	1	21	0	0	170	55	39	7	73	301	453	128	2
Sr	ppm	660	266	658	340	240	110	10	4600	3	570	310	76	196	0	0	478	1191	439	178	248	18	10	64	169
Y	ppm	19	14	20	37	28	25	143	22	0	16	21	8	22	0	0	11	119		25	18	87	166	39	19
Zr	ppm	231	108	230	184	550	220	300	1100	20	235	150	11	92	10	0	309	517		51	116	98	1494	290	59

Table IV. Mean of Relative Deviation (RD%) from 25th June to 5th October 2008

	AGV 2	BCR 2	RGM 1		meanRD (Weighted)	meanRD Oxford
SiO ₂	-0.08	-0.02	-0.40		-0.12	0.22
Al ₂ O ₃	-0.10	0.07	-0.02		-0.03	0.83
CaO	-0.62	-1.34	7.17		0.67	1.39
MgO	-0.44	0.42	4.82		0.82	1.41
MnO	0.23	2.24	-6.51		-0.49	1.7
P ₂ O ₅	5.13	-1.19	12.33		4.69	2.51
Fe ₂ O ₃	0.75	0.50	6.53		1.79	0.9
Na ₂ O	0.62	1.10	1.14		0.86	1.73
K ₂ O	0.35	-1.66	0.56		-0.19	1.18
TiO ₂	-0.56	0.21	0.06		-0.22	2.08
Ce	-3.05	-0.52	1.91		-1.37	
La	-2.73	-9.64	7.08		-2.84	
Th	8.68	-16.67	-7.33		-1.71	2.14
Ni	-3.12	-72.22	97.73		-3.66	3.1
V	1.23	-0.09	1.54		0.91	3.04
Ba	-0.40	-0.39	1.09		-0.11	4.79
Cr	6.10	83.33			27.21	12.39
Cu	-2.31	-32.74	3.33		-10.00	15.12
Ga	3.52	-15.76	18.00		0.74	1.41
Hf	4.26	14.80	-14.52		3.69	
Nb	-11.60	1.19	-10.11		-7.63	6.68
Pb	4.56	-5.68	0.42		0.81	10.98
Rb	-0.82	-3.52	0.47		-1.35	3.06
Sr	1.23	-3.09	-6.45		-1.49	2.63
Y	-9.81	-19.59	5.60		-9.67	8.97
Zr	-3.75	0.48	-3.45		-2.48	4.86
n	27	15	10		52	

Table V. Coefficients of Variation (CV%) from 25th June to 25th September 2008

	AGV 2	BCR 2	RGM 1	Argent,in Pease, 1997	Lee & McConchie, 1982
SiO ₂	0.07	0.09	0.06	0.07	0.13
Al ₂ O ₃	0.54	0.47	0.54	0.10	0.16
CaO	0.48	0.36	0.46	0.16	0.12
MgO	0.53	0.45	2.70	0.85	0.78
MnO	0.56	0.40	2.58	1.10	2.10
P ₂ O ₅	1.67	2.43	9.65	1.15	0.10
Fe ₂ O ₃	0.61	0.27	2.56	0.15	0.16
Na ₂ O	0.38	0.68	0.36	0.49	1.40
K ₂ O	0.41	0.58	0.30	0.14	0.14
TiO ₂	0.32	0.17	0.32	0.34	0.19
Ce	6.77	9.54	6.34		
La	5.88	11.51	12.04		
Th	10.37	12.03	4.08	4.80	
Ni	6.26	24.80	7.76	1.70	
V	2.01	0.84	9.97	2.40	4.30
Ba	0.41	0.68	0.87	0.60	0.50
Cr	4.21	8.82		3.40	
Cu	3.72	38.20	12.72	3.80	12.70
Ga	4.98	5.34	5.36	1.50	2.40
Hf	38.42	52.01	30.88		
Nb	4.95	7.72	8.33	4.10	
Pb	5.86	12.47	3.63	4.50	9.10
Rb	1.12	1.42	0.77	0.60	4.50
Sr	0.74	0.63	1.07	0.30	1.00
Y	11.96	13.54	1.96	4.50	13.00
Zr	1.67	4.15	3.22	0.30	2.20
n	27	15	10		

Table VI. Counts per second per unit of concentration for 2 standards.

	AGV 2 cps/weight% or cps/ppm	BCR 2 cps/weight% or cps/ppm	Lower limit of accurate detection Weight% (*) or ppm
Si-K α	14405	14349	0.032 *
Al-K α	15767	15424	0.078 *
Ca-K α	28331	29514	0.012 *
Mg-K α	3815	3791	0.075 *
Mn-K α	61543	59028	0.001 *
P-K α	34071	33508	0.031 *
Fe-K α	70470	68800	0.004 *
Na-K α	2536	2530	0.233 *
K-K α	124059	125228	0.021 *
Ti-K α	19070	19672	0.001 *
Ce-L β 1	0.64	0.61	10
La-L α	1.09	0.85	10
Th-L α	15.64	12.68	5
Ni-K α	29.64	22.53	15
V-K α	4.06	3.66	10
Ba-L α	0.54	0.60	15
Cr-K α	23.74	29.76	10
Cu-K α	15.12	19.70	10
Ga-K α	15.61	11.34	10
Hf-L α	4.21	1.35	5
Nb-K α	43.15	35.10	5
Pb-L β 1	20.28	13.93	5
Rb-K α	34.90	28.65	5
Sr-K α	39.32	31.52	5
Y-K α	94.10	51.25	10
Zr-K α	61.20	46.34	5

Appendix B

Table VII. Mineral abundance data, primary list.

Mineral Volume(%)	DL13-01	DL13-02	DL13-03	DL13-04	DL13-05	DL13-06	DL13-07	DL13-08a	DL13-08b	DL13-09	DL13-10	DL13-11	DL13-12	DL13-13
Pyrite textures	0,00	0,00	0,00	0,00	0,00	0,00	0,00	0,00	0,00	0,00	0,00	0,00	0,00	0,00
Calcite/Aragonite textures	0,82	2,19	2,00	0,90	0,22	0,07	0,07	0,12	0,10	0,25	0,45	0,91	0,82	0,14
Goethite/Lepidocrocite	0,00	0,00	0,01	0,00	0,01	0,01	0,04	0,01	0,01	0,00	0,00	0,01	0,01	0,02
Jarosite	0,00	0,00	0,00	0,00	0,00	0,00	0,00	0,00	0,00	0,00	0,00	0,00	0,00	0,00
Schwertmannite	0,00	0,00	0,00	0,00	0,00	0,00	0,00	0,00	0,00	0,00	0,00	0,00	0,00	0,00
Halotrichite	0,00	0,00	0,00	0,00	0,00	0,00	0,00	0,00	0,00	0,00	0,00	0,00	0,00	0,00
Apatite textures	0,01	0,12	0,08	0,01	0,02	0,01	0,02	0,12	0,01	0,01	0,01	0,01	0,01	0,01
Siderite (Mg-Zn)	0,00	0,00	0,00	0,00	0,00	0,00	0,00	0,00	0,00	0,00	0,00	0,00	0,00	0,00
Dolomite textures	0,34	0,03	0,81	0,33	0,17	0,00	0,03	0,02	0,02	0,05	0,03	0,52	0,17	0,02
Kutnohorite	0,00	0,00	0,00	0,00	0,00	0,00	0,00	0,00	0,00	0,00	0,00	0,00	0,00	0,00
Rhodochrosite	0,00	0,00	0,00	0,00	0,00	0,00	0,00	0,00	0,00	0,00	0,00	0,00	0,00	0,00
Quartz textures	1,02	1,96	2,83	1,53	1,13	1,29	0,41	0,48	0,16	0,30	2,29	1,22	0,59	0,55
Kaolinite textures	4,64	1,22	5,42	5,39	3,57	7,97	1,85	1,24	1,49	1,48	12,28	1,40	1,91	2,90
Clinochrysoile	0,00	0,00	0,00	0,00	0,00	0,00	0,00	0,00	0,00	0,00	0,00	0,00	0,00	0,00
Albite textures	0,06	0,14	0,04	0,20	0,06	0,15	0,09	0,07	0,27	0,05	0,15	0,08	0,08	0,13
Annite	0,03	0,02	0,24	0,00	0,10	0,22	0,41	0,05	0,00	0,02	0,12	0,00	0,06	0,21
Phlogopite	0,00	0,00	0,00	0,00	0,00	0,00	0,00	0,00	0,00	0,00	0,00	0,00	0,00	0,00
Annite-Phlogopite	0,01	0,03	0,15	0,00	0,02	0,15	0,84	0,04	0,00	0,01	0,02	0,00	0,01	0,06
Muscovite textures	0,02	0,01	0,01	0,00	0,00	0,00	0,00	0,00	0,00	0,01	0,00	0,00	0,00	0,00
Illite textures	0,22	0,29	1,09	0,61	0,57	0,75	0,25	0,40	0,05	0,08	1,14	0,22	0,16	0,21
Ripidolite	0,02	0,54	0,15	0,07	0,09	0,00	0,21	0,00	0,01	0,00	0,00	0,19	0,01	0,02
Glaucophane	0,00	0,00	0,00	0,02	0,04	0,00	0,01	0,00	0,00	0,00	0,00	0,01	0,00	0,00
Montmorillonite textures	2,32	3,63	8,76	19,41	23,73	3,03	2,83	3,98	1,74	1,18	2,07	3,02	4,64	2,44
Palygorskite	0,01	0,00	0,01	0,25	0,25	0,00	0,03	0,00	0,00	0,00	0,00	0,03	0,01	0,01
Beidellite	0,37	0,04	0,04	0,03	0,08	0,05	0,04	0,04	0,01	0,09	0,05	0,00	0,23	0,10
Sepiolite	0,00	0,00	0,00	0,00	0,00	0,00	0,00	0,00	0,00	0,00	0,00	0,00	0,00	0,00
Corrensite	0,01	0,00	0,01	0,19	0,03	0,00	0,12	0,03	0,11	0,01	0,00	0,69	0,02	0,02
Clinozoisite	0,00	0,00	0,00	0,00	0,00	0,00	0,00	0,00	0,00	0,00	0,00	0,00	0,00	0,00
Fluorite	0,00	0,00	0,00	0,00	0,00	0,00	0,00	0,00	0,00	0,00	0,00	0,00	0,00	0,00
Pores	0,00	0,00	0,00	0,00	0,00	0,00	0,00	0,00	0,00	0,00	0,00	0,00	0,00	0,00
Rutile/Anatase (S)	0,00	0,14	0,02	0,00	0,00	0,00	0,01	0,01	0,01	0,00	0,00	0,00	0,00	0,01
Cassiterite (S)	0,00	0,00	0,00	0,00	0,00	0,00	0,00	0,00	0,00	0,00	0,00	0,00	0,00	0,00
Baddeleyite (S)	0,00	0,00	0,00	0,00	0,00	0,00	0,00	0,00	0,00	0,00	0,00	0,00	0,00	0,00
Spinel (S)	0,00	0,00	0,00	0,00	0,00	0,00	0,00	0,00	0,00	0,00	0,00	0,00	0,00	0,00
Magnesiochromite (S)	0,00	0,00	0,00	0,00	0,00	0,00	0,00	0,00	0,00	0,00	0,00	0,00	0,00	0,00
Chromite (S)	0,00	0,00	0,00	0,00	0,00	0,00	0,00	0,00	0,00	0,00	0,00	0,00	0,00	0,00
Hercynite (S)	0,00	0,00	0,00	0,00	0,00	0,00	0,00	0,00	0,00	0,00	0,00	0,00	0,00	0,00
Gahnite (S)	0,00	0,00	0,00	0,00	0,00	0,00	0,00	0,00	0,00	0,00	0,00	0,00	0,00	0,00

Ulvospinel (S)	0,00	0,00	0,00	0,00	0,00	0,00	0,00	0,00	0,00	0,00	0,00	0,00	0,00	0,00
Ilmenite (S)	0,00	0,00	0,00	0,00	0,00	0,01	0,01	0,00	0,00	0,00	0,00	0,00	0,00	0,00
Magnetite (S)	0,01	0,00	0,02	0,00	0,01	0,01	0,07	0,01	0,03	0,00	0,00	0,00	0,02	0,02
Hematite (S)	0,01	0,00	0,07	0,00	0,01	0,01	0,16	0,02	0,09	0,01	0,01	0,01	0,04	0,03
Perovskite (S)	0,00	0,00	0,00	0,00	0,00	0,00	0,00	0,00	0,00	0,00	0,00	0,00	0,00	0,00
Calcite (S)	5,86	9,64	5,92	1,46	0,47	0,25	0,47	1,10	3,05	2,74	2,99	6,47	6,29	1,13
Dolomite (S)	0,01	0,00	0,01	0,00	0,00	0,00	0,00	0,00	0,00	0,03	0,00	0,02	0,00	0,00
Ankerite (S)	0,01	0,00	0,00	0,00	0,00	0,00	0,00	0,00	0,00	0,08	0,00	0,01	0,00	0,00
Magnesite (S)	0,00	0,00	0,00	0,00	0,00	0,00	0,00	0,00	0,00	0,00	0,00	0,00	0,00	0,00
Siderite (S)	0,00	0,00	0,01	0,00	0,00	0,00	0,00	0,00	0,00	0,00	0,00	0,00	0,00	0,00
Pyrite (S)	0,00	0,01	0,00	0,02	0,00	0,02	0,00	0,00	0,00	0,00	0,00	0,00	0,00	0,00
Chalcopyrite (S)	0,00	0,00	0,00	0,00	0,00	0,00	0,00	0,00	0,00	0,00	0,00	0,00	0,00	0,00
Sphalerite (S)	0,00	0,00	0,00	0,00	0,00	0,00	0,00	0,00	0,00	0,00	0,00	0,00	0,00	0,00
Galena (S)	0,00	0,00	0,00	0,00	0,00	0,00	0,00	0,00	0,00	0,00	0,00	0,00	0,00	0,00
Anhydrite (S)	0,00	0,00	0,00	0,00	0,00	0,00	0,00	0,00	0,00	0,00	0,00	0,00	0,00	0,00
Gypsum (S)	0,00	0,00	0,00	0,00	0,00	0,00	0,00	0,00	0,00	0,00	0,00	0,00	0,00	0,00
Chlorapatite (S)	0,00	0,00	0,00	0,00	0,00	0,00	0,00	0,00	0,00	0,00	0,00	0,00	0,00	0,00
Fluorapatite (S)	0,00	0,03	0,00	0,00	0,00	0,00	0,00	0,00	0,00	0,00	0,00	0,00	0,00	0,00
Apatite (S)	0,10	0,23	0,03	0,01	0,03	0,02	0,12	0,22	0,07	0,04	0,04	0,03	0,04	0,02
Monazite-(Ce) (S)	0,00	0,00	0,00	0,00	0,00	0,00	0,00	0,00	0,00	0,00	0,00	0,00	0,00	0,00
Monazite-(La) (S)	0,00	0,00	0,00	0,00	0,00	0,00	0,00	0,00	0,00	0,00	0,00	0,00	0,00	0,00
Monazite-(Nd) (S)	0,00	0,00	0,00	0,00	0,00	0,00	0,00	0,00	0,00	0,00	0,00	0,00	0,00	0,00
Xenotime-(Y) (S)	0,00	0,00	0,00	0,00	0,00	0,00	0,00	0,00	0,00	0,00	0,00	0,00	0,00	0,00
Xenotime-(Yb) (S)	0,00	0,00	0,00	0,00	0,00	0,00	0,00	0,00	0,00	0,00	0,00	0,00	0,00	0,00
Zircon (S)	0,00	0,00	0,00	0,00	0,00	0,00	0,00	0,00	0,00	0,00	0,00	0,00	0,00	0,00
Titanite (S)	0,00	0,02	0,01	0,01	0,00	0,02	0,25	0,58	0,06	0,00	0,10	0,03	0,00	0,00
Opal (S)	0,00	0,05	0,01	0,00	0,00	0,00	0,00	0,00	0,00	0,00	0,00	0,00	0,00	0,00
Dravite (S)	0,00	0,00	0,00	0,00	0,00	0,00	0,00	0,00	0,00	0,00	0,00	0,00	0,00	0,00
Dravite-Schorl (S)	0,00	0,00	0,00	0,00	0,00	0,00	0,00	0,00	0,00	0,00	0,00	0,00	0,00	0,00
Schorl (S)	0,00	0,00	0,00	0,00	0,00	0,00	0,00	0,00	0,00	0,00	0,00	0,00	0,00	0,00
Elbaite (S)	0,00	0,00	0,00	0,00	0,00	0,00	0,00	0,00	0,00	0,00	0,00	0,00	0,00	0,00
Almandine (S)	0,02	0,02	0,02	0,00	0,06	0,03	0,03	0,01	0,00	0,00	0,01	0,01	0,04	0,07
Spessartine (S)	0,00	0,00	0,00	0,00	0,00	0,00	0,00	0,00	0,00	0,00	0,00	0,00	0,00	0,00
Pyrope (S)	0,00	0,00	0,00	0,00	0,00	0,00	0,00	0,00	0,00	0,00	0,00	0,00	0,00	0,00
Grossular (S)	0,00	0,00	0,00	0,00	0,00	0,00	0,00	0,00	0,00	0,00	0,00	0,00	0,00	0,00
Andradite (S)	0,00	0,00	0,00	0,00	0,00	0,00	0,00	0,00	0,00	0,00	0,00	0,00	0,00	0,00
Uvarovite (S)	0,00	0,00	0,00	0,00	0,00	0,00	0,00	0,00	0,00	0,00	0,00	0,00	0,00	0,00
Alm-Sp (2:1) (S)	0,00	0,00	0,00	0,00	0,00	0,00	0,00	0,00	0,00	0,00	0,00	0,00	0,00	0,00
Sp-Alm (2:1) (S)	0,00	0,00	0,00	0,00	0,00	0,00	0,00	0,00	0,00	0,00	0,00	0,00	0,00	0,00
Alm-Grs (2:1) (S)	0,00	0,05	0,02	0,08	0,01	0,07	0,02	0,03	0,00	0,00	0,00	0,38	0,00	0,00
Grs-Alm (2:1) (S)	0,00	0,00	0,00	3,04	0,02	1,62	0,57	0,00	0,00	0,00	0,00	5,48	0,00	0,00
Alm-Py (2:1) (S)	0,10	0,88	0,15	0,11	0,16	0,08	0,07	1,62	0,27	0,14	0,03	0,02	0,34	0,08
Py-Alm (2:1) (S)	0,24	0,01	0,12	1,58	3,91	0,09	1,70	0,15	0,41	0,23	0,06	0,30	0,30	0,50
Sp-Grs (2:1) (S)	0,00	0,00	0,00	0,00	0,00	0,00	0,00	0,00	0,00	0,00	0,00	0,00	0,00	0,00
Grs-Sp (2:1) (S)	0,00	0,00	0,00	0,00	0,00	0,00	0,00	0,00	0,00	0,00	0,00	0,00	0,00	0,00
Sp-Py (2:1) (S)	0,00	0,00	0,00	0,00	0,00	0,00	0,00	0,00	0,00	0,00	0,00	0,00	0,00	0,00
Py-Sp (2:1) (S)	0,00	0,00	0,00	0,00	0,00	0,00	0,00	0,00	0,00	0,00	0,00	0,00	0,00	0,00
Alm-Sp-Grs (S)	0,00	0,00	0,00	0,00	0,00	0,00	0,00	0,00	0,00	0,00	0,00	0,00	0,00	0,00

Alm-Sp-Py (S)	0,00	0,00	0,00	0,00	0,00	0,00	0,00	0,00	0,00	0,00	0,00	0,00	0,00	0,00
And-Grs (2:1) (S)	0,00	0,00	0,00	0,00	0,00	0,00	0,00	0,00	0,00	0,00	0,00	0,00	0,00	0,00
Grs-And (2:1) (S)	0,00	0,00	0,00	0,00	0,00	0,00	0,00	0,00	0,00	0,00	0,00	0,00	0,00	0,00
And-Uv (2:1) (S)	0,00	0,00	0,00	0,00	0,00	0,00	0,00	0,00	0,00	0,00	0,00	0,00	0,00	0,00
Uv-And (2:1) (S)	0,00	0,00	0,00	0,00	0,00	0,00	0,00	0,00	0,00	0,00	0,00	0,00	0,00	0,00
Staurolite (S)	0,00	0,00	0,00	0,00	0,00	0,00	0,00	0,00	0,00	0,00	0,00	0,00	0,00	0,00
Sillimanite/Kyanite/Andalu site (S)	0,00	0,00	0,00	0,00	0,00	0,00	0,00	0,00	0,00	0,00	0,00	0,00	0,00	0,00
Epidote-(Fe) (S)	0,00	0,00	0,00	0,00	0,00	0,00	0,00	0,00	0,00	0,00	0,00	0,00	0,00	0,00
Epidote (S)	0,00	0,00	0,01	0,08	0,00	0,01	0,01	0,00	0,00	0,00	0,00	0,21	0,00	0,00
Epidote-(Al) (S)	0,00	0,00	0,00	0,16	0,00	0,17	0,03	0,00	0,00	0,00	0,00	0,21	0,00	0,00
Zoisite (S)	0,00	0,00	0,00	0,00	0,00	0,00	0,00	0,00	0,00	0,00	0,00	0,00	0,00	0,00
Piemontite (S)	0,00	0,00	0,00	0,00	0,00	0,00	0,00	0,00	0,00	0,00	0,00	0,00	0,00	0,00
Allanite-(Ce) (S)	0,00	0,00	0,00	0,00	0,00	0,00	0,00	0,00	0,00	0,00	0,00	0,00	0,00	0,00
Allanite-(La) (S)	0,00	0,00	0,00	0,00	0,00	0,00	0,00	0,00	0,00	0,00	0,00	0,00	0,00	0,00
Allanite-(Y) (S)	0,00	0,00	0,00	0,00	0,00	0,00	0,00	0,00	0,00	0,00	0,00	0,00	0,00	0,00
Cordierite-(Mg) (S)	0,00	0,00	0,00	0,00	0,00	0,00	0,00	0,00	0,00	0,00	0,00	0,00	0,00	0,00
Cordierite (S)	0,06	0,00	0,01	0,00	0,01	0,00	0,00	0,00	0,00	0,01	0,00	0,00	0,03	0,00
Cordierite-(Fe) (S)	0,00	0,00	0,00	0,00	0,00	0,00	0,00	0,00	0,00	0,00	0,00	0,00	0,00	0,00
Albite (S)	32,60	19,67	1,75	12,45	23,19	22,83	20,94	42,94	66,43	51,94	16,88	18,36	38,30	43,33
Oligoclase (S)	0,01	0,02	0,00	0,01	0,00	0,01	0,01	0,02	0,00	0,01	0,00	0,03	0,02	0,00
Andesine (S)	1,99	0,94	0,52	0,87	2,52	1,53	1,12	1,18	0,39	0,72	1,23	0,32	2,58	1,36
Labradorite (S)	0,01	0,01	0,01	0,11	0,00	0,03	0,00	0,00	0,00	0,01	0,01	0,02	0,01	0,00
Bytownite (S)	0,00	0,00	0,00	0,00	0,00	0,00	0,00	0,00	0,00	0,00	0,00	0,00	0,00	0,00
Anorthite (S)	0,00	0,00	0,00	0,00	0,00	0,01	0,00	0,00	0,00	0,00	0,00	0,00	0,00	0,00
Anorthoclase (S)	0,05	0,02	0,00	0,00	0,03	0,34	0,27	0,08	0,03	0,05	0,60	0,02	0,15	0,28
Sanidine (S)	0,00	0,00	0,00	0,00	0,00	0,00	0,00	0,00	0,00	0,00	0,00	0,00	0,00	0,00
Muscovite (S)	5,09	3,02	3,02	0,00	0,26	2,38	1,09	1,00	0,30	5,26	2,57	0,11	5,06	5,53
Biotite (S)	0,69	0,93	3,07	0,00	0,81	2,62	5,32	0,87	0,02	1,35	0,81	0,07	1,14	2,07
Paragonite (S)	0,02	0,00	0,00	0,00	0,00	0,00	0,00	0,00	0,00	0,00	0,00	0,00	0,00	0,00
Clinocllore (S)	1,45	0,69	2,33	4,33	2,81	0,08	4,22	0,30	1,00	0,87	0,12	6,07	1,52	1,02
Chlorite (S)	0,04	0,20	0,09	0,66	0,05	0,03	0,20	0,73	0,78	0,04	0,03	0,87	0,29	0,08
Chamosite (S)	5,13	27,10	11,08	18,65	10,05	1,04	6,83	16,26	6,77	3,54	0,94	18,03	9,97	3,36
Chloritoid (S)	0,00	0,00	0,00	0,00	0,00	0,00	0,00	0,00	0,00	0,00	0,00	0,00	0,00	0,00
Forsterite (S)	0,00	0,00	0,00	0,00	0,00	0,00	0,00	0,00	0,00	0,00	0,00	0,00	0,00	0,00
Olivine Fo90 (S)	0,00	0,00	0,00	0,00	0,00	0,00	0,00	0,00	0,00	0,00	0,00	0,00	0,00	0,00
Olivine Fo80 (S)	0,00	0,00	0,00	0,00	0,00	0,00	0,00	0,00	0,00	0,00	0,00	0,00	0,00	0,00
Olivine Fo70 (S)	0,00	0,00	0,00	0,00	0,00	0,00	0,00	0,00	0,00	0,00	0,00	0,00	0,00	0,00
Olivine Fo60 (S)	0,00	0,00	0,00	0,00	0,00	0,00	0,00	0,00	0,00	0,00	0,00	0,00	0,00	0,00
Olivine Fo50 (S)	0,00	0,00	0,00	0,00	0,00	0,00	0,00	0,00	0,00	0,00	0,00	0,00	0,00	0,00
Olivine Fo40 (S)	0,00	0,00	0,00	0,00	0,00	0,00	0,00	0,00	0,00	0,00	0,00	0,00	0,00	0,00
Olivine Fo30 (S)	0,00	0,00	0,00	0,00	0,00	0,00	0,00	0,00	0,00	0,00	0,00	0,00	0,00	0,00
Olivine Fo20 (S)	0,00	0,00	0,00	0,00	0,00	0,00	0,00	0,00	0,00	0,00	0,00	0,00	0,00	0,00
Olivine Fo10 (S)	0,01	0,00	0,00	0,00	0,02	0,01	0,03	0,00	0,01	0,00	0,02	0,00	0,02	0,04
Fayalite (S)	0,00	0,00	0,01	0,00	0,01	0,00	0,01	0,00	0,00	0,00	0,01	0,00	0,00	0,01
Enstatite (S)	0,00	0,00	0,00	0,00	0,00	0,00	0,00	0,00	0,00	0,00	0,00	0,00	0,00	0,00
OPX En90 (S)	0,00	0,00	0,00	0,00	0,00	0,00	0,00	0,00	0,00	0,00	0,00	0,00	0,00	0,00
OPX En80 (S)	0,00	0,00	0,00	0,00	0,00	0,00	0,00	0,00	0,00	0,00	0,00	0,00	0,00	0,00

OPX En70 (S)	0,00	0,00	0,00	0,00	0,00	0,00	0,00	0,00	0,00	0,00	0,00	0,00	0,00	0,00
OPX En60 (S)	0,00	0,00	0,00	0,00	0,00	0,00	0,00	0,00	0,00	0,00	0,00	0,00	0,00	0,00
OPX En50 (S)	0,00	0,00	0,00	0,00	0,00	0,00	0,00	0,00	0,00	0,00	0,00	0,00	0,00	0,00
OPX En40 (S)	0,00	0,00	0,00	0,00	0,00	0,00	0,00	0,00	0,00	0,00	0,00	0,00	0,00	0,00
OPX En30 (S)	0,00	0,00	0,00	0,00	0,00	0,00	0,00	0,00	0,00	0,00	0,00	0,00	0,00	0,00
OPX En20 (S)	0,00	0,00	0,00	0,00	0,00	0,00	0,00	0,00	0,00	0,00	0,00	0,00	0,00	0,00
OPX En10 (S)	0,01	0,00	0,01	0,00	0,04	0,01	0,05	0,00	0,01	0,00	0,04	0,01	0,04	0,08
OPX En0 (S)	0,00	0,00	0,00	0,00	0,00	0,00	0,01	0,00	0,00	0,00	0,01	0,00	0,00	0,01
Augite (S)	0,00	0,00	0,01	0,00	0,00	0,00	0,00	0,00	0,00	0,00	0,00	0,01	0,00	0,00
Diopside (S)	0,00	0,00	0,00	0,00	0,00	0,00	0,00	0,00	0,00	0,00	0,00	0,00	0,00	0,00
Diopside-Hedenbergite (S)	0,00	0,00	0,00	0,00	0,00	0,00	0,00	0,00	0,00	0,00	0,00	0,00	0,00	0,00
Hedenbergite (S)	0,00	0,00	0,00	0,00	0,00	0,00	0,00	0,00	0,00	0,00	0,00	0,00	0,00	0,00
Aegirine (S)	0,00	0,00	0,00	0,00	0,00	0,00	0,00	0,00	0,00	0,00	0,00	0,00	0,00	0,00
Jadeite (S)	0,52	0,17	0,02	0,10	0,26	0,21	0,19	0,55	0,77	0,49	0,08	0,19	0,42	0,41
Magnesiohornblende (S)	0,00	0,00	0,00	0,00	0,00	0,00	0,00	0,00	0,00	0,00	0,00	0,00	0,00	0,00
Hornblende (S)	0,00	0,00	0,00	0,01	0,00	0,00	0,00	0,00	0,00	0,00	0,00	0,01	0,01	0,00
Ferrohornblende (S)	0,00	0,00	0,01	0,00	0,00	0,00	0,00	0,00	0,00	0,00	0,00	0,00	0,00	0,00
Tremolite (S)	0,00	0,00	0,00	0,00	0,00	0,00	0,00	0,00	0,00	0,00	0,00	0,00	0,00	0,00
Actinolite (S)	0,00	0,00	0,00	0,00	0,00	0,00	0,00	0,00	0,00	0,00	0,00	0,00	0,00	0,00
Anthophyllite (S)	0,00	0,00	0,00	0,00	0,00	0,00	0,00	0,00	0,00	0,00	0,00	0,00	0,00	0,00
Riebeckite-(Mg) (S)	0,00	0,00	0,00	0,00	0,00	0,00	0,00	0,00	0,00	0,00	0,00	0,00	0,00	0,00
Riebeckite (S)	0,00	0,00	0,00	0,00	0,00	0,00	0,00	0,00	0,00	0,00	0,00	0,00	0,00	0,00
Riebeckite-(Fe) (S)	0,00	0,00	0,00	0,00	0,00	0,00	0,00	0,00	0,00	0,00	0,00	0,00	0,00	0,00
Pargasite (S)	0,00	0,00	0,00	0,00	0,00	0,00	0,00	0,00	0,00	0,00	0,00	0,00	0,00	0,00
Talc (S)	0,00	0,00	0,00	0,00	0,00	0,00	0,00	0,00	0,00	0,00	0,00	0,00	0,00	0,00
Illite (S)	2,46	1,20	2,75	0,00	0,51	5,12	7,66	1,21	0,17	1,09	6,17	0,26	2,29	3,61
Kaolinite/Dickite (S)	1,71	0,08	0,16	0,08	0,12	0,09	0,02	0,07	0,00	0,20	0,04	0,00	0,39	0,10
Berthierine (S)	0,05	0,06	0,06	0,00	0,13	0,03	0,04	0,02	0,01	0,01	0,01	0,01	0,04	0,08
Glauconite (S)	0,01	0,01	0,32	0,00	0,01	0,05	0,02	0,00	0,00	0,00	0,08	0,00	0,00	0,03
Montmorillonite (S)	0,54	0,15	0,51	3,39	6,78	1,30	0,74	0,50	0,29	0,20	1,37	0,32	0,62	0,62
Nontronite (S)	0,05	0,23	0,47	0,01	0,74	0,06	0,05	0,11	0,03	0,01	0,12	0,02	0,08	0,17
Saponite (S)	0,00	0,00	0,00	0,06	0,03	0,00	0,05	0,00	0,00	0,00	0,00	0,11	0,00	0,00
Stevensite (S)	0,00	0,00	0,00	0,00	0,00	0,00	0,00	0,00	0,00	0,00	0,00	0,00	0,00	0,00
Gibbsite (S)	0,00	0,00	0,00	0,00	0,00	0,00	0,00	0,00	0,00	0,00	0,00	0,00	0,00	0,00
Halite (S)	0,00	0,00	0,00	0,00	0,00	0,00	0,00	0,00	0,00	0,00	0,00	0,00	0,00	0,00
Aluminium (S)	0,00	0,00	0,00	0,00	0,00	0,00	0,00	0,00	0,00	0,00	0,00	0,00	0,00	0,00
Copper (S)	0,00	0,00	0,00	0,00	0,00	0,00	0,00	0,00	0,00	0,00	0,00	0,00	0,00	0,00
Barite	0,00	0,00	0,00	0,00	0,00	0,00	0,00	0,00	0,00	0,00	0,00	0,00	0,00	0,00
Ferrosilite	0,00	0,00	0,00	0,00	0,00	0,00	0,00	0,00	0,00	0,00	0,00	0,00	0,00	0,00
Halite	0,00	0,00	0,00	0,00	0,00	0,00	0,00	0,00	0,00	0,00	0,00	0,00	0,00	0,00
Fe Oxides	0,08	0,01	0,18	0,00	0,12	0,13	1,31	0,17	0,48	0,06	0,10	0,09	0,24	0,48
Quartz	25,08	20,53	35,68	17,15	12,00	35,81	21,71	17,56	12,51	21,82	34,39	27,65	12,96	16,46
Montmorillonite_Ca_Std	0,00	0,00	0,00	0,01	0,00	0,00	0,00	0,00	0,00	0,00	0,00	0,00	0,00	0,00
Montmorillonite_Na_Std	0,06	0,09	0,02	0,10	0,13	0,09	0,10	0,11	0,24	0,07	0,17	0,07	0,09	0,18
Montmorillonite_Mg_Std	0,00	0,00	0,00	0,00	0,00	0,00	0,00	0,00	0,00	0,00	0,00	0,00	0,00	0,00
Montmorillonite_Mg_Ca_Std	0,00	0,00	0,00	0,00	0,00	0,00	0,00	0,00	0,00	0,00	0,00	0,00	0,00	0,00
Montmorillonite_Na_Ca_Std	0,00	0,00	0,00	0,00	0,00	0,00	0,00	0,00	0,00	0,00	0,00	0,00	0,00	0,00

Montmorillonite_Na_Mg_Std	0,00	0,00	0,00	0,00	0,00	0,00	0,00	0,00	0,00	0,00	0,00	0,00	0,00	0,00
K-Feldspar (A)	0,03	0,13	0,38	0,00	0,00	0,24	0,30	0,01	0,00	0,03	0,63	0,10	0,01	0,14
Illite (Fe) (A)	0,47	0,34	2,02	0,00	0,34	3,10	5,26	0,80	0,02	0,59	3,09	0,17	0,84	2,01
Gypsum/Anhydrite (A)	0,00	0,01	0,00	0,01	0,00	0,02	0,00	0,00	0,00	0,00	0,00	0,00	0,00	0,00
Siderite (Mg) (A)	0,01	0,00	0,00	0,00	0,01	0,00	0,05	0,01	0,02	0,00	0,00	0,05	0,00	0,00
Siderite (Mn) (A)	0,00	0,00	0,00	0,00	0,00	0,00	0,00	0,00	0,00	0,00	0,00	0,00	0,00	0,00
Siderite (Mg_Mn) (A)	0,00	0,00	0,00	0,00	0,00	0,00	0,00	0,00	0,00	0,00	0,00	0,00	0,00	0,00
Pyrophyllite (A)	0,00	0,00	0,00	0,00	0,00	0,00	0,00	0,00	0,00	0,00	0,00	0,00	0,00	0,00
Sylvite (A)	0,00	0,00	0,00	0,00	0,00	0,00	0,00	0,00	0,00	0,00	0,00	0,00	0,00	0,00
Apatite-Quartz (25:75)	0,00	0,06	0,03	0,02	0,01	0,01	0,01	0,11	0,00	0,00	0,01	0,02	0,01	0,00
Calcite-Illite (25:75)	0,03	0,13	0,12	0,00	0,00	0,05	0,02	0,01	0,00	0,02	0,06	0,04	0,02	0,01
Sylvite-Dolomite (75:25)	0,00	0,00	0,00	0,00	0,00	0,00	0,00	0,00	0,00	0,00	0,00	0,00	0,00	0,00
Chlorite-Kutnohorite (75:25)	0,02	0,00	0,05	0,12	0,22	0,00	0,04	0,01	0,00	0,00	0,00	0,05	0,02	0,01
Chlorite-Kutnohorite (25:75)	0,00	0,00	0,00	0,00	0,00	0,00	0,00	0,00	0,00	0,00	0,00	0,00	0,00	0,00
Rutile textures	0,00	0,01	0,01	0,00	0,00	0,00	0,00	0,00	0,00	0,00	0,00	0,00	0,00	0,00
Albite-Quartz (25:75) (A)	0,11	0,08	0,08	0,07	0,01	0,14	0,14	0,04	0,25	0,09	0,69	0,09	0,07	0,21
Biotite-Dolomite (75:25) (A)	0,00	0,00	0,00	0,00	0,00	0,00	0,00	0,00	0,00	0,00	0,00	0,00	0,00	0,00
Chlorite/Illite-Kutnohorite (25:75) (A)	0,00	0,00	0,00	0,00	0,00	0,00	0,00	0,00	0,00	0,00	0,00	0,00	0,00	0,00
Apatite (T)	0,15	0,32	0,89	0,25	0,35	0,15	0,36	2,09	0,13	0,08	0,09	0,50	0,19	0,07
Rutile (T)	0,06	1,08	0,73	0,55	0,02	0,06	0,69	0,81	0,19	0,08	0,31	0,04	0,40	0,34
Kutnohorite-Quartz (75:25)	0,00	0,00	0,00	0,00	0,00	0,00	0,00	0,00	0,00	0,00	0,00	0,00	0,00	0,00
Unclassified	0,06	0,01	0,04	0,01	0,01	0,01	0,01	0,02	0,01	0,01	0,00	0,09	0,10	0,00
Florencite-(Ce) (S)	0,00	0,00	0,00	0,00	0,00	0,00	0,00	0,00	0,00	0,00	0,00	0,00	0,00	0,00
Florencite-(La) (S)	0,00	0,00	0,00	0,00	0,00	0,00	0,00	0,00	0,00	0,00	0,00	0,00	0,00	0,00
Florencite-(Nd) (S)	0,00	0,00	0,00	0,00	0,00	0,00	0,00	0,00	0,00	0,00	0,00	0,00	0,00	0,00
Cr-Spinel R44 (A)	0,00	0,00	0,00	0,00	0,00	0,00	0,00	0,00	0,00	0,00	0,00	0,00	0,00	0,00
Chromite-Spinel R44 (A)	0,00	0,00	0,00	0,00	0,00	0,00	0,00	0,00	0,00	0,00	0,00	0,00	0,00	0,00
Muscovite-(Fe) (A)	0,61	0,12	0,08	0,00	0,06	0,46	0,12	0,22	0,01	1,18	0,43	0,01	0,83	1,11
Ti-Fe-Al Silicate R44 (A)	0,05	0,03	0,03	0,01	0,01	0,01	0,01	0,01	0,00	0,02	0,01	0,00	0,02	0,02
Dolomite (T)	0,00	0,00	0,00	0,00	0,00	0,00	0,00	0,00	0,00	0,00	0,00	0,00	0,00	0,00
K-Al-silicate (lowFe-Mg) (T)	2,98	0,32	0,70	0,00	0,31	3,37	6,14	1,14	0,14	2,94	4,02	0,34	2,82	4,08
Fe-Ox/Carb (T)	0,11	0,01	0,08	0,00	0,17	0,09	0,69	0,11	0,27	0,04	0,08	0,31	0,24	0,45
Staurolite-(Mg) (S)	0,00	0,00	0,00	0,00	0,00	0,00	0,00	0,00	0,00	0,00	0,00	0,00	0,00	0,00
Staurolite-(Mg) (A)	0,00	0,00	0,00	0,00	0,00	0,00	0,00	0,00	0,00	0,00	0,00	0,00	0,00	0,00
Monazite (T)	0,00	0,00	0,00	0,00	0,00	0,00	0,00	0,00	0,00	0,00	0,00	0,00	0,00	0,00
Zircon (T)	0,00	0,01	0,00	0,00	0,00	0,00	0,00	0,00	0,00	0,00	0,00	0,02	0,00	0,00
Cr (T)	0,00	0,00	0,00	0,01	0,00	0,00	0,00	0,00	0,00	0,00	0,00	0,00	0,00	0,00
Illite (A)	0,19	0,05	0,19	0,00	0,03	0,43	0,48	0,10	0,01	0,12	1,06	0,07	0,14	0,35
Ti-Fe Oxide (A)	0,00	0,00	0,00	0,00	0,00	0,00	0,00	0,00	0,00	0,01	0,00	0,00	0,00	0,00
Fe-Ti Oxide (A)	0,04	0,00	0,01	0,00	0,02	0,03	0,87	0,01	0,26	0,03	0,03	0,00	0,36	0,05
Ti-Al-Silicate R09 (A)	0,01	0,39	0,06	0,13	0,00	0,00	0,09	0,01	0,02	0,02	0,02	0,00	0,06	0,12
Ca-Fe-Al-Silicate R09 (A)	0,02	0,03	0,02	5,25	0,05	1,20	0,47	0,01	0,00	0,01	0,02	3,41	0,04	0,00
FeOx-Silica texture R09 (A)	0,12	0,01	0,19	0,00	0,62	0,13	0,54	0,05	0,19	0,04	0,25	0,10	0,31	1,10
Silica-FeOx texture R09 (A)	0,62	0,33	4,04	0,05	2,32	0,55	0,90	0,36	0,17	0,07	1,50	0,27	1,21	1,79
Calcite-FeOx boundary R09 (R)	0,26	0,05	0,04	0,01	0,02	0,00	0,01	0,02	0,04	0,04	0,05	0,12	0,21	0,06

FeOx-Calcite boundary R09 (R)	0,04	0,00	0,01	0,00	0,00	0,00	0,00	0,00	0,00	0,02	0,01	0,01	0,03	0,02	0,01
Pyrite textures	0,00	0,00	0,00	0,00	0,00	0,00	0,00	0,00	0,00	0,00	0,00	0,00	0,00	0,00	0,00
Calcite/Aragonite textures	15,78	15,86	17,00	16,48	17,06	16,45	15,47	15,25	15,11	15,56	15,37	16,47	16,26	15,96	
Goethite/Lepidocrocite	15,45	14,84	16,36	14,84	15,24	16,01	15,91	17,54	15,33	16,69	15,54	17,72	16,48	15,87	
Jarosite	0,00	0,00	0,00	0,00	0,00	0,00	0,00	0,00	0,00	0,00	0,00	0,00	0,00	0,00	0,00
Schwertmannite	14,84	0,00	0,00	0,00	0,00	14,84	14,84	0,00	0,00	0,00	0,00	0,00	0,00	0,00	0,00
Halotrichite	0,00	0,00	0,00	0,00	0,00	0,00	0,00	0,00	0,00	0,00	0,00	0,00	0,00	0,00	0,00
Apatite textures	15,11	15,10	15,47	14,97	15,18	15,12	14,92	14,89	15,00	14,91	15,01	15,10	15,27	14,93	
Siderite (Mg-Zn)	14,84	0,00	0,00	0,00	0,00	0,00	0,00	0,00	0,00	0,00	0,00	0,00	0,00	0,00	0,00
Dolomite textures	15,69	14,84	16,08	15,21	16,08	14,84	15,02	14,88	14,96	15,15	14,91	15,74	15,30	15,14	
Kutnohorite	0,00	0,00	0,00	0,00	0,00	0,00	0,00	0,00	0,00	0,00	15,93	0,00	0,00	0,00	0,00
Rhodochrosite	0,00	0,00	0,00	0,00	0,00	0,00	0,00	0,00	0,00	0,00	0,00	0,00	0,00	0,00	0,00
Quartz textures	15,95	16,10	16,92	16,05	15,82	15,73	15,35	15,49	15,14	15,52	15,75	17,49	16,99	15,71	
Kaolinite textures	18,33	15,59	16,78	17,69	17,04	19,10	15,98	15,56	15,40	16,09	19,10	16,29	16,95	16,64	
Clinochrysotile	0,00	0,00	0,00	14,84	0,00	0,00	0,00	0,00	0,00	14,84	0,00	0,00	0,00	0,00	0,00
Albite textures	15,09	15,02	15,32	15,09	15,12	14,98	14,96	15,11	14,98	15,00	15,03	15,18	15,40	15,00	
Annite	15,98	14,96	15,31	17,53	15,41	16,56	15,74	16,06	15,76	15,45	15,11	15,00	16,49	16,10	
Phlogopite	0,00	0,00	0,00	0,00	0,00	0,00	0,00	0,00	0,00	0,00	0,00	0,00	0,00	0,00	0,00
Annite-Phlogopite	15,52	14,98	15,05	14,84	15,11	15,51	15,77	15,21	14,84	15,14	15,16	16,72	15,48	15,28	
Muscovite textures	14,98	14,99	14,88	0,00	14,84	14,84	14,84	14,84	14,84	15,01	14,84	14,84	14,84	14,84	14,84
Illite textures	15,43	15,11	15,67	15,53	15,40	15,54	15,28	15,29	14,93	15,11	15,44	15,85	15,54	15,23	
Ripidilite	15,93	15,22	15,65	15,13	15,35	14,84	15,33	15,47	15,00	15,06	14,84	15,45	15,59	15,22	
Glaucofanite	14,84	14,84	16,95	14,98	15,06	14,84	14,99	14,84	14,84	14,84	0,00	15,06	14,84	15,43	
Montmorillonite textures	17,29	16,52	18,85	25,19	25,55	17,84	16,94	16,82	15,57	16,83	15,96	18,43	19,64	17,22	
Palygorskite	15,11	15,36	14,96	15,19	15,15	14,92	15,10	15,29	14,84	15,07	15,11	15,21	15,15	15,00	
Beidellite	15,32	15,23	15,04	16,64	15,15	14,95	14,95	14,98	14,92	15,03	14,99	14,84	15,13	15,45	
Sepiolite	0,00	14,84	0,00	0,00	0,00	0,00	0,00	0,00	14,84	0,00	0,00	14,84	0,00	0,00	0,00
Corrensite	15,36	14,84	15,17	15,29	15,20	15,17	15,63	15,20	15,36	15,26	15,78	16,54	15,34	15,12	
Clinzoisite	14,84	14,84	14,84	16,95	14,84	14,84	14,84	0,00	0,00	14,84	0,00	14,84	0,00	0,00	0,00
Fluorite	0,00	0,00	0,00	0,00	0,00	0,00	0,00	0,00	0,00	0,00	0,00	0,00	0,00	0,00	0,00
Pores	0,00	0,00	0,00	0,00	0,00	0,00	0,00	0,00	0,00	0,00	0,00	0,00	0,00	0,00	0,00
Rutile/Anatase (S)	15,19	15,66	15,24	14,84	14,84	14,84	15,00	15,65	15,22	15,68	14,84	0,00	18,40	14,84	
Cassiterite (S)	0,00	0,00	0,00	0,00	0,00	0,00	0,00	0,00	0,00	0,00	0,00	0,00	0,00	0,00	0,00
Baddeleyite (S)	0,00	0,00	0,00	0,00	0,00	0,00	0,00	0,00	0,00	0,00	0,00	0,00	0,00	0,00	0,00
Spinel (S)	0,00	0,00	0,00	0,00	0,00	0,00	0,00	0,00	0,00	0,00	0,00	0,00	0,00	0,00	0,00
Magnesiocromite (S)	0,00	0,00	0,00	0,00	0,00	0,00	0,00	0,00	0,00	0,00	0,00	0,00	0,00	0,00	0,00
Chromite (S)	0,00	0,00	0,00	0,00	0,00	0,00	0,00	0,00	0,00	0,00	0,00	0,00	0,00	0,00	0,00
Hercynite (S)	0,00	0,00	0,00	0,00	0,00	0,00	14,84	0,00	0,00	0,00	0,00	0,00	0,00	0,00	0,00
Gahnite (S)	0,00	0,00	0,00	0,00	0,00	0,00	0,00	0,00	0,00	0,00	0,00	0,00	0,00	0,00	0,00
Ulvospinel (S)	0,00	0,00	0,00	0,00	0,00	0,00	0,00	0,00	0,00	0,00	0,00	0,00	0,00	0,00	0,00
Ilmenite (S)	14,84	14,84	14,84	0,00	14,84	22,55	18,06	15,54	14,84	18,28	17,80	0,00	16,95	14,84	
Magnetite (S)	15,33	14,84	16,01	14,84	15,07	15,26	15,15	14,99	15,16	15,26	14,92	14,96	15,12	15,25	
Hematite (S)	15,35	15,00	18,41	17,80	15,21	15,32	15,51	15,14	15,54	15,33	14,97	15,07	15,60	15,30	
Perovskite (S)	0,00	0,00	0,00	0,00	0,00	0,00	0,00	0,00	0,00	0,00	0,00	0,00	0,00	0,00	0,00
Calcite (S)	36,54	31,53	73,34	28,40	28,32	57,87	34,29	35,99	53,20	43,93	37,33	57,97	54,41	40,99	
Dolomite (S)	14,92	15,09	14,91	14,84	14,84	0,00	14,84	14,84	14,84	15,75	14,84	14,95	15,00	14,84	
Ankerite (S)	15,40	14,84	14,84	14,84	14,84	14,84	14,84	14,84	14,84	19,67	14,84	14,94	14,84	14,84	

Magnesite (S)	0,00	0,00	0,00	0,00	0,00	0,00	0,00	0,00	0,00	0,00	0,00	0,00	0,00	0,00
Siderite (S)	15,03	14,84	16,03	0,00	15,98	14,84	14,84	15,01	14,84	14,84	14,84	14,97	15,44	14,84
Pyrite (S)	14,84	15,95	15,46	16,58	14,84	17,67	15,72	16,69	14,84	16,18	16,69	16,51	14,84	14,84
Chalcopyrite (S)	0,00	0,00	0,00	0,00	0,00	0,00	0,00	0,00	0,00	0,00	0,00	0,00	0,00	0,00
Sphalerite (S)	0,00	0,00	0,00	0,00	0,00	0,00	0,00	0,00	0,00	0,00	0,00	0,00	0,00	0,00
Galena (S)	0,00	0,00	0,00	0,00	0,00	0,00	0,00	0,00	0,00	0,00	0,00	0,00	0,00	0,00
Anhydrite (S)	0,00	14,84	0,00	0,00	0,00	0,00	0,00	0,00	0,00	0,00	0,00	0,00	0,00	0,00
Gypsum (S)	0,00	14,84	0,00	0,00	0,00	14,84	0,00	0,00	0,00	0,00	0,00	0,00	0,00	0,00
Chlorapatite (S)	0,00	0,00	0,00	0,00	0,00	0,00	0,00	0,00	0,00	0,00	0,00	0,00	0,00	0,00
Fluorapatite (S)	14,84	14,97	15,24	14,84	14,84	0,00	14,84	14,84	14,84	14,84	14,84	14,84	14,84	14,84
Apatite (S)	23,34	15,84	16,56	19,97	21,16	19,69	20,87	15,28	21,82	21,57	17,55	17,98	19,28	19,18
Monazite-(Ce) (S)	0,00	0,00	0,00	0,00	0,00	0,00	0,00	0,00	0,00	0,00	0,00	0,00	0,00	0,00
Monazite-(La) (S)	0,00	0,00	0,00	0,00	0,00	0,00	0,00	0,00	0,00	0,00	0,00	0,00	0,00	0,00
Monazite-(Nd) (S)	0,00	0,00	0,00	0,00	0,00	0,00	0,00	0,00	0,00	0,00	0,00	0,00	0,00	0,00
Xenotime-(Y) (S)	14,84	0,00	0,00	0,00	0,00	0,00	0,00	0,00	0,00	0,00	0,00	0,00	0,00	0,00
Xenotime-(Yb) (S)	0,00	0,00	0,00	0,00	0,00	0,00	0,00	0,00	0,00	0,00	0,00	0,00	0,00	0,00
Zircon (S)	40,60	14,84	0,00	0,00	27,05	14,84	32,37	0,00	14,84	14,84	14,84	16,32	0,00	14,84
Titanite (S)	14,84	15,21	14,88	15,63	15,25	16,04	16,24	15,94	16,44	14,84	17,02	15,63	14,84	14,84
Opal (S)	14,84	14,90	14,84	0,00	0,00	0,00	0,00	0,00	0,00	16,58	0,00	0,00	0,00	0,00
Dravite (S)	0,00	0,00	0,00	0,00	0,00	0,00	0,00	0,00	0,00	0,00	0,00	0,00	0,00	0,00
Dravite-Schorl (S)	14,84	0,00	0,00	0,00	0,00	0,00	0,00	0,00	0,00	14,84	0,00	0,00	14,84	0,00
Schorl (S)	14,84	0,00	0,00	0,00	0,00	0,00	0,00	0,00	0,00	0,00	0,00	0,00	0,00	0,00
Elbait (S)	14,84	14,84	14,84	0,00	0,00	0,00	0,00	0,00	0,00	0,00	0,00	0,00	0,00	0,00
Almandine (S)	16,42	14,96	15,40	14,84	16,04	16,61	15,30	15,77	14,84	15,66	14,92	16,54	17,88	15,91
Spessartine (S)	0,00	0,00	0,00	0,00	0,00	0,00	0,00	0,00	0,00	0,00	0,00	0,00	0,00	0,00
Pyrope (S)	0,00	0,00	0,00	0,00	14,84	0,00	14,84	0,00	0,00	0,00	0,00	0,00	0,00	0,00
Grossular (S)	0,00	14,84	0,00	14,84	0,00	0,00	14,84	0,00	14,84	0,00	14,84	0,00	0,00	0,00
Andradite (S)	0,00	0,00	0,00	0,00	0,00	0,00	0,00	22,25	14,84	0,00	0,00	0,00	0,00	0,00
Uvarovite (S)	0,00	0,00	0,00	0,00	0,00	0,00	0,00	0,00	0,00	0,00	0,00	0,00	0,00	0,00
Alm-Sp (2:1) (S)	0,00	0,00	0,00	0,00	0,00	0,00	0,00	0,00	0,00	0,00	0,00	0,00	0,00	0,00
Sp-Alm (2:1) (S)	0,00	0,00	0,00	0,00	0,00	0,00	0,00	0,00	0,00	0,00	0,00	0,00	0,00	0,00
Alm-Grs (2:1) (S)	15,95	15,10	15,39	15,54	15,77	18,16	15,41	15,66	16,40	15,63	15,43	17,31	16,52	16,58
Grs-Alm (2:1) (S)	14,84	14,84	0,00	22,95	21,84	32,03	27,00	17,80	14,84	14,84	14,84	33,38	14,84	14,84
Alm-Py (2:1) (S)	15,35	15,24	15,13	15,28	15,68	15,71	15,35	15,86	15,00	15,23	15,36	15,83	15,75	15,26
Py-Alm (2:1) (S)	15,44	15,00	15,11	16,42	17,61	15,39	16,28	15,20	15,06	15,33	15,18	15,98	15,56	15,57
Sp-Grs (2:1) (S)	0,00	0,00	0,00	0,00	0,00	0,00	0,00	0,00	0,00	0,00	0,00	0,00	0,00	0,00
Grs-Sp (2:1) (S)	0,00	0,00	0,00	0,00	0,00	0,00	0,00	0,00	0,00	0,00	0,00	0,00	0,00	0,00
Sp-Py (2:1) (S)	0,00	0,00	0,00	0,00	0,00	0,00	0,00	0,00	0,00	0,00	0,00	0,00	0,00	0,00
Py-Sp (2:1) (S)	0,00	0,00	0,00	0,00	0,00	0,00	0,00	0,00	0,00	0,00	0,00	0,00	0,00	0,00
Alm-Sp-Grs (S)	0,00	0,00	0,00	0,00	0,00	0,00	0,00	0,00	0,00	0,00	0,00	0,00	0,00	0,00
Alm-Sp-Py (S)	0,00	0,00	0,00	0,00	0,00	0,00	14,84	0,00	0,00	0,00	0,00	0,00	0,00	0,00
And-Grs (2:1) (S)	0,00	14,84	0,00	14,84	0,00	0,00	0,00	14,84	0,00	0,00	14,84	0,00	0,00	0,00
Grs-And (2:1) (S)	14,84	14,84	0,00	16,25	0,00	0,00	0,00	14,84	0,00	0,00	14,84	16,69	0,00	0,00
And-Uv (2:1) (S)	0,00	0,00	0,00	0,00	0,00	0,00	0,00	0,00	0,00	0,00	0,00	0,00	0,00	0,00
Uv-And (2:1) (S)	0,00	0,00	0,00	0,00	0,00	0,00	0,00	0,00	0,00	0,00	0,00	0,00	0,00	0,00
Staurolite (S)	0,00	14,84	0,00	0,00	0,00	14,84	0,00	0,00	0,00	0,00	0,00	0,00	0,00	0,00
Sillimanite/Kyanite/Andalusite (S)	0,00	0,00	0,00	0,00	0,00	0,00	0,00	0,00	0,00	0,00	0,00	0,00	0,00	0,00

Epidote-(Fe) (S)	14,84	14,84	14,84	0,00	14,84	0,00	0,00	0,00	0,00	0,00	14,84	19,78	14,84	14,84
Epidote (S)	16,41	14,99	15,68	15,73	17,18	15,66	15,46	20,54	14,84	16,07	16,05	16,36	18,00	17,18
Epidote-(Al) (S)	0,00	17,53	0,00	15,78	15,89	17,15	15,56	0,00	0,00	0,00	14,84	15,86	14,84	14,84
Zoisite (S)	0,00	0,00	14,84	14,84	0,00	14,84	0,00	0,00	0,00	0,00	0,00	0,00	14,84	0,00
Piemontite (S)	0,00	0,00	0,00	0,00	0,00	0,00	0,00	0,00	0,00	0,00	0,00	0,00	0,00	0,00
Allanite-(Ce) (S)	0,00	0,00	0,00	0,00	0,00	0,00	0,00	0,00	0,00	0,00	0,00	0,00	0,00	0,00
Allanite-(La) (S)	0,00	0,00	0,00	0,00	0,00	0,00	0,00	0,00	0,00	0,00	0,00	0,00	0,00	0,00
Allanite-(Y) (S)	0,00	0,00	0,00	0,00	0,00	0,00	0,00	0,00	0,00	0,00	0,00	0,00	0,00	0,00
Cordierite-(Mg) (S)	0,00	0,00	0,00	0,00	0,00	0,00	0,00	0,00	0,00	0,00	0,00	0,00	0,00	0,00
Cordierite (S)	15,21	14,84	14,88	14,84	14,98	14,84	14,84	14,84	14,84	14,96	14,84	0,00	15,24	15,00
Cordierite-(Fe) (S)	15,13	15,17	14,84	14,84	16,95	14,84	0,00	14,84	0,00	15,43	14,84	0,00	14,96	16,37
Albite (S)	58,58	36,92	23,65	31,23	32,81	50,96	29,06	43,09	72,52	115,60	23,45	71,14	59,17	53,60
Oligoclase (S)	15,20	14,93	16,72	15,03	15,10	15,26	14,89	14,98	14,94	15,12	15,03	15,23	15,25	15,74
Andesine (S)	16,04	15,63	15,72	15,94	16,52	16,08	15,55	15,45	15,02	15,34	15,44	15,80	16,31	15,62
Labradorite (S)	15,99	15,13	15,34	15,53	15,79	15,39	15,14	15,24	14,84	15,15	15,26	15,30	15,51	15,99
Bytownite (S)	0,00	14,84	0,00	14,84	0,00	0,00	0,00	0,00	0,00	0,00	0,00	0,00	0,00	0,00
Anorthite (S)	15,20	14,84	15,39	15,54	14,84	14,97	14,84	0,00	0,00	15,27	14,84	14,84	14,84	14,84
Anorthoclase (S)	14,89	14,88	14,93	14,84	15,00	15,18	15,05	14,98	14,85	14,87	15,13	14,97	14,99	15,00
Sanidine (S)	14,84	14,84	14,84	0,00	0,00	14,84	15,29	14,84	0,00	14,84	14,98	15,13	14,84	14,84
Muscovite (S)	21,86	19,07	20,52	16,85	16,69	18,92	15,74	15,72	16,53	22,79	16,30	18,18	21,63	19,52
Biotite (S)	16,56	15,85	17,93	16,11	16,44	19,95	18,54	16,10	16,00	17,52	15,56	16,70	19,12	17,52
Paragonite (S)	15,28	14,84	14,84	14,84	0,00	0,00	0,00	0,00	0,00	17,31	0,00	0,00	0,00	0,00
Clinocllore (S)	18,99	15,30	18,16	17,87	17,30	15,65	19,45	15,38	15,92	17,49	16,38	22,91	17,56	17,01
Chlorite (S)	15,64	15,08	15,42	15,76	15,42	16,25	15,79	16,02	16,48	15,43	15,51	16,40	15,73	15,44
Chamosite (S)	24,01	37,52	26,60	31,58	21,19	22,63	22,11	27,42	25,70	24,99	27,29	39,54	33,52	22,38
Chloritoid (S)	0,00	0,00	0,00	0,00	0,00	0,00	0,00	0,00	0,00	0,00	0,00	0,00	0,00	0,00
Forsterite (S)	0,00	0,00	0,00	0,00	0,00	0,00	0,00	0,00	0,00	0,00	0,00	0,00	0,00	0,00
Olivine Fo90 (S)	0,00	0,00	0,00	29,67	0,00	0,00	0,00	0,00	0,00	0,00	0,00	0,00	0,00	0,00
Olivine Fo80 (S)	0,00	0,00	0,00	0,00	0,00	0,00	0,00	0,00	0,00	0,00	0,00	0,00	0,00	0,00
Olivine Fo70 (S)	0,00	0,00	0,00	0,00	0,00	0,00	0,00	0,00	0,00	0,00	0,00	0,00	0,00	0,00
Olivine Fo60 (S)	0,00	0,00	0,00	0,00	0,00	0,00	0,00	0,00	0,00	0,00	0,00	0,00	0,00	0,00
Olivine Fo50 (S)	0,00	0,00	0,00	0,00	0,00	0,00	0,00	0,00	0,00	0,00	0,00	0,00	0,00	0,00
Olivine Fo40 (S)	0,00	0,00	0,00	0,00	0,00	0,00	0,00	0,00	0,00	0,00	0,00	14,84	0,00	0,00
Olivine Fo30 (S)	0,00	0,00	14,84	0,00	14,84	29,67	14,84	0,00	0,00	0,00	0,00	15,71	0,00	14,84
Olivine Fo20 (S)	14,84	0,00	0,00	0,00	15,18	14,84	15,72	14,84	14,84	0,00	0,00	16,07	14,84	16,25
Olivine Fo10 (S)	15,16	14,84	15,13	14,84	15,61	15,45	15,44	15,09	15,06	15,53	15,10	15,56	15,94	15,69
Fayalite (S)	15,76	14,84	15,51	14,84	15,61	15,31	15,37	15,57	14,84	14,84	15,06	15,89	15,56	15,54
Enstatite (S)	0,00	0,00	0,00	0,00	0,00	0,00	17,80	0,00	25,96	0,00	0,00	0,00	0,00	0,00
OPX En90 (S)	0,00	0,00	0,00	0,00	0,00	0,00	0,00	0,00	14,84	0,00	0,00	0,00	0,00	0,00
OPX En80 (S)	0,00	0,00	0,00	0,00	0,00	0,00	0,00	0,00	0,00	0,00	0,00	0,00	0,00	0,00
OPX En70 (S)	0,00	0,00	0,00	0,00	0,00	0,00	0,00	0,00	0,00	0,00	0,00	0,00	0,00	0,00
OPX En60 (S)	0,00	14,84	0,00	0,00	0,00	0,00	0,00	0,00	0,00	0,00	0,00	14,84	0,00	0,00
OPX En50 (S)	0,00	0,00	0,00	0,00	14,84	0,00	14,84	0,00	0,00	0,00	0,00	14,84	0,00	0,00
OPX En40 (S)	14,84	0,00	14,84	14,84	14,84	14,84	14,84	0,00	14,84	0,00	0,00	15,60	14,84	14,84
OPX En30 (S)	14,84	0,00	14,84	0,00	15,17	14,84	15,10	14,84	14,84	14,84	0,00	16,95	17,80	14,84
OPX En20 (S)	14,84	0,00	0,00	0,00	15,12	16,95	15,01	16,48	14,84	14,84	14,84	15,71	15,89	15,45
OPX En10 (S)	15,09	14,84	15,36	16,18	15,62	15,43	15,52	15,55	15,27	15,77	15,10	15,83	16,11	15,54

OPX En0 (S)	15,08	14,84	14,84	14,84	15,38	15,06	15,41	14,84	14,84	14,84	15,07	15,28	15,45	15,22
Augite (S)	14,84	14,84	15,59	15,47	16,07	14,84	14,84	14,84	14,84	14,84	14,84	16,03	17,31	14,84
Diopside (S)	0,00	0,00	0,00	0,00	0,00	0,00	0,00	0,00	0,00	0,00	0,00	0,00	0,00	0,00
Diopside-Hedenbergite (S)	14,84	0,00	14,84	0,00	14,84	0,00	14,84	0,00	0,00	0,00	0,00	14,84	0,00	0,00
Hedenbergite (S)	14,84	14,84	0,00	0,00	0,00	0,00	14,84	0,00	0,00	0,00	14,84	14,84	0,00	0,00
Aegirine (S)	14,84	0,00	14,84	0,00	14,84	0,00	0,00	0,00	14,84	0,00	14,84	0,00	0,00	14,84
Jadeite (S)	15,17	14,98	15,30	15,12	15,27	15,04	15,03	15,11	15,02	15,00	15,05	15,20	15,11	15,11
Magnesiohornblende (S)	0,00	0,00	0,00	0,00	0,00	0,00	0,00	0,00	0,00	0,00	0,00	0,00	0,00	0,00
Hornblende (S)	15,36	15,17	14,84	15,37	15,18	14,84	14,84	15,92	14,84	16,62	15,89	16,21	15,61	19,78
Ferrohornblende (S)	14,84	15,08	15,77	16,07	15,41	14,84	14,84	14,84	14,84	14,84	15,66	15,64	17,39	14,84
Tremolite (S)	0,00	0,00	0,00	0,00	0,00	0,00	0,00	0,00	0,00	0,00	0,00	0,00	0,00	0,00
Actinolite (S)	0,00	0,00	0,00	0,00	0,00	0,00	0,00	0,00	0,00	0,00	0,00	14,84	14,84	0,00
Anthophyllite (S)	0,00	0,00	0,00	0,00	0,00	0,00	0,00	0,00	0,00	0,00	0,00	0,00	0,00	0,00
Riebeckite-(Mg) (S)	0,00	0,00	0,00	0,00	0,00	0,00	0,00	0,00	0,00	0,00	0,00	0,00	0,00	0,00
Riebeckite (S)	0,00	0,00	0,00	0,00	14,84	0,00	0,00	0,00	0,00	0,00	0,00	0,00	0,00	0,00
Riebeckite-(Fe) (S)	14,84	0,00	14,84	0,00	15,45	14,84	15,66	0,00	14,84	14,84	14,84	14,84	14,84	14,84
Pargasite (S)	0,00	0,00	0,00	14,84	16,18	0,00	14,84	0,00	0,00	0,00	0,00	14,84	0,00	14,84
Talc (S)	14,84	14,84	0,00	0,00	0,00	0,00	17,80	0,00	16,48	0,00	14,84	0,00	14,84	0,00
Illite (S)	16,71	15,63	16,50	16,18	15,94	18,68	18,88	15,64	15,17	15,66	17,11	17,30	16,57	16,77
Kaolinite/Dickite (S)	18,66	15,37	15,24	19,31	15,31	15,12	15,05	15,13	14,84	15,50	15,07	14,84	15,62	15,86
Berthierine (S)	17,18	14,98	16,02	14,84	16,92	16,55	15,36	16,05	14,98	15,12	15,18	16,40	17,23	16,24
Glauconite (S)	15,21	14,99	15,17	14,84	15,31	15,13	15,38	14,95	0,00	14,84	15,10	14,84	15,04	15,13
Montmorillonite (S)	15,41	15,00	15,20	17,18	18,22	15,77	15,44	15,25	14,96	15,10	15,52	15,52	15,69	15,36
Nontronite (S)	14,97	14,94	15,33	14,87	15,29	15,01	14,88	14,88	14,85	14,84	14,86	14,98	15,09	15,03
Saponite (S)	16,48	14,84	15,03	15,07	15,09	14,84	15,20	14,84	14,84	14,84	19,78	15,56	14,84	15,06
Stevensite (S)	0,00	0,00	0,00	0,00	0,00	0,00	0,00	0,00	14,84	0,00	0,00	0,00	0,00	14,84
Gibbsite (S)	0,00	0,00	0,00	0,00	0,00	0,00	0,00	0,00	0,00	0,00	0,00	0,00	0,00	0,00
Halite (S)	0,00	0,00	0,00	0,00	0,00	0,00	0,00	0,00	0,00	0,00	0,00	0,00	0,00	0,00
Aluminium (S)	0,00	0,00	14,84	0,00	0,00	0,00	0,00	0,00	0,00	0,00	0,00	0,00	0,00	0,00
Copper (S)	0,00	0,00	0,00	0,00	0,00	0,00	0,00	0,00	0,00	0,00	0,00	0,00	0,00	0,00
Barite	0,00	14,84	0,00	0,00	0,00	14,84	14,84	0,00	0,00	0,00	0,00	0,00	0,00	0,00
Ferrosilite	0,00	0,00	0,00	14,84	14,84	14,84	14,84	0,00	14,84	0,00	14,84	14,84	0,00	14,84
Halite	0,00	0,00	0,00	25,96	0,00	0,00	0,00	0,00	14,84	0,00	0,00	0,00	0,00	0,00
Fe Oxides	19,22	15,17	26,78	22,25	20,71	28,25	21,84	16,89	20,10	20,75	17,14	18,69	24,15	21,64
Quartz	54,04	43,51	41,77	31,39	28,57	64,32	39,31	33,17	27,36	95,77	28,42	77,16	46,01	36,85
Montmorillonite_Ca_Std	15,66	15,11	14,84	15,30	14,84	14,84	14,84	15,14	14,84	16,18	16,58	15,15	15,71	14,84
Montmorillonite_Na_Std	15,11	14,93	15,04	14,97	15,12	14,93	15,03	15,00	14,94	14,93	15,05	15,10	15,19	15,13
Montmorillonite_Mg_Std	14,84	14,84	14,84	15,14	14,93	14,84	15,54	14,84	14,84	14,84	14,84	14,84	14,84	14,84
Montmorillonite_Mg_Ca_Std	0,00	0,00	0,00	0,00	0,00	0,00	0,00	0,00	0,00	0,00	0,00	0,00	0,00	0,00
Montmorillonite_Na_Ca_Std	0,00	0,00	0,00	0,00	0,00	0,00	0,00	0,00	0,00	0,00	0,00	0,00	0,00	0,00
Montmorillonite_Na_Mg_Std	0,00	0,00	0,00	0,00	0,00	0,00	0,00	0,00	0,00	0,00	0,00	0,00	0,00	0,00
K-Feldspar (A)	14,98	15,08	15,15	29,67	14,84	15,16	15,17	14,98	14,84	14,95	15,19	15,49	15,24	15,19
Illite (Fe) (A)	15,45	15,15	16,02	14,84	15,67	17,99	17,92	15,65	15,01	15,54	16,17	16,77	16,00	16,30
Gypsum/Anhydrite (A)	15,38	14,84	15,09	16,55	14,84	19,52	15,66	15,89	15,38	14,84	14,84	16,07	16,48	15,82
Siderite (Mg) (A)	17,92	14,84	15,13	14,84	15,17	16,04	15,13	14,88	15,03	15,73	14,84	15,51	14,84	14,95
Siderite (Mn) (A)	0,00	0,00	0,00	0,00	0,00	0,00	14,84	0,00	0,00	0,00	0,00	0,00	0,00	0,00
Siderite (Mg_Mn) (A)	14,84	0,00	0,00	0,00	0,00	0,00	0,00	0,00	0,00	0,00	0,00	0,00	0,00	0,00

Pyrophyllite (A)	14,84	14,84	14,84	14,84	0,00	0,00	0,00	14,84	0,00	14,84	0,00	0,00	14,84	14,84
Sylvite (A)	0,00	0,00	0,00	0,00	0,00	0,00	0,00	0,00	0,00	0,00	0,00	0,00	0,00	0,00
Apatite-Quartz (25:75)	15,00	15,04	15,12	15,04	15,32	15,27	14,93	15,14	15,10	15,13	15,22	15,53	15,80	15,18
Calcite-Illite (25:75)	15,93	15,32	15,51	29,67	15,56	15,58	15,59	15,23	14,84	15,54	15,57	17,28	16,41	15,81
Sylvite-Dolomite (75:25)	0,00	0,00	0,00	0,00	0,00	0,00	0,00	0,00	0,00	0,00	0,00	0,00	0,00	0,00
Chlorite-Kutnohorite (75:25)	15,63	14,97	15,80	15,28	15,30	17,20	15,12	15,30	14,84	15,30	15,01	15,65	15,96	15,15
Chlorite-Kutnohorite (25:75)	0,00	0,00	0,00	0,00	0,00	0,00	0,00	0,00	0,00	0,00	0,00	0,00	0,00	0,00
Rutile textures	14,84	14,97	15,21	14,84	0,00	0,00	14,84	14,84	14,84	14,84	14,84	0,00	16,25	14,84
Albite-Quartz (25:75) (A)	15,03	14,93	14,94	14,94	15,06	14,92	15,04	15,05	14,95	14,94	15,16	15,11	15,14	15,06
Biotite-Dolomite (75:25) (A)	17,31	14,84	15,70	0,00	14,84	14,84	15,33	14,84	0,00	17,03	16,95	17,12	14,84	16,48
Chlorite/Illite-Kutnohorite (25:75) (A)	17,18	14,84	15,21	14,84	18,74	14,84	14,84	14,84	14,84	16,48	17,31	18,54	17,01	14,84
Apatite (T)	18,54	15,52	18,09	15,33	17,24	17,58	16,43	15,73	16,54	18,26	15,83	19,67	19,19	17,13
Rutile (T)	16,55	20,06	19,11	15,80	16,32	19,20	17,30	17,37	16,41	17,65	16,85	15,53	17,52	15,79
Kutnohorite-Quartz (75:25)	0,00	0,00	0,00	0,00	0,00	0,00	0,00	0,00	0,00	0,00	0,00	0,00	0,00	0,00
Unclassified	30,92	31,42	31,51	29,87	30,77	33,02	31,80	30,98	33,00	30,39	29,97	30,96	31,49	29,46
Florencite-(Ce) (S)	0,00	0,00	0,00	0,00	0,00	0,00	0,00	0,00	0,00	0,00	0,00	0,00	0,00	0,00
Florencite-(La) (S)	0,00	0,00	0,00	0,00	0,00	0,00	0,00	0,00	0,00	0,00	0,00	0,00	0,00	0,00
Florencite-(Nd) (S)	0,00	0,00	0,00	0,00	0,00	0,00	0,00	0,00	0,00	0,00	0,00	0,00	0,00	0,00
Cr-Spinel R44 (A)	0,00	0,00	0,00	19,45	0,00	0,00	0,00	0,00	0,00	0,00	0,00	0,00	0,00	0,00
Chromite-Spinel R44 (A)	0,00	0,00	0,00	14,84	0,00	0,00	0,00	0,00	0,00	0,00	0,00	0,00	0,00	0,00
Muscovite-(Fe) (A)	15,74	15,06	15,04	19,07	15,42	15,72	15,02	15,28	15,03	16,70	15,29	15,49	16,29	15,93
Ti-Fe-Al Silicate R44 (A)	15,81	14,94	15,03	14,88	14,99	14,99	14,84	14,93	14,84	15,18	14,84	14,84	15,00	14,95
Dolomite (T)	14,84	0,00	0,00	14,84	0,00	0,00	0,00	0,00	14,84	14,84	0,00	0,00	0,00	0,00
K-Al-silicate (lowFe-Mg) (T)	17,76	15,49	16,10	15,48	16,08	17,92	18,51	15,89	15,38	18,25	16,52	18,54	17,49	17,43
Fe-Ox/Carb (T)	16,79	14,99	17,38	18,13	17,01	18,82	16,67	15,70	16,02	15,86	15,18	17,06	19,25	17,75
Staurolite-(Mg) (S)	0,00	0,00	0,00	0,00	0,00	0,00	0,00	0,00	0,00	0,00	0,00	0,00	0,00	0,00
Staurolite-(Mg) (A)	0,00	0,00	0,00	0,00	14,84	0,00	0,00	0,00	0,00	0,00	0,00	0,00	0,00	0,00
Monazite (T)	0,00	14,84	0,00	0,00	0,00	0,00	0,00	0,00	0,00	0,00	0,00	0,00	0,00	0,00
Zircon (T)	15,58	15,05	14,84	14,84	16,95	15,71	15,98	15,62	15,89	14,84	15,53	16,63	16,95	16,88
Cr (T)	14,84	14,84	0,00	21,24	22,25	0,00	14,84	0,00	14,84	14,84	14,84	0,00	0,00	14,84
Illite (A)	15,18	15,01	15,04	14,84	15,19	15,23	15,20	15,14	14,90	15,01	15,33	15,26	15,05	15,13
Ti-Fe Oxide (A)	14,84	15,05	14,84	14,84	0,00	14,84	15,61	15,06	15,50	17,56	14,84	0,00	16,81	14,84
Fe-Ti Oxide (A)	23,74	14,84	16,88	14,84	19,67	32,11	29,23	15,17	21,98	18,95	17,95	14,84	40,32	24,89
Ti-Al-Silicate R09 (A)	15,40	18,95	16,99	16,27	17,22	15,87	17,08	16,73	15,19	16,39	15,62	14,84	17,84	16,36
Ca-Fe-Al-Silicate R09 (A)	16,06	15,27	15,39	24,34	22,00	24,08	21,86	15,78	15,13	15,88	15,69	23,07	16,36	16,97
FeOx-Silica texture R09 (A)	17,02	14,94	19,45	20,50	21,44	19,50	17,03	16,12	15,40	17,30	15,47	19,16	21,89	21,37
Silica-FeOx texture R09 (A)	17,63	15,07	19,11	15,54	18,90	18,50	17,43	15,39	15,54	15,80	15,64	17,11	23,65	20,43
Calcite-FeOx boundary R09 (R)	17,30	14,89	15,70	14,88	17,63	18,00	14,99	15,10	15,98	16,00	15,35	16,37	17,47	17,87
FeOx-Calcite boundary R09 (R)	15,65	14,84	16,62	14,84	16,47	15,71	15,52	14,84	15,74	16,40	15,23	16,42	16,26	15,60

All data provided in the following spreadsheets are calculated from the QEMSCAN. The grains of the mineral of interest have been extracted from the map, and grain: Grains that are touching (including matrix grains) have been reported as single, lar Inclusions of other phases within a grain, or intergrowths of other phases within a For each dataset, a corresponding QEMSCAN image is shows, displaying only the n These are visual representations of the actual data used to calculate the mineral g

mineral maps generated with 2.5 μ m point spacing.

Grains of 1 or 2 pixels in size have been removed.

Grains that are too small, elongated, or often irregularly shaped grains, thus biasing data.

Grains that are not included in the grains from which size data are calculated and may thus bias the data for the mineral for which grain size data are displayed.

Grain sizes and thus give a clear picture of whether the numbers in the table are derived from clear

ita.

arily separated, individual grains, or from unrepresentative textures or intergrowths.